Scattering of Electrons by Atomic Systems with Configurations $(1S)^2 (2S)^2 (2P)^6 (3S)^2 (3P)^9$

by

Michael Joseph Conneely

Submitted to the University of London
in partial fulfilment of the
requirements for the degree of
Doctor of Philosophy

To Helen

ABSTRACT

The close-coupling approximation has been used to compute cross sections for a wide range of processes (electron impact, photodetachment and photoionization). Errors in previous formulations have been pointed out and corrected. The results are compared with previous calculations and experiments and are correlated to recent work on the effects of configuration interaction.

A description of the computer code used is also given.

ACKNOWLEDGEMENTS

I would like to record my gratitude to my supervisor Professor Kenneth Smith for suggesting the topic of this thesis and for his invaluable guidance throughout the work.

I am indebted to Royal Holloway College for financial support and to the Atlas Computer Laboratory, Chilton, Berkshire and to the University of Nebraska Computer Centre, Lincoln, Nebraska, U.S.A. for use of their facilities.

In addition, I would like to acknowledge the hospitality of the Institute of Computational Sciences, The University of Nebraska where the latter part of this work was carried out. I am also grateful to Dr. L. Lipsky for helpful conversations.

Contents

Chapter I (Introduction)

a) Continuum atomic processes in astrophysical problems
b) The Close-coupling Method
c) The Fesbach Formalism
d) Configuration Interaction

Chapter II

a) Wave functions for the $(np)^q$ system
b) Antisymmetrization of the wave function
c) Electron impact cross sections
d) Photoionization

Chapter III

a) Photoionization of N and N^+
b) Photoionization of P
c) Photoionization of Aℓ, Si, S, Cℓ
d) Photodetachment of Si^-, S^-, $Cℓ^-$

Chapter IV

A description of the code and the numerical methods used

References

Bound Papers

Trial Wave Functions in the Close-Coupling Approximation
Photoionization of Atoms with Configurations $(1S)^2(2S)^2$
$(2p)^6(3S)^2(3P)^q$

List of Tables

		Page
Table I	Partial wave contributions to the excitation cross sections for O^+ N^+, O^{++}	52
Table II	Partial wave contributions to the excitation cross sections for P^+	56
Table III	Partial wave contributions to the excitation cross sections for S^+	58
Table IV	Partial wave contributions to the excitation cross sections for Cl^+	60
Table V	Comparison of collision strengths for various $(3p)^q$ ions between present and previous calculations	61
Table VI	Parameterization of the resonance series in the photoionization of N (^2P) (a) L=0 (b) L=1 (c) L=2	118
Table VII	Parameterization of the resonance series in the photoionization of N (^2D) (a) L=1 (b) L=2 (c) L=3	121
Table VIII	Photoionization cross sections for N (^4S, ^2D, ^2P) above all thresholds	124
Table IX	Photoionization cross sections for N^+ (^3P, ^1D, ^1S)	126
Table X	Parameterization of the resonance series in the photoionization of P (^2P) (a) L=0 (b) L=1 (c) L=2	128
Table XI	Parameterization of the resonance series in the photoionization of P (^2D) (a) L=1 (b) L=2 (c) L=3	130

List of Tables (continued)

		Page
Table XII	Photoionization cross sections for P (^4S, ^2D, ^2P) above all thresholds	133
Table XIII	Photoionization cross sections for Aℓ	135
Table XIV	Photoionization cross sections for Si	136
Table XV	Parameterization of the resonance series in the photoionization of S(^3P) (a) L=0 (b) L=1 (c) L=2	138
Table XVI	Parameterization of the resonance series in the photoionization of S(^1D)	140
Table XVII	Parameterization of the resonance series in the photoionization of S(^1S)	142
Table XVIII	Photoionization cross sections for S (^3P, ^1D, ^1S) above all thresholds	143
Table XIX	Parameterization of the resonance series in the photoionization of Cℓ(^2P) (a) L=0 (b) L=1 (c) L=2	144
Table XX	Photoionization cross sections for Cℓ(^2P) above all thresholds	146
Table XXI	Photodetachment cross sections for S_i^- (^4S) and $Cℓ^-$ (^1S)	147
Table XXII	Photodetachment cross sections for S^- (^2P)	149

List of Figures

		Page
Figure 1	Scattering potentials for electrons incident of carbon and silicon.	50
Figure 2	$^3D^o$ partial wave contribution to the ^4S-^2D excitation cross section of S^+ showing resonance effects.	51
Figure 3	Photoionization cross section of $N(^4S)$ and comparison with experiment.	79
Figure 4	$^2S^e$ partial wave contribution to the photoionization cross section of $N(^2P)$ showing resonance series.	80
Figure 5	$^2P^e$ partial wave contribution to the photoionization cross section of $N(^2P)$ showing resonance series.	81
Figure 6	$^2D^e$ partial wave contribution to the photoionization cross section of $N(^2P)$ showing resonance series.	82
Figure 7	$^2P^e$ partial wave contribution to the photoionization cross section of $N(^2D)$ showing resonance series.	83
Figure 8	$^2D^e$ partial wave contribution to the photoionization cross section of $N(^2D)$ showing resonance series.	84
Figure 9	$^2F^e$ partial wave contribution to the photoionization cross section of $N(^2D)$ showing resonance series.	85
Figure 10	$N^+(^3P)$ photoionization cross section and comparison with Dalgarno et.al. and Armstrong et.al.	86
Figure 11	Photoionization cross sections of $P(^4S)$ and $N(^4S)$.	88
Figure 12	$^2S^e$ partial wave contribution to the photoionization cross section of $P(^2P)$ showing resonance series.	90

List of Figures (continued)

		Page
Figure 13	$^2P^e$ partial wave contribution to the photoionization cross section of P(^{2}P) showing resonance series.	91
Figure 14	$^2D^e$ partial wave contribution to the photoionization cross section of P(^{2}P) showing resonance series.	92
Figure 15	$^2P^e$ partial wave contribution to the photoionization cross section of P(^{2}D) showing resonance series.	93
Figure 16	$^2D^e$ partial wave contribution to the photoionization cross section of P(^{2}D) showing resonance series.	94
Figure 17	$^2F^e$ partial wave contribution to the photoionization cross section of P(^{2}D) showing resonance series.	95
Figure 18	Comparison of three computed values (in the dipole length approximation) of the photoionization cross section of Al.	97
Figure 19	Comparison of the present results on the photoionization cross section of Si with the experimental observations of Rich.	99
Figure 20	$^3S^o$ partial wave contribution to the photoionization cross section of S(^{3}P) showing resonance series.	101
Figure 21	$^3P^o$ partial wave contribution to the photoionization cross section of S(^{3}P) showing resonance series.	102
Figure 22	$^3D^o$ partial wave contribution to the photoionization cross section of S(^{3}P) showing resonance series.	103
Figure 23	$^1P^o$ partial wave contribution to the photoionization cross section of S(^{1}D) showing resonance series.	104
Figure 24	$^1D^o$ partial wave contribution to the photoionization cross section of S(^{1}D) showing resonance series.	105

List of Figures (continued)

		Page
Figure 25	$^1F^o$ partial wave contribution to the photoionization cross section of $S(^1D)$ showing resonance series.	106
Figure 26	Total photoionization cross section of $S(^1S)$ showing a single resonant series.	107
Figure 27	$S(^3P)$ total photoionization cross section.	108
Figure 28	$^2P^e$ partial wave contribution to the photoionization cross section of $Cl(^2P)$ showing resonance series.	110
Figure 29	$^2P^e$ partial wave contribution to the photoionization cross section of $Cl(^2P)$ showing resonance series.	111
Figure 30	$^2D^e$ partial wave contribution to the photoionization cross section of $Cl(^2P)$ showing resonance series.	112
Figure 31	Comparison of Robinson and Geltman's calculation with the present calculation of the photodetachment cross section of S_i^-	114
Figure 32	Comparison of Robinson and Geltman's prediction with the present calculation of the photodetachment cross section of S^-.	115
Figure 33	Comparison of Robinson and Geltman's results with the present results for photodetachment of Cl^-.	116

THE IMPORTANCE OF CONTINUUM ATOMIC PROCESSES IN ASTROPHYSICAL PROBLEMS

The interaction of electrons and photons with matter in astrophysical sources covers a very wide range of conditions from that of interstellar clouds, where the atomic concentrations are very low (~8 atoms/cm^3), to that of the interior of stars where the density is very high (~10^{25} atoms/cm^3). The need for photoionization and electron excitation cross-sectional values is apparent whenever these processes are significant for the energy balance of a particular system and situation. In this introduction instances where the need for photoionization and electron excitation arises, will be indicated.

Planetary Atmospheres

The nonsphere of the Earth is produced mainly by the ionization of the neutral particle constitients of the atmosphere by solar ultraviolet radiation, leading to the production of free electrons and positive ions. The electrons initially possess a broad range of kinetic energies. As they slow down by collisions, the electrons cause excitation of the neutral particles and the resulting luminosity is an important component of the dayglow. The excitation processes

$$\begin{aligned} e + O(^3P) &\longrightarrow e + O(^1D) \\ e + O(^3P) &\longrightarrow e + O(^1S) \end{aligned} \qquad \ldots.(1.1)$$

which lead to emission of the oxygen red and green lines, together with the fine-structure transition.[1]

$$e + O(^3P_J) \longrightarrow e + O(^3P_{J'}) \qquad \ldots.(1.2)$$

are amongst the most efficient energy loss mechanisms in the neutral atmosphere.

At high altitudes the electron gas cools more efficiently in collisions with positive ions than with neutral particles and the ion gas temperature also uses above the neutral particle temperature.

The rate at which the electron gas loses heat to a positive ion mixture of O^+ He^+ and H^+ is given approximately by [2]

$$\mathcal{L}_e = 5 \times 10^{-7}(T_e - T_i)\, n_e \{ n(O^+) + 4\, n(He^+) + 16\, n(H^+) \} \text{ ev cm}^{-3}\text{sec}^{-1} \quad \ldots.(1.3)$$

where T_i is the positive ion temperature.

The thermal electron gas is removed by recombination process, and the recombination of electrons and positive ions is an important source of heating of the neutral particle atmosphere.

Electrons can also be removed by attachment processes leading to the formation of negative ions at low altitudes.

The Planetary Nebulae

Planetary nebulae are clouds of ionized gas surrounding certain very hot stars. The emitted light gives the nebulae a pale green disk like appearance resembling that of the planets Uranus and Neptune, hence the name planetary.

The model usually employed in the analogous of such stellar objects is one of a thin spherical shell surrounding a black body radiating at a high temperature T. The intensity I_ν of the radiation reaching the inner surface of the shell can be expressed by

$$I_\nu = \frac{R_s^2}{4r^2} \frac{2h\nu^3}{c^2} \frac{1}{e^{h\nu/kT} - 1} \quad \ldots.(1.4)$$

where R_s is the radius of the central star and r the inner shell radius of the nebula.

The black body intensity is thus diluted by the geometrical factor of $R_s^2/4r^2$ and since this is very small ($\sim 10^{-13}$), the nebula is exposed and radiation whose density is 10^{-13} times that for thermal equilibrium at temperature T.

The primary physical process that occurs in the nebula itself is photoionization due to the absorption of stellar ultraviolet radiation i.e.

$$h\nu + A \rightarrow A^+ + e$$

and occurs in atoms in the ground state. The electrons are then recaptured leaving the atoms in highly excited levels from which they cascade to lower levels emitting lines of allowed transitions. While this recombination occurs primarily in hydrogen and helium, it also has been observed in heavier elements such as oxygen, carbon, and nitrogen.

Collisional excitations are responsible for the strongest lines in most planetary nebulae. These lines are due to the forbidden transitions[3] which arise from the collisional excitation of the metastable levels that lie a few electron volts above the ground level. After the electrons have been excited to the metastable levels by inelastic collisions they cascade back to a lower level with the emmission of a forbidden quarter of the magnetic dipole or magnetic quadrupole type, or by a collision of the second kind.

The number of collisional excitations /cm^3/ sec. from a lower level n to an upper level n^1, F_{nn^1} depends on the

ion density N_n in level n, the electron density Ne, the electron temperature Te, the excitation potential $X_{nn}1$, of the upper level, the statistical weight W_n of the lower level and the collision strength $\Omega(nn^1)$ of the particular ion and the transition involved i.e.

$$F_{nn'} = 8.63 \times 10^{-6} N_n Ne Te^{-\frac{1}{2}} \frac{\Omega(n n')}{w_n} e^{-\chi_{nn'}/kTe} \quad \ldots.(1.5)$$

where $\Omega(n\ n^1)$, or the collision strength[4] is defined by

$$Q(n n') = \frac{\pi \Omega(n n')}{w_n K_n^2} \quad \ldots.(1.6)$$

where $Q(n\ n^1)$ is the cross-section and $K_n = mv_n/\hbar$ where v_n is the velocity of the incident electron. Equating the number of collisional excitations to the number of radiative de-excitations enables one to derive an expression, which involves Te and Ne, for the intensity of a forbidden line. From the intensity lines Te and Ne may be determined[5,6].

Interstellar Gas Clouds

To obtain information about the abundance of elements in the interstellar medium, it is necessary to study their degree of ionization. The steady state requires that the ionization rate equal the recombination rate. Denote by N' and N'' the number densities of some ion in two necessive stages of ionization. The radiative recombination rate n (rec) per unit volume is given by

$$n(rec) = \alpha N'' Ne \quad \ldots.(1.7)$$

where the recombination rate α is a function of electron temperature Te and is given by

$$\alpha = \frac{8\pi}{c^2}(2\pi m kTe)^{-3/2} \sum \frac{g_j'}{2g_1''} e^{\chi_j/kTe} \times \int (h\nu)^2 A_j(\nu)\, e^{-h\nu/kTe} \quad \ldots.(1.8)$$

where g_j' denotes the statistical weight, X_j the ionization potential, $A_j(\nu)$ the absorption cross section of the jth excited state of the atom in the lower stage of ionization and g_1'' the statistical weight of the ground state in the next state of ionization. If it is assumed that ionization is produced only by radiation of intensity $I(\nu)$ the photoionization rate is

$$n(ion) = 4\pi N' \int_{\nu_1}^{\infty} A_1(\nu) \frac{I(\nu)}{h\nu} d\nu = N'\Gamma \quad \ldots.(1.9)$$

where $A_1(\nu)$ is the absorption co-efficient for the ground state of the lower state of ionization and ν_1 is the ionization limit. Thus the ionization equation can be written in the form

$$\frac{N'' Ne}{N'} = \frac{\Gamma}{\alpha} \quad \ldots.(1.10)$$

The ionization rate Γ may be significantly altered by phenomena of auto-ionization.

Its influence on Γ has been discussed by Burgess[7] et al in their investigation of the lines of neutral aluminum.

Stromgen[8], who developed the interstellar ionization theory in its modern form, has shown that the abundance ratio of

$Ca/_{Na}$ could be deduced from the ratio $CaII/_{NaI}$ by

$$N_{Ca}/N_{Na} = (N_{CaII}/N_{NaI}) \times \left\{ \left[N_e + \left(\frac{\Gamma}{\alpha}\right) Ca\,II \right] / \left[N_e + \left(\frac{\Gamma}{\alpha}\right) Na\,I \right] \right\} \quad \ldots(1.11)$$

which leads to the curious results that the abundance ratio is about 0.03 compared to its value of 0.7 in the sun and other stars. It is possible that the photoionization rates are in error[9] because transitions in Na and CaII from their ground states to auto-ionizing states have not been taken into account. Possible transitions of this sort are shown in the diagram

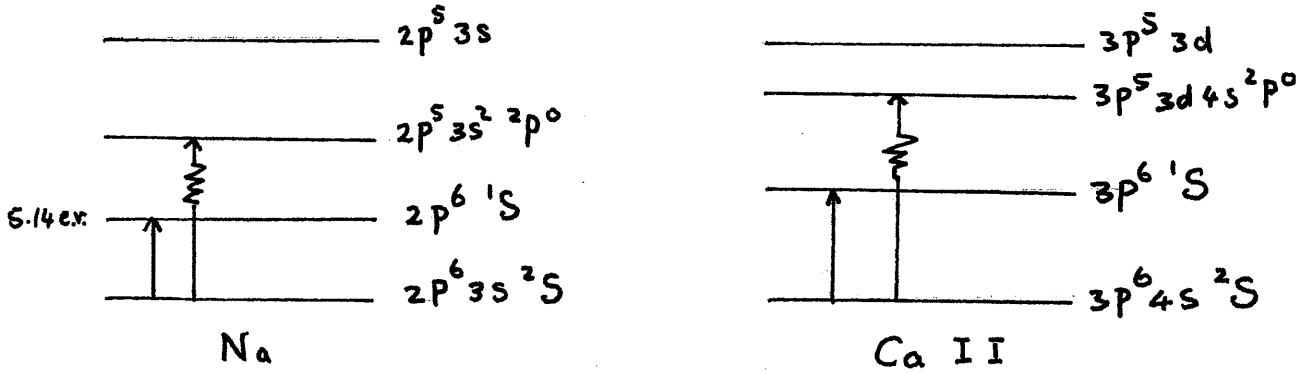

Golgberg[9] and Goldberg and Dupree[9a] have drawn attention to several astrophysical consequences of auto-ionization. The inverse process called delectronic recombination has been shown by Burgess[10] to play an important role in solar corona.

Other atomic processes of importance in the cooling interstellar gas

(a) atom molecule collisions[11]

$$H + H_2(J=0) \rightarrow H + H_2(J=0) \quad \ldots(1.12a)$$

(b) molecule-molecula collisions

$$H_2(J=0) + H_2(J=0) \rightarrow H_2(J=0) + H_2(J=2) \quad \ldots(1.12b)$$

(c) Excitation of the fine structure levels of Si^+ and C^+.

Stellar Atmopsheres

The stellar atmosphere problem may be defined in terms of the transfer equation[12]

$$\mu \frac{d}{dr} I_\nu = -K_\nu [I_\nu - B_\nu(T)] \quad \ldots.(1.13)$$

the equation of radiative equilibrium.

$$\int K_\nu J_\nu \, d\nu = \int K_\nu B_\nu \, d\nu \quad \ldots.(1.14)$$

and the equation of hydrostatic equilibrium

$$\frac{d}{dr} P_g = -\rho g + \frac{1}{c} \int K_\nu F_\nu \, d\nu \quad \ldots.(1.15)$$

where B_ν is the Planck function, J_ν the mean intensity

$J_\nu = \frac{1}{4\pi} \int I_\nu \, d\omega$ and F_ν being the flux,

$F_\nu = \int I_\nu \mu \, d\omega$ Pg is the gas pressure, Pg=NKT where N is the total number of particles per unit volume and $N=\sum_i N_i$.

For a given value of Pg and T one may calculate N_i using the Boltzmann and Saha equations and calculate the absorption coefficient.

$$K_\nu(PgT)=\sum_i N_i A_i(\nu) \quad \ldots.(1.16)$$

assuming all the absorption cross section A_i to be known. For principle one may solve the foregoing equations and hence obtain a complete model for the atmosphere. The unknowns Te and g and chemical composition have to be adjusted so as to obtain agreement between the calculated and observed star spectrum.

To explain the observed absorption in the solar atmosphere Wildt[13] suggested that the excess could be attributed to the negative hydrogen ion H^-.

Vardya[14] has compiled bound-free absorption co-efficients of $C\ell^-$ and other negative ions which are an important source of opacity in the atmospheres of cool stars.

$$h\nu + A^- \longrightarrow A + e$$

Also significant contributions might arise from the bound-free absoprtion of H_2^+ ions

$$h\nu + H_2^+(1s\sigma) \longrightarrow H + H^+$$

In order to explain absorption further in the red one must include the absorption due to the free-free transitions.

$$H + e + h\nu \longrightarrow H + e$$

The absorption co-efficients due to free-free transitions in H^- were evaluated by T. Ohmura and H. Ohmura[15]. Similiar work has been done recently for nitrogen and oxygen by Mjolsness and Ruffel.[16]

The Close-Coupling Approximation

In order to calculate the scattering cross section, within the framework of non-relativistic wave mechanics it is necessary to approximate the Schrodinger equation. One of the most useful approximation schemes is to expand the overall wave function of the projectile plus target in terms of the complete set of eigenstates of the target Hamiltonian. The method, called the close coupling approximation[17], was first introduced by Massey and Mohr[18], and has been since shown by Fesbach[19,20,21] to give rise naturally to resonance of the closed channel type. In order to make the method numerically tractable only a few of the lower stationary states are retained in the expansion. Apart from approximations inherent in the choice of eigenstates for complex atoms this is the only approximation made in the method.

The Hamiltonian for an electron colliding with an atomic system having N electrons and nuclear charge Z, neglecting magnetic and relativistic effects is

$$H = \sum_{i=1}^{N+1} H_1(i) + \sum_{i<j}^{N+1} \frac{1}{r_{ij}} \qquad \ldots.(1.17a)$$

where

$$H_1(i) = -\frac{1}{2}\left(\nabla_i^2 + \frac{2Z}{r_i}\right) \qquad \ldots.(1.17b)$$

$$r_{ij} = |\underline{r}_i - \underline{r}_j| \qquad \ldots.(1.17c)$$

Since spin orbit coupling is neglected the total orbital angular momentum and total spin are separately conserved, the calculation

may be simplified by using a representation which is diagonal in L, S and π. The unsymmetrized wave function for the N+1 electron system may be written[22]

$$\Psi_u = \sum_{\gamma_T} \Psi(\gamma_T \underline{X}_N) \bar{F}_{\gamma_T}(\underline{x}_{N+1}) \quad \ldots.(1.18)$$

where $\underline{X}_{N+1}$ denote the co-ordinates $\underline{x}_1 \ldots \underline{x}_{N+1}$ and $\underline{x}_k = \underline{r}_k \sigma_k$ i.e. the space and spin variables of the Kth electron. We now expand the continuum wave functions $\bar{F}_{\gamma_T}(\underline{x}_{N+1})$ in terms of a central fold type function.

$$\bar{F}_{\gamma_T}(\underline{x}_{N+1}) = \sum_{\substack{\ell_T m_T \\ m_s}} f_{\gamma_T \ell_T m_T m_s}(r_{N+1}) \, Y_{\ell_T m_T}(\hat{r}_{N+1}) \, \chi_{\frac{1}{2}}^{m_s}(\sigma_{N+1}) \, r_{N+1}^{-1} \quad \ldots.(1.19)$$

Hence

$$\Psi_u(X_{N+1}) = \sum_{\substack{\gamma_T \ell_T \\ m_T m_s}} \Psi(\gamma_T X_N) Y_{\ell_T m_T}(\hat{r}_{N+1}) \chi_{\frac{1}{2}}^{m_s}(\sigma_{N+1}) f_{\gamma_T \ell_T m_T m_s}(r_{N+1}) \, r_{N+1}^{-1} \quad \ldots.(1.20)$$

The angular and spin parts of $\bar{F}_{\gamma_T}(x_{N+1})$ are now coupled to those of $\Psi(\gamma_T \underline{X}_N)$ to give a new basis function $\Psi(\Gamma : \underline{X}_N \hat{x}_{N+1})$ where Γ denotes the complete set of quantum numbers.

$$\Gamma \equiv \{ \gamma_T \ell_T L M_L S M_S \pi \}$$

Since

$$\Psi(\gamma_T \underline{X}_N) \chi_{\frac{1}{2}}^{m_s}(\sigma_{N+1}) Y_{\ell_T m_T}(\hat{r}_{N+1}) = \sum_{L M_L S M_S} (L_T \ell_T M_{L_T} m_T | L M_L) \times (S_T \tfrac{1}{2} M_{S_T} m_s | S M_S) \Psi(\Gamma : \underline{X}_N \hat{x}_{N+1}) \quad \ldots.(1.21)$$

we have

$$\Psi_u(\underline{X}_{N+1}) = \sum \Psi(\Gamma : \underline{X}_N \hat{x}_{N+1}) \frac{\tilde{F}_\Gamma(r_{N+1})}{r_{N+1}} \quad \ldots.(1.22)$$

where

$$\tilde{F}_\Gamma(r_{N+1}) = \sum_{m_s m_T} (L_T \ell_T M_{L_T} m_T | L M_L)(S_T \tfrac{1}{2} M_{S_T} m_s | S M_S) \times f_{\gamma_T \ell_T m_T m_s}(r_{N+1}) \quad \ldots.(1.23)$$

In the asymptotic region we require

$$\tilde{F}_\Gamma(r) \sim A_\Gamma e^{-i\theta_\Gamma} - B_\Gamma e^{i\theta_\Gamma} \quad \ldots.(1.24)$$

The S-matrix is defined by the relationship

$$B_\Gamma = \sum_{\Gamma'} S_{\Gamma\Gamma'} A_{\Gamma'} \quad \ldots.(1.25)$$

Hence

$$F_\Gamma(r) \sim \sum A_\Gamma(\delta_{\Gamma\Gamma'} e^{-i\theta_\Gamma} - S_{\Gamma\Gamma'} e^{i\theta_\Gamma}) \quad \ldots.(1.26)$$

$$\theta_\Gamma = k_\Gamma r - \tfrac{1}{2}\ell_\Gamma\pi - \frac{Z-N}{k_\Gamma}\log(2k_\Gamma r) + \arg\left[\Gamma\left(\ell_\Gamma+1-i\frac{Z-N}{k_\Gamma}\right)\right] \quad \ldots.(1.27)$$

We define a new radial function $F_{\alpha\beta}$ by the transformation

$$\tilde{F}_\beta(r) = i\sum (I-iR)^{-1}_{\alpha\beta} F_{\alpha\beta}(r), \quad k_\beta^2 > 0 \quad \ldots.(1.28)$$

where $$R_{\alpha\beta} = i\left[\frac{I-S}{I+S}\right]_{\alpha\beta} \quad \ldots.(1.29)$$

With this definition the $F_{\alpha\beta}$ will be real everywhere and will have the asymptotic form

$$F_{\alpha\beta}(r) \sim \frac{1}{k_\alpha^{\frac{1}{2}}}(\delta_{\alpha\beta}\sin\theta_\alpha + R_{\alpha\beta}\cos\theta_\alpha), \quad k_\alpha^2 > 0 \quad \ldots.(1.30a)$$

$$F_\gamma(r) \sim N_\gamma \exp\left[-|k_\gamma|r + \mathrm{Im}\left(\frac{Z-N}{k_\gamma}\right)\log(2|k_\gamma|r)\right], \quad k_\gamma^2 < 0 \quad \ldots.(1.30b)$$

Consequently

$$\bar{\Psi}_u(\underline{X}_{N+1}) = \sum_{\Gamma_i,\Gamma_j} \Psi(\Gamma_i; \underline{X}_N \hat{x}_{N+1}) F_{\Gamma_i\Gamma_j}(r_{N+1}) r_{N+1}^{-1} \quad \ldots.(1.31)$$

For the system initially in state Γ_j the wave function is

$$\bar{\Psi}_u(\Gamma_j \underline{X}_{N+1}) = \sum_{\Gamma_i} \Psi(\Gamma_i \underline{X}_N \hat{x}_{N+1}) F_{ij}(r_{N+1}) r_{N+1}^{-1} \quad \ldots.(1.32)$$

Finally we construct a properly antisymmetrized wave function

$$\bar{\Psi}(\Gamma_j \underline{X}_{N+1}) = \frac{1}{(N+1)^{\frac{1}{2}}} \sum_{K=1}^{N+1} (-1)^{N+1-K} \bar{\Psi}_u(\Gamma_j \underline{X}^{-K} \underline{x}_K) \quad \ldots.(1.33)$$

where $\underline{X}^{-K} = \underline{x}_1\ \underline{x}_2 \cdots \underline{x}_{K-1}\ \underline{x}_{K+1} \cdots \underline{x}_{N+1}$

The S-Matrix

The elements of the S-matrix are defined in equation (1.25) in terms of the amplitudes of the ingoing and out going waves. It also may be obtained from the R-matrix

$$S = \frac{I + iR}{I - iR} \qquad \ldots.(1.34)$$

The fact that it is unitary and symmetric means that it can be diagonalized by a real orthogonal matrix U

$$\tilde{U} S U = e^{2i\eta_\alpha} \qquad \ldots.(1.35)$$

where the eigenphase shifts η_α are real. The same matrix U will also diagonalize the R-matrix

$$\tilde{U} R U = \tan \eta_\alpha \delta_{\alpha\beta} \qquad \ldots.(1.36)$$

The transition matrix is defined by

$$T = S - I \qquad \ldots.(1.37)$$

The total cross section for the transition $L_i\text{-}S_i \to L_j S_j$ is defined by [23]

$$\sigma(L_i S_i \to L_j S_j) = \sum_{\substack{S L \pi \\ \ell_i \ell_j}} \frac{(2L+1)(2S+1)}{2k_i^2(2L_i+1)(2S_i+1)} |T_{ij}|^2 \qquad \ldots.(1.38)$$

The Radial Equations

We consider the integral

$$I_{ij} = \int \Psi^*(\Gamma_i\, \underline{X}_{N+1}) [H_{N+1} - E] \Psi(\Gamma_j\, \underline{X}_{N+1})\, d\underline{X}_{N+1} \qquad \ldots.(1.39)$$

where

$$H_{N+1} = -\tfrac{1}{2}\nabla^2_{N+1} - \frac{Z}{r_{N+1}} + \sum_{\alpha=1}^{N} \frac{1}{r_{N+1,\alpha}} + H_N \qquad \ldots.(1.40)$$

Equation (1.39) can be written in terms of the unsymmetrized functions as

$$I_{ij} = \int (N+1)^{\frac{1}{2}} \Psi_u(\Gamma_i\, \underline{X}_N\, \underline{x}_{N+1}) [H_{N+1} - E] \times \sum_{k=1}^{N+1} (-1)^{N+1-k} (N+1)^{-\frac{1}{2}} \Psi_u(\Gamma_j\, \underline{X}^{-k}\, \underline{x}_k)\, dX \qquad \ldots.(1.41)$$

using the symmetry with respect to interchange of variable.

The atomic eigen functions satisfy

$$\int \Psi(\gamma_T\, X_N)\,[H_N - E_\xi]\,\Psi(\gamma_T',\, X_N)\, d X_N = 0 \qquad \ldots.(1.42)$$

Thus equation (1.41) becomes using eq. (1.42)

$$I_{ij} = \int_0^\infty \sum_{k\ell} F_{k\ell}^{(r)} \left[-\tfrac{1}{2}\left(\frac{d^2}{dr^2} - \frac{\ell_k(\ell_k+1)}{r^2} + \frac{2z}{r} + k_k^2\right)\delta_{k\ell} + V_{k\ell}^{(r)} \right] F_{\ell j}^{(r)}\, dr$$

$$\equiv \int_0^\infty F^T \mathcal{L}\, F\, dr \qquad \ldots.(1.43)$$

where the potential $V_{k\ell}^{(r)}$ involves direct and exchange interaction.

We now consider variation of the function F about the exact solution which satisfy the boundary conditions.

$$\begin{aligned} \delta F_{ij} &\sim a_i\, r^{\ell_i+1}, \quad r \to 0 \\ \delta F_{ij} &\sim \kappa^{-\frac{1}{2}}\, \delta R_{ij} \cos\theta_i, \quad r \to \infty \end{aligned} \qquad \ldots.(1.44)$$

The corresponding variation in I is

$$\delta I = \int_0^\infty \left[\delta F^T \mathcal{L}\, F + F^T \mathcal{L}\, \delta F\right] dr$$

$$= 2\int_0^\infty \delta F^T \mathcal{L}\, F\, dr - \tfrac{1}{2}\left[F^T \frac{d}{dr}\delta F - \delta F^T \frac{d}{dr} F\right]_0^\infty \qquad \ldots.(1.45)$$

using the boundary conditions (1.30) and (1.44) we obtain

$$\delta I = 2\int_0^\infty \delta F^T \mathcal{L}\, F\, dr + \tfrac{1}{2}\,\delta R \qquad \ldots.(1.46)$$

Thus the variational principle

$$\delta\left(I - \tfrac{1}{2} R\right) = 0 \qquad \ldots.(1.47)$$

for arbritary variations of F subject to the appropriate boundary conditions, leads to the coupled equations

$$\mathcal{L}\, F \equiv \left(\frac{d^2}{dr^2} - \frac{\ell_i(\ell_i+1)}{r^2} + \frac{2z}{r} + k_i^2\right) F_{ik}^{(r)} - 2\sum_{j=1}^{m} V_{ij}\, F_{jk}^{(r)} = 0 \qquad \ldots.(1.48)$$

for the radial function F. These equations will be discussed further in Chapter 2.

The Fesbach Formalism

The formal properties of the solution to equations (1.48) can be conveniently discussed using the projection operator ofrmalism introduced by Fesbach[20,21]. We write our coupled equations formally as

$$P[H-E](P+Q)\Psi = 0 \qquad \ldots.(1.49a)$$

$$Q[H-E](P+Q)\Psi = 0 \qquad \ldots.(1.49b)$$

where P projects onto the open channel subspace and Q projects onto the closed channel subspace. The operators P and Q satisfy the relations

$$P+Q=1\ ,\quad P^2=P\ ,\quad Q^2=Q\ ,\quad PQ=0$$

We now formally solve eq. (27b) for $Q\Psi$

$$Q\Psi = -Q\frac{1}{Q(H-E)Q}QHP\Psi \qquad \ldots.(1.50)$$

Equation (1.49a) then gives

$$P\left[H - PHQ\frac{1}{Q(H-E)Q}QHP - E\right]P\Psi = 0 \qquad \ldots.(1.51)$$

The term P(H-E)P in equation (1.51) is just the close coupling operator obtained by retaining only the open channels in the expansion. The remaining term is just an optical potential. Denoting the eigenfunctions of the operator QHQ by Φ_n we have

$$QHQ\,\Phi_n = \mathcal{E}_n\,\Phi_n \qquad \ldots.(1.52)$$

The operator QHQ has in general a discreet spectrum plus a continuum starting from the lowest threshold in the closed channel subspace. It is the discreet spectrum which corresponds physically to an electron bound in the field of an excited atom

or ion, that gives use to closed channel resonance solutions of equation (1.51).

The optical potential is now expanded using the Φ_n and consequently equation (1.51) becomes

$$P\left[H - \sum_n \frac{PHQ|\Phi_n\rangle\langle\Phi_n|QHP}{\mathcal{E}_n - E} - E\right]\Psi = 0 \quad \ldots.(1.53)$$

We wish to consider the behaviour of the solution in the neighbourhood of an eigenvalue E_s of QHQ. Equation (1.53) is written as

$$(H'-E)P\Psi = -\frac{PHQ|\Phi_s\rangle\langle\Phi_s|QHP\Psi\rangle}{E-\mathcal{E}_s} \quad \ldots.(1.54)$$

where

$$H' = PHP + \sum_{n\neq s} \frac{PHQ|\Phi_n\rangle\langle\Phi_n|QHP}{E-\mathcal{E}_s}$$

Equation (1.54) can be formally solved to yield

$$P\Psi = P\Psi_0 + \frac{1}{E-\mathcal{E}_s} G\,PHQ\Phi_s\rangle\langle\Phi_s QHP\Psi\rangle \quad \ldots.(1.55)$$

where G and ψ_0 are the Greens function and regular solution of the operator H^1-E. Multiplying eq. (1.55) on the left by $\langle\Phi_s QHP$ we obtain

$$\langle\Phi_s QHP\Psi\rangle = \frac{\langle\Phi_s QHP\Psi_0\rangle}{1 - \frac{1}{E-\mathcal{E}_s}\langle\Phi_s QHPG\,PHQ\Phi_s\rangle} \quad \ldots.(1.56)$$

and substituting in eq. (1.55) gives

$$P\Psi = P\Psi_0 + \frac{GPHQ\Phi_s\rangle\langle\Phi_s QHP\Psi_0\rangle}{E-\mathcal{E}_s-\Delta_s} \quad \ldots.(1.57)$$

where

$$\Delta_s = \langle\Phi_s QHPG\,PHQ\Phi_s\rangle \quad \ldots.(1.58)$$

is the shift in energy caused by the interaction with the continuum.

O'Malley and Geltman[24] have shown that for a two electron system, that asymptotically equation (1.57) becomes

$$P\Psi \underset{r_2\to\infty}{\sim} \sqrt{\frac{2}{\pi k}}\frac{U_{1s}(r_1)}{r_2}Y_\ell^m(\hat{r}_2)\sin\left[kr_2 - \frac{\ell\pi}{2} + \eta_0 - \pi\frac{|\langle\Psi_0 PHQ\Phi_s\rangle|^2}{E-\mathcal{E}_s-\Delta_s}\cos\left(kr_2 - \frac{\ell\pi}{2} + \eta_0\right)\right] \quad \ldots.(1.59)$$

$$= \sqrt{\frac{2}{\pi k}}\, u_{1S}(r_1)\, Y_\ell^m(\hat{r}_2)\, \frac{\sin(kr_2 - \frac{\ell\pi}{2} + \eta_0 + \eta_r)}{r_2 \cos\eta_r}$$

where

$$\tan\eta_r = \frac{-\Gamma_s/2}{E - \varepsilon_s - \Delta_s}\,, \quad \Gamma_s = 2\pi |\langle \Psi_0 | PHQ | \Phi_s \rangle|^2 \qquad \ldots.(1.60)$$

In equation (1.59) the resonance position E_r can be seen to be $E_r = \varepsilon_s + \Delta_s$. The background phase shift is denoted by η_0 and the resonant part by η_r.

The partial wave cross section can be expressed in terms of the phase shift $\eta = \eta_0 + \eta_r$ by

$$\sigma_\ell = \frac{4\pi}{k^2} \sin^2\eta \qquad \ldots.(1.61)$$

In the neighborhood of an isolated resonance this gives

$$\sigma_\ell = \frac{4\pi}{k^2} \sin^2\eta_0 \, \frac{(q+\epsilon)^2}{1+\epsilon^2} \qquad \ldots.(1.62)$$

where $\epsilon = (E - E_r)/\frac{1}{2}\Gamma$, $q = -\cot\eta_0$. The Breit-Wigner one level formula[25] follows immediately by putting $\eta_0 = 0$.

Configuration Interaction

We now consider an alternative model for describing resonant or autoionizing states proposed by Fano.[26,27] A review of theoretical models which predict and interpret resonance phenomena has been given by Smith[17].

We consider a discreet state ϕ interacting with one continuum Ψ_E, and assume the normalization

$$\langle \phi | \phi \rangle = 1 \,, \quad \langle \phi | \Psi_E \rangle = 0 \qquad \ldots.(1.63)$$

The expectation value of the Hamiltonian is

$$\begin{aligned} \langle \phi | H | \phi \rangle &= E_\phi \\ \langle \Psi_E | H | \phi \rangle &= V_E \\ \langle \Psi_{E''} | H | \Psi_{E'} \rangle &= E' \delta(E'' - E') \end{aligned} \qquad \ldots.(1.64)$$

where it is assumed for simplicity that the sub matrix in the continuum states has been prediagonalized. Each energy value E within the range considered is an eigenvalue of the matrix and its corresponding eigenvector we write as

$$\Psi_E = a\phi + \int dE' \, b_{E'} \, \psi_{E'} \qquad \ldots.(1.65)$$

Then pre-multiplying the Schroedinger equation $(H - E)\Psi_E = 0$ by ϕ and Ψ_E and integrating yields, having used equations ....(1.62)

$$\begin{aligned} E_\phi \, a + \int dE' \, V_{E'} \, b_{E'} &= E\, a \\ V_{E'} \, a + E' \, b_{E'} &= E \, b_{E'} \end{aligned} \qquad \ldots.(1.66)$$

The second of equations (1.66) can be solved formally[28] to give

$$b_{E'} = \left[\frac{P}{E - E'} + Z(E)\, \delta(E - E') \right] V_{E'} \, a \qquad \ldots.(1.67)$$

where $Z(E)$ depends on the contour of integration round the singularity at $E=E'$ and P means that the principle value of the integral is taken.

If the states Ψ_E are represented by a wave function with the asymptotic form

$$\psi_E \sim \sin [\, kr + \delta_0(E) \,] \qquad \ldots.(1.68)$$

where $\delta_0(E)$ is a slowly varying potential phase shift, then the total wave function has the asymptotic form

$$\begin{aligned} \Psi_E &\sim \int dE' \, b_{E'} \, \Psi_{E'} \qquad \ldots.(1.69) \\ &\sim V_E \, a \left[-\pi \cos(kr + \delta_0(E)) + Z(E) \sin(kr + \delta_0(E)) \right] \\ &\sim V_E \, a \sqrt{\pi^2 + Z^2} \sin(kr + \delta_0 + \delta_r) \end{aligned}$$

where $$\delta_r = -\tan^{-1}\left(\frac{\pi}{Z(E)} \right) \qquad \ldots.(1.70)$$

Now upon substitution of equation (1.69) into the first of equations (1.66) one obtains

$$E_\phi \, a + P \int \frac{dE' \, |V_{E'}|^2 a}{E - E'} + Z(E) |V_E|^2 a = E\, a \qquad \ldots.(1.71)$$

Thus

$$Z(E) = \frac{E - E_\phi - \Delta E}{|V_E|^2} \quad \ldots.(1.72)$$

where the shift of the level due to interaction with the continuum is defined

$$\Delta(E) = P \int \frac{|V_E|^2}{E - E'} dE' \quad \ldots.(1.70)$$

The resonance with is

$$\Gamma = 2\pi |V_E|^2 = 2\pi |\langle \Psi_E | H | \phi \rangle| \quad \ldots.(1.71)$$

The normalization condition $\langle \Psi_E | \Psi_{E'} \rangle = \delta(E - E')$ gives

$$a = \frac{\sin \delta_r}{\pi V_E} \quad \ldots.(1.72)$$

Use of equation (1.67) yields

$$b_{E'} = P \frac{V_{E'}}{\pi V_E} \frac{\sin \delta_r}{E - E'} - \cos \delta_r \, \delta(E - E') \quad \ldots.(1.73)$$

The transition matrix element from source initial state i to a resonant final state is

$$\langle \Psi_E | T | i \rangle = \frac{1}{\pi V_E^*} \langle \Phi | T | i \rangle \sin \delta_r - \langle \Psi_E | T | i \rangle \cos \delta_r \quad \ldots.(1.74)$$

where $\Phi = \phi + P \int \frac{dE' \, V_{E'} \Psi_{E'}}{E - E'}$

Hence we obtain that the ratio of the absorption cross section to the modified continuum to that of the unperturbed continuum is

$$\frac{\sigma}{\sigma_a} = \frac{|\langle \Psi_E | T | i \rangle|^2}{|\langle \Psi_E | T | i \rangle|^2} = \frac{(q + \epsilon)^2}{1 + \epsilon^2} \quad \ldots.(1.75a)$$

where $\epsilon = -\cot \delta_r = \frac{E - E_r}{\Gamma/2}$ $\quad \ldots.(1.75b)$

$$q = \frac{\langle \Phi | T | i \rangle}{\pi \langle \phi | H | \Psi_E \rangle \langle \Psi_E | T | i \rangle} \quad \ldots.(1.75c)$$

In the case of more than one continuum say Ψ_E , Ψ_E .... it is possible to find linear combinations of these states such that the discreet state ϕ only interacts with one of these

combinations say ψ'_E . The form of the photoionization cross section in this case is

$$\sigma = \sigma_a \frac{(q+\epsilon)^2}{1+\epsilon^2} + \sigma_b \qquad \ldots.(1.76)$$

where the smooth background σ_b is due to the states orthogonal to ψ'_E

The Rydberg Series Lines

The case of several discreet lines superimposed upon a continuum and converging to a series limit at some excited state of the atomic ion is one which is frequently encountered in absorption studies in the far ultraviolet. In terms of autoionization effects the Rydberg series of lines can be treated as a set of discrete states which experience configuration interaction with the continuum. This case has been treated in detail by Fano[37] and Fano and Cooper[28]. Because of the second order interaction among the discrete states arising from their coupling with the continuum, the discreet states ϕ_n and their energies $E_{\phi(n)}$ will be perturbed by a matrix $Z^{(E)}_{nm}$ analogous to $Z(E)$ of equation (1.72)

$$Z^{(E)}_{nm} = P \int \frac{V_{n,E'} V_{E',m}\, dE'}{E - E'} \qquad \ldots.(1.77)$$

The states ϕ_n are replaced by new states $\bar{\phi}_\nu$ which in turn are modified by an admixture of states from the continuum

$$\bar{\Phi}_\nu = \bar{\phi}_\nu + P \int \frac{\psi_{E'} V_{E',\nu}\, dE'}{E - E'} \qquad \ldots.(1.78a)$$

$$q_\nu = \frac{\langle \bar{\Phi}_\nu | T | i \rangle}{\pi V_{E,\nu} \langle \psi_E | T | i \rangle} \qquad \ldots.(1.78b)$$

$$\Gamma_\nu = 2\pi |V_{E,\nu}|^2 \qquad \ldots.(1.78c)$$

Fano and Cooper[27] showed that in the interval between successive resonances the same line shapes occur for the single discrete level and a single continuum. In particular the matrix element $\langle \Psi_E | T | i \rangle$ vanishes once in each successive interval. The shape parameter q is approximately constant along a series and the width Γ_ν decreases in proportion to the spacing between the resonances.

Mies[29] has extented Fano's resonance theory to include the interaction of many resonances with many continua, as well as overlaping resonances. Shore[30] has also treated this problem from a different approach.

Chapter 2

Wave Functions for the $(np)^q$ system

We wish to construct from the one-electron wave functions $\psi_{n\ell m\mu}(\xi_1)$, $\psi_{n'\ell'm'\mu'}(\xi_2)$ the wave function of the 2-electron system. $\Psi_{LSM_LM_S}(\ell_1\ell_2)$ We have

$$\Psi_{LSM_LM_S}(\ell_1\ell_2') = \sum_{m\mu m'\mu'} (\ell m \ell' m' | L M_L)(\tfrac{1}{2}\mu\tfrac{1}{2}\mu' | S M_S)\psi_{n\ell m\mu}(\xi_1)\,\psi_{n'\ell'm'\mu'}(\xi_2) \quad \ldots.(2.1)$$

and

$$\Psi_{LSM_LM_S}(\ell_2\ell_1') = \sum_{m\mu m'\mu'} (\ell m \ell' m' | L M_L)(\tfrac{1}{2}\mu\tfrac{1}{2}\mu' | S M_S)\psi_{n\ell m\mu}(\xi_2)\,\psi_{n'\ell'm'\mu'}(\xi_1) \quad \ldots.(2.2)$$

These two functions differ in the fact that in the first case the first electron is in a state with angular momentum ℓ and in the second case it is in a state with angular momentum ℓ'. The wave function for the two electron system, can be obtained by composing an antisymmetric combination of the above functions.

$$\Psi_{LSM_LM_S} = \frac{1}{\sqrt{2}}\left\{\Psi_{LM_LSM_S}(\ell_1\ell_2') - \Psi_{LM_LSM_S}(\ell_2\ell_1')\right\} \quad \ldots.(2.3)$$

Noting the fact

$$(\ell m \ell' m' | L M_L) = (-1)^{\ell+\ell'-L}(\ell' m' \ell m | L M_L)$$
$$(\tfrac{1}{2}\mu\tfrac{1}{2}\mu' | S M_S) = (-1)^{1-S}(\tfrac{1}{2}\mu'\tfrac{1}{2}\mu | S M_S) \quad \ldots.(2.4)$$

We see that

$$\Psi_{LM_LSM_S}(\ell_2\ell_1') = (-1)^{\ell+\ell'-1-L-S}\Psi_{LM_LSM_S}(\ell_1'\ell_2)$$

Therefore we obtain

$$\Psi_{LM_LSM_S} = \frac{1}{\sqrt{2}}\left\{\Psi_{LM_LSM_S}(\ell_1\ell_2') + (-1)^{\ell+\ell'-L-S}\Psi_{LM_LSM_S}(\ell_1'\ell_2)\right. \quad \ldots.(2.5)$$

where

$$\Psi_{LM_LSM_S}(\ell_1'\ell_2) = \sum(\ell' m' \ell m | L M_L)(\tfrac{1}{2}\mu'\tfrac{1}{2}\mu | S M_S)\psi_{n'\ell'm'\mu'}(\xi_1)\,\psi_{n\ell m\mu}(\xi_2) \quad \ldots.(2.6)$$

In the case of two equivalent electrons $\ell=\ell'$ and noting that

$$\bar{\Psi}_{LM_LSM_S}(\ell_1\ell_2') = \Psi_{LM_LSM_S}(\ell_1'\ell_2) = \Psi_{LM_LSM_S}(\ell_1\ell_2) \quad \ldots.(2.7)$$

we obtain

$$\Psi_{LM_LSM_S} = \bar{\Psi}_{LM_LSM_S}(\ell_1\ell_2) \quad L+S \text{ even}$$

$$\Psi_{LM_LSM_S} = 0 \quad L+S \text{ odd} \quad \ldots.(2.8)$$

and the normalization factor is equal to $\frac{1}{2}$ and not $1/\sqrt{2}$.

We now wish to write the wave function $\Psi_{LM_LSM_S}(\ell^n)$ of a group of n equivalent electrons in terms of a linear combination of the functions $\Psi_{LM_LSM_S}(\ell^{n-1}(S'L')\ell\, LS)$ corresponding to different initial terms $L'S'$ of the configuration ℓ^{n-1}. Amongst the states $\{\ell^{n-1}(L'S')\ell\, LS\, M_L\, M_S\}$ obtained according to the rules of addition of angular momenta will be some which are forbidden by the Pauli exclusion principle. Only a linear combination of these functions will satisfy the Pauli principle. We write

$$\Psi_{LM_LSM_S}(\ell^n) = \sum_{L'S'}(\ell^n LS|\}\ell^{n-1}L'S')\,\Psi_{LSM_LM_S}(\ell^{n-1}(L'S')\ell\, LS) \quad \ldots.(2.9)$$

The co-efficients $(\ell^n LS|\}\ell^{n-1}L'S')$ are called the fractional parentage co-efficients : In the case of two equivalent electrons we have from the previous discussion that all the c.f.p.'s are equal to unity.

In the case of three equivalent electrons we will add a third ℓ electron to the configuration ℓ^2 and construct the function $\Psi_{LM_LSM_S}(\ell_1\ell_2(L'S')\ell_3)$ according to the rules

of addition of angular momenta. The function is antisymmetric in electrons 1 and 2 but not with respect to the third electron. We now couple electrons 2 and 3 and obtain

$$\Psi_{LM_LSM_S}(\ell_1\ell_2(S'L')\ell_3) = \sum (\ell\ell(L'S')\ell SL \mid \ell,\ell\ell(L''S'')LS) \times \Psi_{LM_LSM_S}(\ell_1:\ell_2\ell_3(L''S'')) \quad \ldots.(2.10)$$

where the transformation co-efficient

$$(\ell\ell(L'S')\ell LS \mid \ell,\ell\ell(L''S'')LS) = (2L'+1)(2L''+1)(2S'+1) \times (2S''+1)\,W(\ell_1\ell_2L\ell_3:L'L'')\,W(\tfrac{1}{2}\tfrac{1}{2}S\tfrac{1}{2}:S'S'') \quad \ldots.(2.11)$$

The function $\Psi_{LM_LSM_S}(\ell_1:\ell_2\ell_3(L''S''))$ is also built according to the rules of addition of angular momenta from the functions $\Psi_{\ell_1 m_1 s_1 \mu_1}^{(\ell_1)}$ and $\Psi_{L''S''M_{L''}M_{S''}}^{(\ell_2\ell_3)}$. Only those functions for which $L'' + S''$ is even are antisymmetric with respect to transposition of electrons, 2 and 3. Consequently we require combinations of the functions $\Psi_{LM_LSM_S}(\ell_1\ell_2(L'S')\ell_3)$ which do not contain functions $\Psi_{LM_LSM_S}(\ell_1:\ell_2\ell_3(S''L''))$ with odd values of $L'' + S''$. This condition is fulfilled provided

$$\sum_{L'S'} (\ell^3LS\}\}\ell^2L'S')(2L'+1)(2L''+1)(2S'+1)(2S''+1)\,W(\ell\ell L\ell:L'L'') \times W(\tfrac{1}{2}\tfrac{1}{2}S\tfrac{1}{2}:S'S'') = 0 \quad S''+L'' = \text{odd} \quad \ldots.(2.12)$$

Consider the ^2P term of the p^3 configuration. The forbidden terms of the P^2 configuration are $^3P, ^1D, ^1S$. Putting $L=1$, $S=\frac{1}{2}$ $L''=0$ $S''=1$ in the previous equation we get

$$\tfrac{1}{6}(P^3\,{}^2P\}\}P^2\,{}^1S) - \tfrac{1}{6}(P^3\,{}^2P\}\}P^2\,{}^3P) + \tfrac{\sqrt{5}}{6}(P^3\,{}^2P\}\}P^2\,{}^1D) = 0 \quad \ldots.(2.13)$$

Similiarly putting $L''=1$ and $S''=0$

$$\tfrac{1}{6}(P^3\,{}^2P\}\}P^2\,{}^1S) + \tfrac{1}{4}(P^3\,{}^2P\}\}P^2\,{}^3P) - \tfrac{\sqrt{5}}{12}(P^3\,{}^2P\}\}P^2\,{}^1D) = 0 \quad \ldots.(2.14)$$

We also must have (normalization)

$$\sum_{L'S'} (p^3\,{}^2P|\}\, p^2 L'S')^2 = 1 \qquad \ldots.(2.15)$$

These equations determine the c.f.p.'s up to a phase factor of ± 1. The procedure may be repeated for the ^2D and ^4S terms. The results are in the following table.

	^1S	^1D	^3P
^4S	0	0	1
^2D	0	$\frac{-1}{\sqrt{2}}$	$\frac{1}{\sqrt{2}}$
^2P	$\frac{\sqrt{2}}{3}$	$-\frac{\sqrt{5}}{3\sqrt{2}}$	$\frac{-1}{\sqrt{2}}$

The sign of each row in the table was chosen following Racah[31]. Although the sign of each row is at our disposal the relative signs of the entries in each row is not.

The same method may also be applied to the configuration ℓ^n of the c.f.p.'s of the ℓ^{n-1} configuration are known. In this case we have

$$\Psi_{LM_LSM_S}(\ell^n) = \sum_{S'L'} (\ell^n SL|\}\, \ell^{n-1}S'L')\, \Psi_{LM_LSM_S}(\ell^{n-1}(L'S')\,\ell)$$
$$= \sum_{S'L'S''L''} (\ell^n SL|\}\, \ell^{n-1}S'L')(\ell^{n-1}S'L'|\}\, \ell^{n-2}S''L'')\, \Psi_{LM_LSM_S}(\ell^{n-2}(S''L'')\,\ell(S'L')\ell) \qquad \ldots.(2.16)$$

Recoupling ℓ_n and ℓ_{n-1} we see that the c.f.p.'s must satisfy the equations

$$\sum_{S'L'} (S''L'', \ell\ell(S'''L''')\, SL \,|\, S''L''\,\ell(S'L')\,\ell\, SL)(\ell^n SL|\}\, \ell^{n-1}S'L')$$
$$\times (\ell^{n-1}S'L'|\}\, \ell^{n-2}S''L'') = 0 \qquad \ldots.(2.17)$$

for $L'' + S'' = \text{odd}$ where

$$(S''L'', \ell\ell(S'''L''')SL \mid S''L''\ell(S'L')\ell SL) = \sqrt{(2L'+1)(2L'''+1)(2S'+1)(2S''+1)} \times W(L''\ell L\ell : L'L''')W(S''\tfrac{1}{2}S\tfrac{1}{2} : S'S''') \quad \ldots.(2.18)$$

As before this system of equations do not fix the phases of the eigenfunctions of the different terms.

We apply the foregoing euqtions to the ^1D term of the p^4 configuration. We chose $L''' = 1, S''' = 0$, $L'' = 2$ $S'' = 0$, $L = 2, S = 0$ and $L'S' = {}^4S$, ^2D, and ^2P. Consequently

$$(p^4\,{}^1D \| p^3\,{}^4S)(p^3\,{}^4S \| p^2\,{}^1D)\, 2\sqrt{3}\, W(2121:01)\, W(0\tfrac{1}{2}0\tfrac{1}{2}:\tfrac{3}{2}0) +$$
$$(p^4\,{}^1D \| p^3\,{}^2D)(p^3\,{}^2D \| p^2\,{}^1D)\, \sqrt{30}\, W(2121:21)\, W(0\tfrac{1}{2}0\tfrac{1}{2}:\tfrac{1}{2}0) +$$
$$(p^4\,{}^1D \| p^3\,{}^2P)(p^3\,{}^2P \| p^2\,{}^1D)\, 3\sqrt{2}\, W(2121:11)\, W(0\tfrac{1}{2}0\tfrac{1}{2}:\tfrac{1}{2}0) = 0$$

$\ldots.(2.19)$

Using the previously obtained values for $(p^3LS \| p^2L'S')$ and evaluating the Racah co-efficients W(abcd:ef) equation (2.19) yields.

$$\frac{(p^4\,{}^1D \| p^3\,{}^2D)}{(p^4\,{}^1D \| p^3\,{}^2P)} = \sqrt{3} \quad \ldots.(2.20)$$

Using equation (2.15) we obtain.

$$(p^4\,{}^1D \| p^3\,{}^2P) = \tfrac{1}{2}\,,\ (p^4\,{}^1D \| p^3\,{}^2D) = \tfrac{\sqrt{3}}{2}\,,\ (p^4\,{}^1D \| p^3\,{}^4S) = 0$$

$\ldots.(2.21)$

Similarly we obtain the rest of the c.f.p.'s for the p^4 configuration

	^4S	^2D	^2P
^3P	$\frac{1}{\sqrt{3}}$	$\frac{-\sqrt{5}}{2\sqrt{3}}$	$\frac{1}{2}$
^1D		$\frac{\sqrt{3}}{2}$	$\frac{1}{2}$
^1S			1

Note: we have chosen $(P^4\ {}^1S|\}P^3\ {}^2P) = +1$ to agree with Smith[32] et al, where as Saraph[33] et al. choses the value -1.

I.I. Sobelman[34] has published c.f.p.'s at variance with the above. He has used the relation given by Racah[31] between the fractional parentages of the terms of an almost closed shell $\ell^{4\ell+2-n}$ and those of ℓ^{n+1} i.e.

$$(\ell^{4\ell+2-n}\ SL|\}\ell^{4\ell+1-n}\ S'L') = (-1)^{S+S'+L+L'-\ell-\frac{1}{2}} \left[\frac{(n+1)(2S'+1)(2L'+1)}{(4\ell+2-n)(2S+1)(2L+1)}\right]^{\frac{1}{2}} \times (\ell^{n+1}\ S'L'|\}\ell^n\ SL) \quad \ldots.(2.22)$$

However for $\ell^{2\ell+2}$ i.e. p^4 in the case we are considering, the above equation leads to difficulty and a change of sign may be necessary[31] which obviously was not taken into account. However we may use it for the configuration P^5 and we obtain

	^3P	^1D	^1S
^2P	$\sqrt{3/5}$	$1/\sqrt{3}$	$1/\sqrt{15}$

which agrees with ref. (33). For $(P^5\ {}^2P|\}P^4\ {}^1S)$ Smith[32] et al. used the value $-1/\sqrt{15}$ which is incorrect.

If we denote the antisymmetric wave function for $(q+1)$ electrons by $\Psi(P^{q+1}L_i S_i)$ and introduce the vector coupled function

$$\Psi(P^q L_j S_j\ P L_i S_i\ \underline{x}_q\ \underline{x}_{q+1}) = \sum (L_j\ M_{L_j}\ m_\ell | L_i M_{L_i})(S_j\ \tfrac{1}{2}\ M_{S_j}\ m_s | S_i M_{S_i}) \times \Psi(P^q L_j S_j M_{L_j} M_{S_j}\ \underline{X}_q)\ Y_1^{m_\ell}(\hat{r}_{q+1})\ \frac{P_{np}(r)}{r_{q+1}}\ \chi_{\frac{1}{2}}^{m_s}(\sigma_{q+1}) \quad \ldots.(2.23)$$

then

$$\Psi(P^{q+1}L_i S_i) = \sum_j (P^{q+1}L_i S_i|\}P^q L_j S_j)\ \Psi(P^q L_j S_j\ P L_i S_i) \quad \ldots.(2.24)$$

For our one-electron orbitals, $P_{n\ell}(r)$ we use the analytic SCF functions of Roothan and Kelly[35] or Clementi[36].

$$P_{n\ell}(r) = \sum_{i=1}^{M} C_i r^{I_i} e^{-Z_i r} \qquad \ldots.(2.25)$$

where M is the number of terms taken to represent an orbital. The functions are normalized such that

$$\int_0^\infty P_i(r) P_j(r) dr = \delta_{ij} \qquad \ldots.(2.26)$$

Reduction of the integrals

Considerable simplicfication of equation (1.39) is achieved if we impose the condition

$$\langle P_{np} | F_{ij} \rangle = 0 \quad \text{for } \ell_i = l \qquad \ldots.(2.27)$$

However, without this constraint F would contain a component of the bound p^q orbital. The unconstrained continuum orbital could then be written

$$\tilde{F} = F + \alpha P \;, \quad \langle F | P \rangle = 0 \qquad \ldots.(2.28)$$

Consequently we write

$$\Psi'(r_j \; \underline{x}_{N+1}) = \Psi(r_j \; \underline{x}_{N+1}) + c_j \Phi(1s \cdots np^{q+1} L S)$$

Substituting this Ψ' into equation (1.39) yields upon using equation (1.42) and the symmetry properties of the wave function we may write

$$I_{ij} = L^D_{ij} + L^E_{ij} + L^C + L^{C_2}$$

where we employ the notation of Smith Henry and Burke[32] except that we omit the subscripts which label the particular solution vector we are refering to since the equations are independent of the boundary conditions imposed upon them. We find

$$L^D_{ij} = \langle \Psi_u(r_i \; \underline{x}_N \, x_{N+1}) | H_{N+1} - E | \Psi_u(r_j \; \underline{x}_N \, x_{N+1}) \rangle$$
$$= \int dr_{N+1} F_i(r_{N+1}) \left[-\tfrac{1}{2}\left(\frac{d^2}{dr^2_{N+1}} - \frac{\ell_i(\ell_i+1)}{r^2_{N+1}} + \frac{2z}{r_{N+1}} + k_i^2\right)\delta_{ij} + V_{ij}(r_{N+1}) \right] F_j(r_{N+1}) \qquad \ldots.(2.29)$$

where

$$V^{(r)}_{ij} = \sum_{n'\ell'} 2(2\ell'+1) Y_0(P_{n'\ell'} P_{n'\ell'} r) + \delta_{S_i S_j} 3q \left[(2\ell_i+1)(2L_i+1)\right.$$
$$\left. \times (2\ell_j+1)(2L_j+1)\right]^{\frac{1}{2}} \sum \frac{1}{2\lambda+1} (\ell_i \ell_j 00 | \lambda 0)(1100 | \lambda 0)$$
$$\times W(\ell_i L_i \ell_j L_j : L\lambda) \sum_{L_2 S_2}^{\lambda} (-1)^{L+L_i+L_j+L_2} (p^q L_i S_i | \} L_2 S_2)$$
$$\times (p^q L_j S_j | \} L_2 S_2) W(1 L_i 1 L_j : L_2 \lambda) Y_\lambda(P_{np} P_{np} r) \qquad \ldots.(2.30)$$

We have used the fact that

$$H_{N+1} = H_N + H(x_{N+1}) + \sum_{\alpha=1}^{N} \frac{1}{r_{N+1,\alpha}}$$

$$H(x_{N+1}) = -\frac{1}{2}\nabla^2_{N+1} - \frac{Z}{r_{N+1}}$$

$$L^E_{ij} = \int dr_{N+1} F_i W_{ij} F_j = -N\langle \Psi_u(r_i \underline{x}_N x_{N+1}) | H_{N+1} - E | \Psi_u(r_j \underline{x}^{-N} \underline{x}_N)\rangle \quad \ldots.(2.31)$$

$$= -\delta_{ij} \sum_{\substack{n'l' \\ ((\alpha\beta\gamma\delta))}} \sum_{\lambda} R_\lambda(P_{n'l'} F_i F_j P_{n'l'}) \frac{(2l'+1)}{(2l_i+1)} (l'\lambda 00 | l_i 0)^2$$

$$- 3q\left[(2l_i+1)(2L_i+1)(2S_i+1)(2l_j+1)(2L_j+1)(2S_j+1)\right]^{\frac{1}{2}} \sum_{L_2 S_2} (p^q L_i S_i | \} p^{q-1} L_2 S_2)$$

$$(p^q L_j S_j | \} p^{q-1} L_j S_j) W(S_j \tfrac{1}{2} \tfrac{1}{2} S_i : S S_2) \sum_{\lambda} (l\, l_j 00 | \lambda 0) \frac{1}{2\lambda+1} (l_i 100 | \lambda 0)$$

$$\begin{Bmatrix} L_2 & 1 & L_j \\ \lambda & l_i & l_j \\ L_i & & L \end{Bmatrix} R_\lambda(P_{np} F_i F_j P_{np}) \quad \ldots.(2.32)$$

Equations (2.30) and (2.32) are exactly the same as equations (19) and (22) of Smith et al.[32]

We now wish to evaluate the terms linear in C. This has been incorrectly done by Smith et al[32]. These authors separated off a p-electron from $\Phi(1s^2 \cdots np^{q+1} LS)$ using the co-efficients of fractional parentage, which of course is only valid for equivalent electron. Consequently, the exchange interactions with the core electrons were not accounted for. We write

$$L^C = C_i \langle \Psi(r_i \underline{x}_{N+1}) | H_{N+1} - E | \Phi(1s^2 \cdots np^{q+1} LS)\rangle$$

$$+ C_j \langle \Phi(1s^2 \cdots np^{q+1} SL) | H_{N+1} - E | \Psi(r_j \underline{x}_{N+1})\rangle \quad \ldots.(2.33)$$

We take

$$\Phi(1s^2 2s^2 2p^{q+1} LS) \equiv |1s^2 2s^2 2p^{q+1} LS\rangle$$

$$= \frac{A_{N+1}}{\sqrt{2!\,2!\,(N+1)!\,(q+1)!}} \varphi(1s^2 | 12)\varphi(2s^2 | 34)\varphi(2p^{q+1} | 5 \cdots N{+}1\, LS) \quad \ldots.(2.34)$$

where A_{N+1} is a antisymmetrization operator. This function is normalized. We note that if $\phi(1 \to M)$ is a function antisymmetric in m variable and ϕ is already normalized, then

$$\frac{1}{\sqrt{M!\,m!}} A_M \phi(1 \to M)$$

is completely antisymmetric and normalized. Furthermore

$$\langle A_N \phi | \theta | A_N \psi \rangle = N! \langle \phi | \theta | A_N \psi \rangle \quad \ldots.(2.35)$$

provided that $[\theta, A_N] = 0$

We also write

$$\Psi(\Gamma_i \underline{x}_{N+1}) \equiv | \Gamma_i 1s^2 2s^2 2p^q (S_i L_i) \ell_i SL \rangle$$
$$= \frac{1}{\sqrt{N+1}} \sum_t (-1)^{N+1-t} \psi(\Gamma_i 1s^2 2s^2 2p^q (S_i L_i) \ell_i SL) \frac{F_i(r_t)}{r_t} \ldots (2.36a)$$

where

$$\psi(\Gamma_i 1s^2 2s^2 2p^q x_1 \cdots x_{N+1} - x_N \hat{x}_t (S_i L_i) \ell_i SL)$$
$$= \sum (L_i M_{L_i} \ell_i m_{\ell_i} | L M_L)(S_i M_{S_i} \tfrac{1}{2} m_s | S M_S) \frac{A_N}{\sqrt{2!\,2!\,N!\,q!}} \varphi(1s^2|12)\varphi(2s^2|34)$$
$$\times \varphi(2p^q | S \cdots N \hat{t} S_i L_i) Y_{\ell_i}^{m_{\ell_i}}(\hat{r}_t) \chi_{\frac{1}{2}}^{m_s}(\sigma_t) \quad \ldots.(2.36b)$$

We obtain, for the first matrix element in equation (2.33) since the right hand side is antisymmetric, upon interchanging t

$$\langle \Psi(\Gamma_i \underline{x}_{N+1}) | H_{N+1} - E | \Phi(1s^2 2s^2 2p^{q+1} LS) \rangle$$
$$= \frac{N+1\sqrt{q+1}}{\sqrt{N+1}\,2!\,2!\,\sqrt{N+1}\,N!\,(q+1)!} \langle A_N \varphi(1s^2|12)\varphi(2s^2|34)\psi(\Gamma_i 2p^q S \cdots N \hat{N+1}) \frac{F_i(r_{N+1})}{r_{N+1}}$$
$$| H_{N+1} - E | A_{N+1} \varphi(1s^2|12)\varphi(2s^2|34)\varphi(2p^{q+1}|S \cdots N+1\, LS) \rangle \quad \ldots.(2.36)$$

Using equation (2.31) we see that the integral over H_N and E will give integrals $\int F_i P_{n\ell}\, dr$ which we set equal to zero since we require the F's to be orthogonal to all bound orbitals.

Consider the matrix element of the 1-electron operator $H(x_{N+1})$ Since

$$[A_N, H(x_{N+1})] = 0$$

we can take it through the operator and operta on the function in the right hand side of the matrix element, which is already antisymmetric, so consequently it gives us a factor N!

Therefore the matrix element of the one-electron operator in equation (2.36) becomes

$$\frac{(q+1)^{\frac{1}{2}}}{2!\,2!\,(q+1)!}\left\langle \varphi(1s^2|12)\,\varphi(2s^2|34)\,\Psi(\Gamma;\,2p^q|5\cdots N\hat{N+1})\frac{F(r_{N+1})}{r_{N+1}}\right|\,H(x_{N+1})\,\Big|$$

$$\times\,\mathcal{A}_N\,\varphi(1s^2|12)\,\varphi(2s^2|34)\,\varphi(2p^{q+1}|5\cdots N+1\;LS)\Big\rangle \qquad \ldots.(2.37)$$

We cannot mix the p-electrons on the R.H.S. with 1s or 2s electrons, or the 1s with the 2s electrons as the orbitals are orthogonal. The φ's are already antisymmetric so A_{N+1} operating on the R.H.S. give a factor of $2!\,2!\,(q+1)!$. Using equation (2.24) we obtain

$$\left\langle \Psi(\Gamma;\,\underline{x}_{N+1})\,|H(x_{N+1})|\,\Phi(1s^2\,2s^2\,2p^{q+1}\,LS)\right\rangle$$

$$=\delta_{\ell;1}\,(2p^{q+1}LS|\{2p^q L_i S_i)\left\langle F\left|-\tfrac{1}{2}\left(\frac{d^2}{dr^2}+\frac{\ell(\ell+1)}{r^2}-\frac{2z}{r}\right)\right|P_{2p}\right\rangle \qquad \ldots.(2.38)$$

We consider now the matrix element of the 2-electron operator

$$\left\langle \Psi(\Gamma;\,\underline{x}_{N+1})\left|\sum_{\alpha}\frac{1}{r_{N+1,\alpha}}\right|\,\Phi(1s^2 2s^2\,2p^{q+1}\,LS)\right\rangle$$

$$=\frac{(q+1)^{\frac{1}{2}}}{2!\,2!\,N!\,(q+1)!}\left\langle A_N\,\varphi(1s^2|12)\,\varphi(2s^2|34)\,\Psi(\Gamma;\,2p^q|5\cdots N\hat{N+1})\frac{F(r_{N+1})}{r_{N+1}}\right.$$

$$\left|\sum_{\alpha=1}^{N}\frac{1}{r_{N+1,\alpha}}\right|\,A_{N+1}\,\varphi(1s^2|12)\,\varphi(2s^2|34)\,\varphi(2p^{q+1}|5\cdots N+1\;LS)\Big\rangle$$

$$\ldots.(2.39)$$

We have

$$\sum_{\alpha=1}^{N}\frac{1}{r_{N+1,\alpha}}=\sum_{\alpha=1}^{2}\frac{1}{r_{N+1,\alpha}}+\sum_{\alpha=3}^{4}\frac{1}{r_{N+1,\alpha}}+\sum_{\alpha=5}^{N}\frac{1}{r_{N+1,\alpha}} \qquad \ldots.(2.40)$$

We next consider the contribution of $\sum_{\alpha=5}^{N} \frac{1}{r_{N+1,\alpha}}$ to the matrix element. As before we get

$$\langle \Psi(\Gamma; \chi_{N+1}) | \sum_{\alpha=5}^{N} \frac{1}{r_{N+1,\alpha}} | \Phi(1s^2 2s^2 2p^{q+1} LS) \rangle$$

$$= \frac{(q+1)^{\frac{1}{2}}}{2!\,2!\,N!\,(q+1)!} \langle A_N \varphi(1s^2|12)\varphi(2s^2|34)\Psi(\Gamma; 2p^q 5\cdots N\hat{N+1}) \frac{F_i(r_{N+1})}{r_{N+1}} \Big| \sum_{\alpha=5}^{N} \frac{1}{r_{N+1,\alpha}} \Big| \cdots \quad (2.37)$$

$$\times A_{N+1} \varphi(1s^2|12)\varphi(2s^2|34)\varphi(2p^{q+1}|5\cdots N+1\, LS)\rangle$$

Since both sides of the matrix element are antisymmetric in co-ordinates 5 to N we can replace $\sum_{\alpha=5}^{N} \frac{1}{r_{N+1,\alpha}}$ by $\frac{q}{r_{q,q+1}}$ As before

$$A_N \longrightarrow N!$$

$$A_{N+1} \longrightarrow A_{(1,2)} \cdot A_{(3,4)} \cdot A_{(5,q+1)}$$

also

$$\longrightarrow 2! \cdot 2! \cdot (q+1)!$$

Consequently equation (2.37) becomes

$$(q+1)^{\frac{1}{2}} q \langle \Psi(\Gamma; 2p^q|5\cdots N\hat{N+1}) \frac{F_i(r_{N+1})}{r_{N+1}} | \frac{1}{r_{q,q+1}} | \varphi(2p^{q+1}|5\cdots N+1\, LS)\rangle$$

$$= (q+1)^{\frac{1}{2}} 3q \sum_{L'S'} \delta_{S'S_i} (p^{q+1} LS|\}p^q L'S') [3(2l_i+1)(2L'+1)(2L_i+1)]^{\frac{1}{2}}$$

$$\times \sum_{\lambda L_2 S_2} (-1)^{L_2+L+L'+L_i} (p^q L'S'|\}p^{q-1} L_2 S_2)(p^{q-1} L_2 S_2|\}p^{q-1} L_i S_i) \frac{1}{2\lambda+1} (1\,1\,0p|\lambda 0)$$

$$\times (1\,l;0\,0|\lambda 0) W(1L'l;L_i:L\lambda) W(1L'1L_i:L_2\lambda) R_\lambda(P_{2p} P_{2p} P_{1s} P_{2p}). \quad (2.38)$$

We now investigate the contribution of $\sum_{\alpha=1}^{2} \frac{1}{r_{N+1,\alpha}}$ to the matrix element. As before we obtain

$$\frac{(q+1)^{\frac{1}{2}}}{2!\,2!\,N!\,(q+1)!} \langle A_N \varphi(1s^2|12)\varphi(2s^2|34)\Psi(\Gamma; 2p^q|5\cdots N\hat{N+1}) \frac{F_i(r)}{r} \Big| \sum_{\alpha=1}^{2} \frac{1}{r_{N+1,\alpha}} \Big| A_{N+1} \varphi(1s^2|12) \cdots \quad (2.39)$$

$$\times \varphi(2s^2|34)\varphi(2p^{q+1}|5\cdots N+1\, LS)\rangle$$

As before when we let A_N operate on the R.H.S. of the matrix element we obtain a factor of N!. Also if we try to anti-symmetrize the R.H.S. with respect to particles 3 and 4 and 5 through N+1 we get a factor of $2!\cdot(q+1)!$ Since both sides

of the matrix element are antisymmetric in particles 1 and 2 the summation can be replaced by a factor of 2. Thus equation (2.39) becomes

$$(q+1)^{\frac{1}{2}} \langle \varphi(1s^2|12)\,\psi(r_i\, 2p^q|s\cdots N\,N+1)\,\Big|\,\frac{1}{r_{N+1,2}}\,\Big|\,A_{2,N+1}\,\varphi(1s^2|12)\times\varphi(2p^{q+1}|s\cdots N+1\,LS)\rangle$$

$$= (q+1)^{\frac{1}{2}}\,\delta_{\ell_i 1}\,(p^{q+1}LS|\}\,p^q L_i S_i)\Big\{2R_0(P_{1s}F_i P_{1s}P_{2p}) - \sum_{\lambda}\frac{1}{2\ell_i+1}(0\lambda 00|\ell_i 0)\,R_\lambda(P_{1s}F_i P_{2p}P_{1s})\Big\} \quad \ldots.(2.40)$$

There will also be a similiar contribution from the 2s electrons and in general the contribution from the core will be

$$\sum_{n'\ell'=\text{closed}}\Big\{2(2\ell'+1)R_0(P_{n'\ell'}F_i P_{n\ell'}P_{np}) - \sum_{\lambda}\frac{2\ell'+1}{2\ell_i+1}\times R_\lambda(P_{n'\ell'}F_i P_{np}P_{n'\ell'})\Big\}$$

Therefore the term linear in C becomes

$$L^C = \sum_i C_i \int V_i F_i\, dr$$

where

$$V_i(r) = (q+1)^{\frac{1}{2}}\Big\{\delta_{\ell_i 1}(p^{q+1}LS|\}\,L_iS_i)\Big[\Big(-\tfrac{1}{2}\frac{d^2}{dr^2}+\frac{l}{r}-\frac{Z}{r}\Big)P_{np}(r) + \sum_{n'\ell'=\text{closed}}2(2\ell'+1)Y_0(P_{n'\ell'}P_{n'\ell'}r)\,P_{np}(r) - \sum_{\lambda}\frac{2\ell'+1}{2\ell_i+1}(\ell'\lambda 00|\ell_i 0)$$

$$\times Y_\lambda(P_{n'\ell'}P_{np}r)\,P_{n'\ell'}(r)\Big] + 39\sum_{L'S'}\delta_{S'S_i}(p^{q+1}LS|\}L'S')\Big[3(2\ell_i+1)$$

$$\times(2L'+1)(2L_i+1)\Big]^{\frac{1}{2}}\sum_{\lambda L_2 S_2}(-1)^{L_2+L+L'+L_i}(p^q L'S'|\}\,L_2S_2)(p^q L_iS_i|\,L_2S_2)$$

$$\times\frac{1}{2\lambda+1}(1100|\lambda 0)(1\ell_i 00|\lambda 0)\,W(1L'\ell_i L_i:L\lambda)\,W(1L'1L_i:L_2\lambda)$$

$$\times Y_\lambda(P_{np}P_{np}r)\,P_{np}(r) \quad \ldots.(2.41)$$

This is the expression given by Smith, Conneely and Morgan[37] and differs from equation (24) of Smith et al[32] in as much as

the above includes terms which arise from exchange with the core. These terms are absent in reference (32) since $\Phi(1 \cdots N+1\, LS)$ was not properly antisymmetrized. We now have to evaluate the term guadratic in C

$$L^{c^2} = c_i c_j \langle \Phi(1s^2 \cdots np^{q+1} LS | H_{N+1} - E | \Phi(1s^2 \cdots np^{q+1} LS) \rangle$$
$$= c_i c_j (E_{N+1} - E) \qquad \ldots.(2.43)$$

where E_{N+1} is the energy of the $1s^2 \cdots np^{q+1}\, LS$ configuration evaluated with the wave functions of the np^q configuration.

The Hamiltonian may be broken up into single particle operators and 2-particle operators since

$$H_{N+1} = \sum_{i=1}^{N+1} H(i) + \sum_{i<j}^{N+1} \frac{1}{r_{ij}} \qquad \ldots.(2.44)$$

The single particle operators give a contribution

$$-\frac{1}{2} \sum_{n_\lambda \ell_\lambda = \text{closed}} 2(2\ell_\lambda+1) \int_0^\infty P_{n_\lambda \ell_\lambda} \left(\frac{d^2}{dr^2} - \frac{\ell_\lambda(\ell_\lambda+1)}{r^2} + \frac{2Z}{r} \right) P_{n_\lambda \ell_\lambda} dr$$
$$- \frac{1}{2}(q+1) \int P_{n\ell} \left(\frac{d^2}{dr^2} - \frac{2}{r^2} + \frac{2Z}{r} \right) P_{n\ell}\, dr \qquad \ldots.(2.45)$$

The matrix element of the electrostatic interaction between groups of inequivalent electrons may be evaluated by the methods of de Shalit and Thalmi[38].

(a) The elctrons in each closed subshell will give a contribution

$$(2\ell'+1)^2 \left[2R_0(n'\ell'4) - \sum_\lambda (-1)^\lambda \frac{1}{2\lambda+1} (\ell'\ell'00|\lambda 0)^2 R_\lambda(n'\ell'4) \right. \qquad (2.46a)$$

(b) From each pair of closed subshells there will be a contribution

$$2(2\ell+1)(2\ell'+1)\left[2R_0(n\ell\, n'\ell'\, n\ell\, n'\ell') - \sum_\lambda (-1)^{\ell+\ell'+\lambda} \frac{1}{2\lambda+1} (\ell\, \ell' 0 0 | \lambda 0)^2 \times R_\lambda(n\ell\, n'\ell'\, n'\ell'\, n\ell)\right] \quad \ldots.(2.46b)$$

(c) From the $n\ell^{q+1}$ open shell there will be a contribution

$$(q+1)(2\ell'+1)\left[2R_0(n\ell\, n'\ell'\, n\ell\, n'\ell') - \sum_\lambda (-1)^{\ell+\ell'+\lambda} \frac{1}{2\lambda+1} (\ell\, \ell' 0 0 | \lambda 0)^2 R_\lambda(n\ell\, n'\ell'\, n'\ell'\, n\ell)\right] \quad \ldots.(2.46C)$$

for each $n'\ell'$ closed subshell. <u>This is independent of the total angular momenta of the open shell.</u>

(d) From the np^{q+1} open subshell we will have the contribution

$$\mathcal{E} = \langle np^{q+1} LS | \sum \frac{1}{r_{ij}} | np^{q+1} LS \rangle$$

$$= \frac{q(q+1)}{2} \langle np^{q+1} LS | \frac{1}{r_{q,q+1}} | np^{q+1} LS \rangle$$

since

$$|np^{q+1} LS\rangle = \sum \langle p^{q+1} LS | \{ p^q L_i S_i)(p^q L_i S_i | \} p^{q-1} L_i' S_i') | np^{q-1}(L_i' S_i') p(L_i S_i) p LS \rangle$$

and

$$|np^{q-1}(L_i' S_i') p(L_i S_i) p LS\rangle = \sum_{L_2} (-1)^{L+L_i'} \sqrt{(2L_i+1)(2L_2+1)} \begin{Bmatrix} L_i' & 1 & L_i \\ 1 & L & L_2 \end{Bmatrix} \times |np^{q-1}(L_i' S_i') p p(L_2 S_2) LS\rangle$$

where we use the 6-j symbols[39] instead of Racah W-co-efficients since they are more symmetrical.

Consequently

$$\mathcal{E} = \frac{q(q+1)}{2} \sum_{\substack{L_i S_i L_j S_j \\ L_i' S_i' L_j' S_j' \\ L_2 L_2'}} \delta_{S_i S_j} \delta_{S_i' S_j'} \delta_{L_i L_j} \delta_{L_2 L_2'} (p^{q+1} LS | \{ p^q L_i S_i)(p^{q+1} LS | \} p^q L_j S_j)$$

$$\times (p^q L_j S_j | \{ p^{q-1} L_j' S_j') \sqrt{(2L_i+1)(2L_2+1)(2L_j+1)(2L_2'+1)} \begin{Bmatrix} L_i' & 1 & L_i \\ 1 & L & L_2 \end{Bmatrix}$$

$$\times \begin{Bmatrix} L_j' & 1 & L_j \\ 1 & L & L_2 \end{Bmatrix} (-1)^{L_i+L_j} \langle p^{q-1}(L_i' S_i') p p(L_2 S_2) LS | \frac{1}{r_{q,q+1}} | p^{q-1}(L_j' S_j') p p(L_2' S_2) LS \rangle$$

We note that

$$\langle p^{q-1}(L_i' S_i')\, p\, p\,(L_2 S_2)\, LS \left| \frac{1}{r_{q,q+1}} \right| p^{q-1}(L_i' S_i')\, p\, p\,(L_2 S_2)\, LS \rangle$$

$$= \sum_{\lambda} (-1)^{L_2} \begin{pmatrix} 1 & 1 & \lambda \\ 0 & 0 & 0 \end{pmatrix} \begin{pmatrix} 1 & 1 & \lambda \\ 0 & 0 & 0 \end{pmatrix} \frac{q}{2\lambda+1} \begin{Bmatrix} 1 & 1 & \lambda \\ 1 & 1 & L_2 \end{Bmatrix} R_\lambda(np^4)$$

where $\lambda = 0$ or 2.

Therefore

$$\xi = \frac{q(q+1)}{2} \sum_{\substack{L_i L_j S_i \\ L_i' S_i' L_2 \lambda}} (p^{q+1} LS \| p^q L_i S_i)(p^{q+1} LS \| p^q L_j S_j)(p^q L_i S_i \| p^{q-1} L_i' S_i')$$

$$\times (p^q L_j S_j \| p^{q-1} L_i' S_i') \sqrt{(2L_i+1)(2L_j+1)} \begin{Bmatrix} L_i' & 1 & L_i \\ 1 & L & L_2 \end{Bmatrix} \begin{Bmatrix} L_j' & 1 & L_j \\ 1 & L & L_2 \end{Bmatrix}$$

$$\times \begin{Bmatrix} 1 & 1 & \lambda \\ 1 & 1 & L_2 \end{Bmatrix} \begin{pmatrix} 1 & 1 & \lambda \\ 0 & 0 & 0 \end{pmatrix} \begin{pmatrix} 1 & 1 & \lambda \\ 0 & 0 & 0 \end{pmatrix} \frac{q}{2\lambda+1} (-1)^{L_2} (2L_2+1)\, R_\lambda(np^4).$$

We now use the Biedenharn-Elliott sum rule

$$\sum_{L_2} (2L_2+1)(-1)^{L_2} \begin{Bmatrix} L_i' & 1 & L_i \\ 1 & L & L_2 \end{Bmatrix} \begin{Bmatrix} L_j' & 1 & L_j \\ 1 & L & L_2 \end{Bmatrix} \begin{Bmatrix} 1 & 1 & \lambda \\ 1 & 1 & L_2 \end{Bmatrix}$$

$$= (-1)^{L+L_i+L_j+L_i'} \begin{Bmatrix} L_j & L_i' & 1 \\ \lambda & L_i & L \end{Bmatrix} \begin{Bmatrix} L_i & L_j & \lambda \\ 1 & 1 & L \end{Bmatrix}$$

So finally we obtain

$$\xi = \frac{q(q+1)}{2} \sum_{L_i L_j L' S_i S' \lambda} (p^{q+1} LS \| p^q L_i S_i)(p^{q+1} LS \| p^q L_j S_j)$$

$$\times (p^q L_i S_i \| p^{q-1} L' S')(p^q L_j S_j \| p^{q-1} L' S') \sqrt{(2L_i+1)(2L_j+1)} \begin{Bmatrix} L_i & L_j & \lambda \\ 1 & 1 & L \end{Bmatrix}$$

$$\times \begin{Bmatrix} L_j & L' & 1 \\ \lambda & L_i & 1 \end{Bmatrix} \frac{q}{2\lambda+1} (-1)^{L+L_i+L_j+L'} \begin{pmatrix} 1 & 1 & \lambda \\ 0 & 0 & 0 \end{pmatrix} \begin{pmatrix} 1 & 1 & \lambda \\ 0 & 0 & 0 \end{pmatrix} R_\lambda(np^4) \quad \ldots\ (2.46d)$$

Equations (2.46 a,b,c,d) give us E_{N+1}. The above expressions are equivalent to that given by reference (37), but differs substantially form that given by Smith et al[32]. Furthermore the expression

$$E = \tfrac{1}{2} k_1^2 + E_N(S_1 L_1) \quad , \quad E_N = \langle 1s^2 \cdots np^q L_1 S_1 | H_N | 1s^2 \cdots np^q L_1 S_1 \rangle \quad (2.47)$$

is calculated using the same methods, where Kl^2 is the energy of the incident electron in Rydbergs and S_1L_1 are the quantum numbers of the lowest term of the target ion.

In order to obtain better agreement with experiment for the positions of the levels of a Rydberg series converging on one of the excited terms we use the experimentally determined $E_N(S_iL_i)$, or theoretical values given by references (35) and (36).

However these value should not be used in equation (2.47) since they are inconsistent with our method of calculating E_{N+1}.

Derivation of the Radial Equations

Application of the Kohn variational principle (equation (1.47) yields, after analysis equivalent to that of reference (32), the equations satisfied by the radial equations F_{ij} where the subscript j refers to the j^{th} solution of the vector function F.

$$\sum_j \mathcal{L}_{ij} F_{jk}(r) + \frac{V_i}{E-E_{N+1}} \sum_j \int V_j(r') F_{jk}(r') dr' + \sum_\lambda m_\lambda^i P_{n_\lambda \ell_\lambda} \quad \ldots.(2.48)$$

where

$$\mathcal{L}_{ij} = -\frac{1}{2}\left[\frac{d^2}{dr^2} - \frac{\ell_i(\ell_i+1)}{r^2} + \frac{2Z}{r} + k_i^2\right]\delta_{ij} + V_{ij} + W_{ij}$$

The direct potential V_{ij} is defined by equation (2.30) and the integral operator W_{ij} by equation (2.32). The m_λ^i

are unknown Lagrange multipliers as we require the radial functions F_{ij} for s-waves to be orthogonal to the 1s 2s and 3s subshells, and for $\ell_i = 1$ to be orthogonal to the $\bar{2}p$ and np subshells. The numerical solution of these equations is discussed in Chapter 4.

Results

The results for the cross sections for electron scattering by carbon, nitrogen and oxygen have been discussed by Smith, Conneely and Morgan[37]. Henry et al[40] have pointed out that the peaks in elastic cross sections in the results for carbon and nitrogen are due to a low energy shape resonance which is supported essentailly by the angular momentum barrier term which corresponds to $\ell=1$. This feature is absent for the corresponding $(3p)^q$ cases i.e. for silicon and phosphorus. The reason for this is that the effective potential that our electron with angular momentum equal to unity incident on phosphorus sees, cannot support a bound state. In Figure 1 we plot the effective potential V_{11}' against 'r' for carbon and phosphrous.

$$V_{11}' = \frac{\ell(\ell+1)}{r^2} - \frac{2Z}{r} + 2.V_{11}$$

where V_{11} is given by equation (2.30).

In Table I we present the partial wave contributions to the excitation cross sections $Q(n,n')$ for O^+, N^+ and O^{++}. We have used the theoretical values[35] for the energy differences between the terms. Henry et al[40] have used experimental energy differences for the terms and furhtermore have used the Hartree-Fock energy for the lowest term (i.e. equation 2.47) which we

have pointed out to be inconsistent. We note that the dominant contributions to the cross sections come from the p-waves. This is not the case for $(3p)^q$ ions.

We have tabulated the partial wave contributions to the excitation cross sections for P^+, S^+ and Cl^+ as well as the total collision strengths in Tables 2,3, and 4. In this case the most important contributions to the cross sections come from the d-waves. For these ions we have used the experimental energy differences between the terms. Table 5 gives a comparsion of collision strengths for various ions between the present results and other calculations. We see that the agreement between the various calculations is poorer for the $(3p)^q$ system than for the $(2p)^q$ system where excellent agreement was obtained[37]. This may be due to the large number exchange terms, which we have treated exactly, i.e. for a particular set of coupled equations there may be as many as 33 distinct exchange terms, all of which we have taken into account. We have calculated the collision strength well above all thresholds as near threshold our method of fitting our solutions to the asymptotic form of Burke and Schey breaksdown. Below the highest term of course our model will predict an infinite number of resonances. In figure 2 we present the $^3D^0$ partial wave contribution to the $^4S-^2D$ transition in S^+ which shows a number of thses resonance profiles.

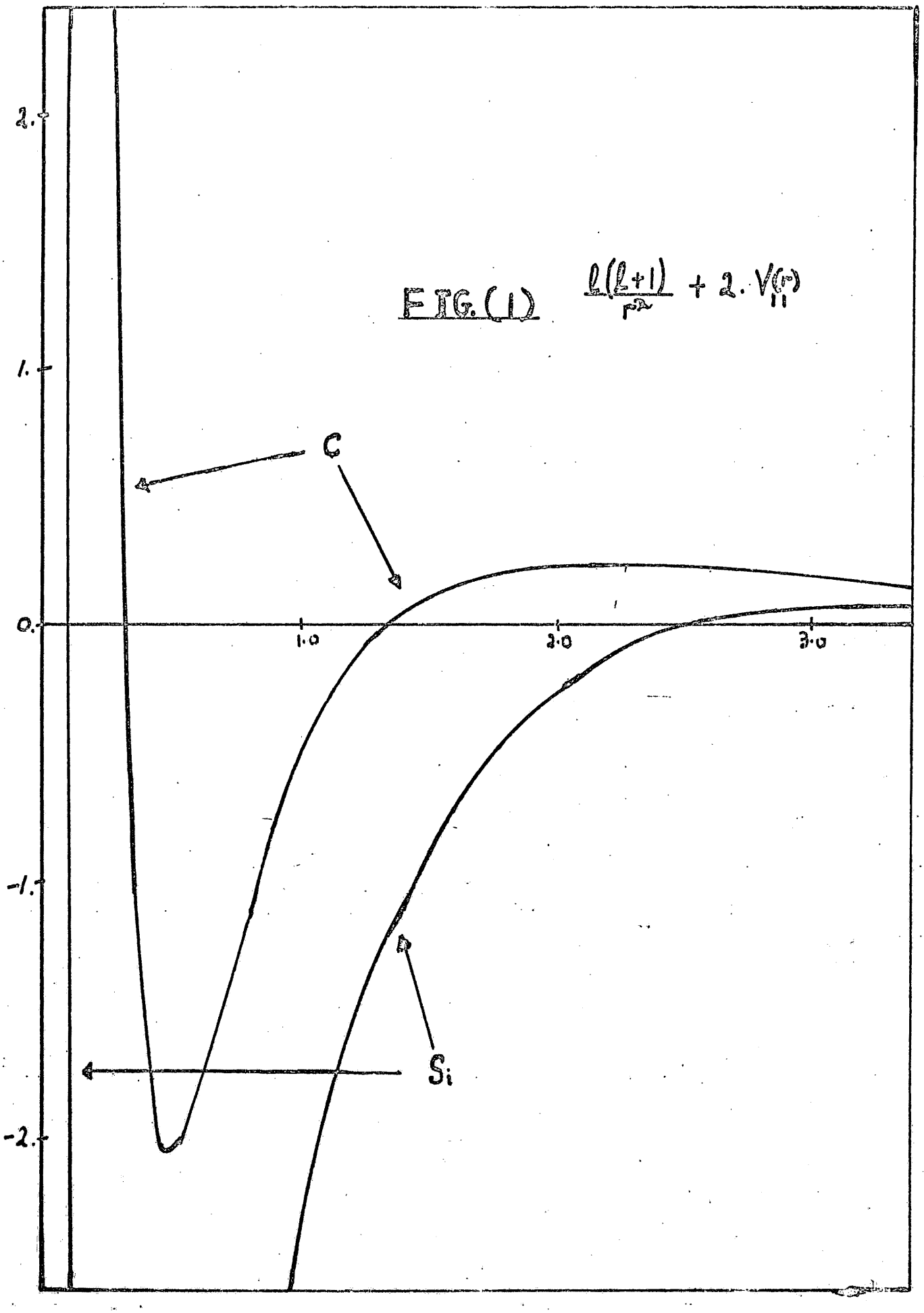

FIG. (1) $\frac{l(l+1)}{r^2} + 2.V_{11}(r)$

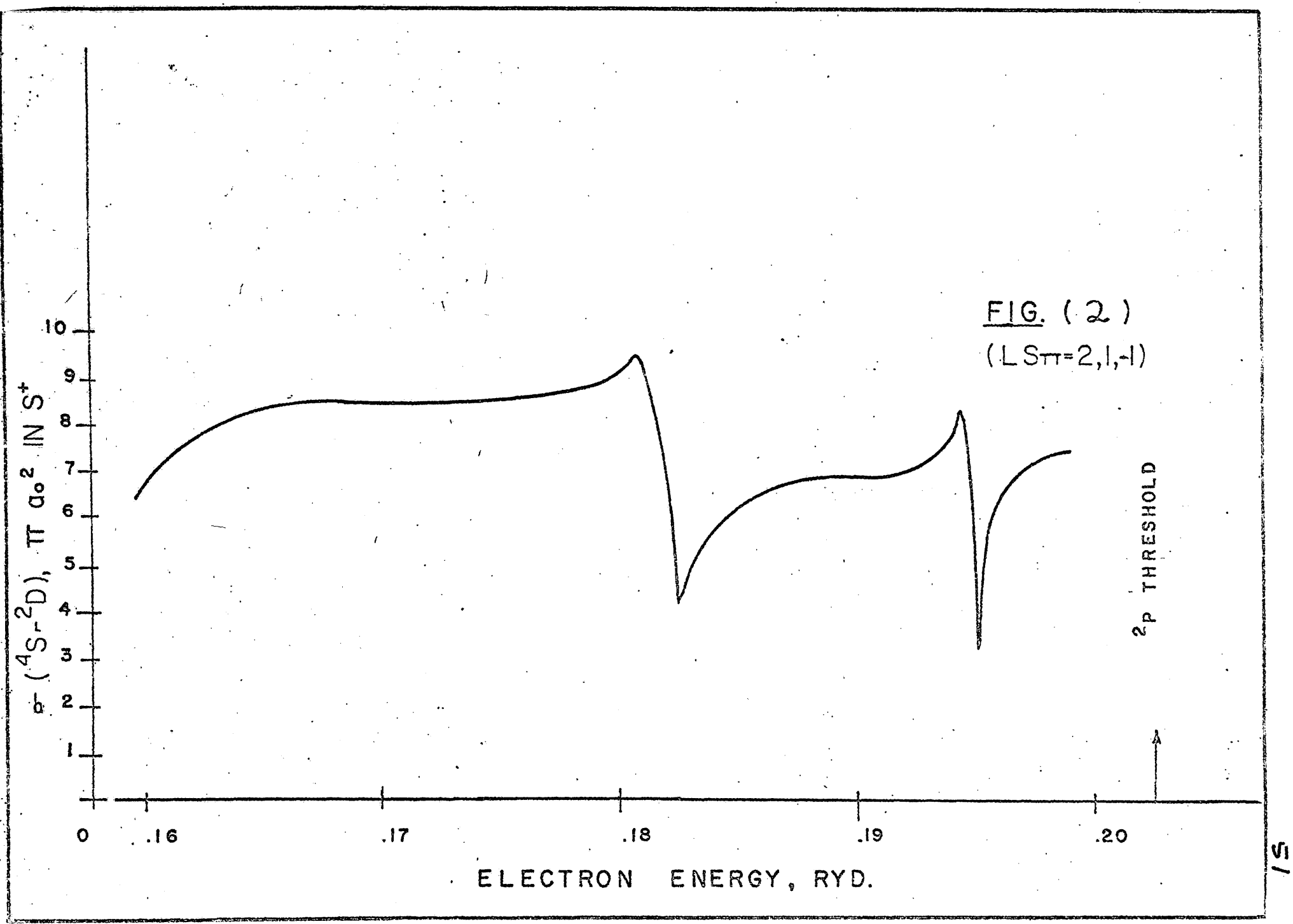
FIG. (2)
(LSπ=2,1,-1)
σ (4S-2D), π a0² IN S+
10
9
8
7
6
5
4
3
2
1
0
.16
.17
.18
.19
.20
2P THRESHOLD
ELECTRON ENERGY, RYD.

TABLE I

Partial wave contribution to the excitation cross sections for N^+, O^{++} and O^+

Ion	K_3^2	$LS\pi$	$Q(^3p, ^1D)$	$Q(^1D, ^3P)$
N^+	.2	$^2P^e$	.01735	.04285
		$^2P^o$	.16525	.40782
		$^2D^e$	.00322	.00795
		$^2D^o$	.32403	.80006
		$^2F^e$	.10370	.25591
		$^2F^o$	.00043	.00106
		Total	.61398	1.51563
			$Q(^3P-^1S)$	$Q(^1S-^3P)$
		$^2P^o$	.06617	1.77379
		$^2D^e$	.01358	.36440
		$^2F^o$	.00002	.00058
		Total	.07977	2.13877
			$Q(^1D, ^1S)$	$Q(^1S-^1D)$
		$^2S^e$	.04074	.44254
		$^2P^o$	.04076	.44276
		$^2D^e$	.08325	.90431
		$^2F^o$	.03210	.34867
		Total	.19685	2.13826
			$Q(^3P, ^1D)$	$Q(^1D, ^3P)$

TABLE I

(continued)

O^{++}	.2	$^2P^e$	.02061	.05230
		$^2P^o$	.08902	.22594
		$^2D^e$	.00312	.00792
		$^2D^o$	.16582	.42090
		$^2F^e$	.12068	.30632
		$^2F^0$	.00039	.00100
		Total	.39964	1.01438
			$Q(^3P, ^1S)$	$Q(^1S, ^3P)$
		$^2P^o$	.03443	1.09661
		$^2D^e$	.02346	.74729
		$^2F^o$	.00005	.00167
		Total	.05794	1.84557
			$Q(^1D, ^1S)$	$Q(^1S, ^1D)$
		$^2S^e$	.02269	.28468
		$^2P^o$	.01647	.20667
		$^2D^e$	.04969	.62348
		$^2F^o$	.02813	.35295
		Total	.11698	1.46778
O^+	.2		$Q(^4S, ^2D)$	$Q(^2D, ^4S)$
		$^3S^o$	.00090	.00062
		$^3P^e$	.50721	.34830

TABLE I

(continued)

$^3D^o$	.07185	.04967
$^3F^e$	.00060	.00042
Total	.58056	.39901
	$Q(^4S, ^2P)$	$Q(^2P, ^4S)$
$^3P^e$	.17406	.38354
$^3D^o$	.02518	.05550
$^3F^e$	.00002	.00005
Total	.19928	.43910
	$Q(^2D, ^2P)$	$Q(^2P, ^2D)$
$^1P^e$	.03507	.11179
$^1P^o$	.03564	.11359
$^3P^e$	.03135	.09993
$^3P^o$	.08057	.25684
$^1D^e$	.09199	.29323
$^1D^o$	.03211	.10236
$^3D^e$	.06041	.19286
$^3D^o$	.03711	.11829
$^1F^e$	.00328	.10147
$^1F^o$	.00401	.01280
$^3F^e$	.00925	.02946
$^3F^o$	.07723	.24618
Total	.49386	1.57421

TABLE I

(continued)

Collision Strengths, $\Omega(n,n^1)$

	N^+	O^{++}	O^+
$\Omega(1,2)$	3.29286	2.54556	1.53510
$\Omega(2,1)$	3.29285	2.54553	1.53623
$\Omega(1,3)$	.42768	.36906	.52692
$\Omega(3,1)$	.42775	.36911	.52692
$\Omega(2,3)$	.42767	.29355	1.90538
$\Omega(3,2)$	.42765	.29355	1.90540

TABLE II

Partial wave contributions to the excitation cross sections of P^+

$Q(n,n^1)$	$LS\pi/k^2$	.3	.4	.6	.8	1.0
$^3P\text{-}^1D$	$^2P^e$	.979	.406	.209	.112	.063
	$^2P^o$	.272	.195	.117	.077	.053
	$^2D^e$	.125	.089	.054	.035	.023
	$^2D^o$	.468	.332	.195	.127	.088
	$^2F^e$	2.192	1.594	.950	.588	.358
	$^2F^o$	.002	.002	.002	.001	.001
	$^2G^o$	.014	.018	.025	.028	.030
	Total	4.052	2.636	1.552	.969	.616
$^3P\text{-}^1S$	$^2P^o$	.092	.065	.038	.024	.016
	$^2D^e$	.650	.501	.302	.181	.105
	$^2F^o$	.001	.002	.003	.004	.004
	Total	.743	.568	.343	.209	.125
$^1D\text{-}^1S$	$^2S^e$	.162	.078	.021	.005	.001
	$^2P^o$	.229	.154	.093	.066	.051
	$^2D^e$	.423	.227	.107	.073	.059
	$^2F^o$	.374	.301	.218	.168	.134
	$^2G^e$	.130	.117	.101	.090	.081
	Total	1.318	.877	.540	.402	.326

TABLE II

(continued)

$\Omega(1,2)$	10.940	9.490	8.381	6.977	5.544
$\Omega(1,3)$	2.006	2.045	1.852	1.505	1.125
$\Omega(2,3)$	1.444	1.399	1.401	1.445	1.498

TABLE III

Partial wave contributions to the excitation cross section for S^+

$Q(n,n^1)$	$LS\pi/k^2$	.3	.4	.6	.8	1.0
$^4S-^2D$	$^3S^o$	.035	.022	.007	.001	.000
	$^3P^e$	.934	.690	.434	.300	.218
	$^3D^o$	3.986	2.805	1.694	1.154	.807
	$^3F^e$	.008	.012	.019	.025	.031
	Total	4.963	3.529	2.154	1.480	1.056
$^4S-^2P$	$^3P^e$	.286	.212	.133	.091	.065
	$^3D^o$	1.557	1.384	1.025	.733	.506
	$^3F^e$	.001	.003	.005	.008	.010
	Total	1.844	1.599	1.163	.832	.581
$^2D-^2P$	$^1P^o$	.320	.172	.079	.051	.038
	$^1P^e$	.189	.113	.061	.040	.030
	$^3P^o$	.456	.201	.056	.019	.010
	$^3P^e$	.119	.073	.041	.029	.022
	$^1D^o$	.983	.583	.299	.187	.125
	$^1D^e$	.201	.139	.088	.063	.049
	$^3D^o$	.604	.376	.182	.096	.051
	$^3D^e$	.512	.345	.216	.157	.122

TABLE III

(continued)

$^1F^o$	.153	.189	.197	.163	.120
$^1F^e$	.045	.039	.032	.029	.026
$^3F^o$	2.144	1.029	.406	.232	.160
$^3F^e$	.119	.093	.072	.059	.050
Total	5.854	3.325	1.729	1.125	.802
$\Omega(1,2)$	5.956	5.646	5.169	4.736	4.224
$\Omega(1,3)$	2.213	2.558	2.791	2.662	2.324
$\Omega(2,3)$	9.623	8.861	8.031	7.474	6.932

TABLE IV

Partial wave contributions to the excitation cross sections for Cl^+

$Q(n\ n^1)$	$LS\pi/k^2$	.3	.4	.6	.8	1.0
$^3P\text{-}^1D$	$^2P^e$	1.015	.771	.507	.359	.257
	$^2P^o$	.468	.350	.225	.359	.117
	$^2D^e$	1.097	.814	.529	.384	.289
	$^2D^o$	.008	.007	.007	.008	.009
	$^2F^o$	.002	.002	.003	.004	.004
	Total	2.590	1.945	1.271	.912	.675
$^3P\text{-}^1S$	$^2P^o$	.022	.013	.005	.003	.002
	$^2D^e$	.345	.276	.186	.134	.099
	$^2F^o$	.000	.000	.001	.001	.001
	Total	.367	.289	.192	.138	.102
$^1D\text{-}^1S$	$^2S^e$	.173	.113	.064	.045	.039
	$^2P^o$	.458	.280	.145	.092	.064
	$^2D^e$	1.156	.703	.316	.167	.096
	$^2F^o$	.157	.134	.107	.092	.080
	$^2H^o$	.015	.019	.019	.018	.017
	Total	2.005	1.295	.693	.453	.332
	$\Omega(1,2)$	6.993	7.002	6.863	6.566	6.075
	$\Omega(1,3)$	.991	1.040	1.036	.994	.918
	$\Omega(2,3)$	1.942	1.902	1.711	1.571	1.484

TABLE V

Comparison of collision strengths

(n,n^1) for $(3P)^q$ ions

ION	n	n^1	Present *	Ref (43)	Ref (44) **	Ref (45)
P^+	1	2	10.94	6.31		
	1	3	2.01	1.12		
	2	3	1.44	1.11		
S^+	1	2	5.96		3.06	2.02
	1	3	2.21		1.28	0.38
	2	3	9.62		6.22	12.7
Cl^{++}	1	2	3.372		3.189	
	1	3	1.847		1.967	
	2	3	5.743		6.63	
Ar^{+++}	1	2	1.008		1.432	
	1	3	0.326		0.645	
	2	3	3.651		4.920	

*k_1^2= .3 except for Cl^{++} and A^{+++} where it equals .5 and 1.0 respectively

**k_3^2+ .0005 in these calculations.

Photo-ionization

We now wish to use the continuum wave functions defined by equation (2.48) to calculate photoionization cross sections. The derivation we give is essentially that of Henry and Lipsky[41].

We consider a photon of energy $h\nu$ impinging on a target system of N electrons and Z nuclear charge with quantum number L_o, M_o, S_o, μ_o and energy E_o described by the wave function $\Phi_{L_o S_o M_{L_o} M_{S_o}}(1, \cdots N)$. If $h\nu$ is greater than the lowest ionization potential of the target, ionization can take place and the final states can be described by wave functions ${}^{\Gamma}\Psi_{LSM_L M_S}(1, \cdots N+1)$ where

$$\Gamma = \{ L_\Gamma S_\Gamma \ell_\Gamma \tfrac{1}{2} \}$$

stands for the channel of the emitted electron. The cross section in the dipole velocity form is[42]

$$\sigma_V = \frac{2\pi e^2 \hbar^2}{m^2 c \nu \omega} \sum_{\substack{M M \\ M_S M_{L_o} M_{S_o}}} \left| \left\langle \Phi_{L_o S_o M_{L_o} M_{S_o}}(1, \cdots N) \left| \sum_{i=1}^{N} \nabla_i^m \right| {}^{\Gamma}\Psi_{LSM_L M_S}(1, \cdots N) \right\rangle \right|^2 \quad \ldots . (2.49)$$

where

$$\omega = 2(2L_o+1)(2S_o+1)$$

is the statiscal weight since we assume the target is unpolarized.

$$\nabla_i^{\pm 1} = -\frac{1}{\sqrt{2}} \left(\frac{\partial}{\partial x_i} \pm i \frac{\partial}{\partial y_i} \right), \quad \nabla_i^{0} = \frac{\partial}{\partial z_i}$$

${}^{\Gamma}\Psi_{LSM_L M_S}$ represents an outgoing spherical wave in channel Γ plus incoming spherical waves in all channels, normalized per unit energy range. This condition will be met if we take ${}^{\Gamma}\Psi_{LSM M_S}$ to be of the form

$$\lim {}^{\Gamma}\Psi_{LSM M_S} = (2\pi k_\Gamma)^{-\frac{1}{2}} \phi(\Gamma\, \underline{x}_{N-1}\, \hat{x}_N) \frac{e^{i\theta_\Gamma}}{r_N}$$

$$- \sum_{\Gamma'} S^{+}_{\Gamma\Gamma'} (2\pi k_{\Gamma'})^{-\frac{1}{2}} \phi(\Gamma'\, \underline{x}_{N-1}\, \hat{x}_N) \frac{e^{-i\theta_\Gamma}}{r_N}$$

where

$$\phi(\Gamma\, \underline{x}_{N-1}\, \hat{x}_N) = \sum (L_\Gamma \ell_\Gamma M_{L_\Gamma} m | L M_L)(S_\Gamma \tfrac{1}{2} M_S m_s | S M_S) \times \Phi(L_\Gamma S_\Gamma\, \underline{x}_{N-1}) Y^{m}_{\ell_\Gamma}(\hat{r}_N)\, \sigma^{m_s}_{\frac{1}{2}}(N) \quad \ldots.(2.50)$$

Here k_Γ is the wave number of the electron ejected in the Γth channel and is related to the incident frequency and the Γth ionization potential I_Γ by the Einstein relation

$$\frac{1}{2m} \hbar^2 k_\Gamma^2 = h\nu - I_\Gamma \quad \ldots.(2.51)$$

Application of the commutation relation

$$[\underline{r}\,, H] = \frac{i\hbar}{m} \underline{p} \quad \ldots.(2.52)$$

to equation (2.49) yields the dipole length form of the cross section

$$ {}^{\Gamma}\sigma_L = \frac{8\pi^3 \nu e^2}{c\omega} \sum_{\substack{M m \\ M_S M_0 M_{S_0}}} \left| \left\langle \Phi^{(1 \ldots N)}_{L_0 S_0 M_0 M_{S_0}} \middle| \sum r_i Y^{m_i}_1(\hat{r}_i) \middle| {}^{\Gamma}\Psi^{(1 \ldots N)}_{LSMM_S} \right\rangle \right|^2 \quad \ldots.(2.53)$$

The total cross section will be

$$\sigma_{tot} = \sum_{\Gamma}^{\text{open}} {}^{\Gamma}\sigma_V = \sum_{\Gamma}^{\text{open}} {}^{\Gamma}\sigma_L \quad \ldots.(2.54)$$

Consequently we are interested in evaluating the matrix element

$$P_\Gamma = \frac{1}{(2L_0+1)(2S_0+1)} \sum_{\substack{m M \\ M_S M_0 M_{S_0}}} \left| \left\langle \Phi^{(1 \ldots N)}_{L_0 S_0 M_0 M_{S_0}} \middle| \theta^m_1 \middle| {}^{\Gamma}\Psi^{(1 \ldots N)}_{LSMM_S} \right\rangle \right|^2$$

where

$$\theta^m_1 = \sum_{i=1}^{N} \nabla_i^m \quad \text{or} \quad \theta^m_1 = \sum_{i=1}^{N} r_i Y^m_1(\theta_i, \phi_i) \quad \ldots.(2.55)$$

If ${}^{\Gamma}\phi_{LSMM_S}$ denotes the close coupling wave functions with the boundary conditions given by equations (1.30) then

$$ {}^{\Gamma}\Psi_{LS} = \sum_{\Gamma'} (1 + iR)^{-1}_{\Gamma\Gamma'} {}^{\Gamma}\phi_{LS} $$

will have the asymptotic behaviour of equation (2.50). Thus

$$ P^{\Gamma} = \frac{1}{(2L_0+1)(2S_0+1)} \sum_{m M \Gamma'\Gamma''} \langle \Phi_0 | \theta_1^m | {}^{\Gamma''}\phi \rangle (1 - iR)^{-1}_{\Gamma\Gamma''} $$

$$ \times (1 + iR)^{-1}_{\Gamma\Gamma'} \langle {}^{\Gamma'}\phi | \theta_1^m | \Phi_0 \rangle^{M_S M_0 M_{S_0}} \quad \ldots.(2.56) $$

Since

$$ (1 \pm iR)^{-1}_{\Gamma\Gamma''} = (1+R^2)^{-1}_{\Gamma\Gamma''} \mp i\,(R/(1+R^2))_{\Gamma\Gamma''} $$

and

$$ (1 - iR)^{-1}_{\Gamma\Gamma''} (1+iR)_{\Gamma\Gamma'} = (1+R^2)^{-1}_{\Gamma\Gamma''} (1+R^2)^{-1}_{\Gamma\Gamma'} $$

$$ + (R(1+R^2)^{-1})_{\Gamma\Gamma'} (R(1+R^2)^{-1})_{\Gamma\Gamma''} + i\left[(1+R^2)^{-1}_{\Gamma\Gamma''}\right. $$

$$ \left. \times (R(1+R^2)^{-1})_{\Gamma\Gamma'} - (1+R^2)_{\Gamma\Gamma'} R(1+R^2)^{-1}_{\Gamma\Gamma''}\right] $$

$$ \ldots.(2.57) $$

Since we have

$$ \sum_{\Gamma'\Gamma''} (1+R^2)^{-1}_{\Gamma\Gamma'} (R(1+R^2)^{-1})_{\Gamma\Gamma''} f_{\Gamma'\Gamma''} = \sum_{\Gamma''\Gamma'} (1+R^2)^{-1}_{\Gamma\Gamma''} (R(1+R^2)^{-1})_{\Gamma\Gamma'} \times f_{\Gamma''\Gamma'} $$

and since

$$ f_{\Gamma'\Gamma''} = f_{\Gamma''\Gamma'} $$

then the two imaginary sums over Γ' and Γ'' cancel each other.

So we define the 3-script matrix

$$ A^{\Gamma}_{\Gamma'\Gamma''} = A^{\Gamma}_{\Gamma''\Gamma'} = (1+R^2)^{-1}_{\Gamma\Gamma''} (1+R^2)^{-1}_{\Gamma\Gamma'} + (R(1+R^2)^{-1})_{\Gamma\Gamma'} $$

$$ \times (R(1+R^2)^{-1})_{\Gamma\Gamma''} \quad \ldots.(2.57) $$

Therefore

$$ P^{\Gamma} = \frac{1}{(2L_0+1)(2S_0+1)} \sum_{m M M_0} \langle \Phi^{M_0 M_{S_0}}_{L_0 S_0} | \theta_1^m | {}^{\Gamma'}\phi^{M M_S}_{LS} \rangle A^{\Gamma}_{\Gamma'\Gamma''} $$

$$ \times \langle {}^{\Gamma''}\phi^{M M_S}_{LS} | \theta_1^m | \Phi^{M_0 M_{S_0}}_{L_0 S_0} \rangle^{M_S M_{S_0} \Gamma'\Gamma''} \quad \ldots.(2.58) $$

where

$$\Gamma\Phi_{LS}^{MM_S} = \frac{1}{\sqrt{N}}\left(1 - P_{1,N} \cdots P_{N-1,N}\right) \sum_{\Gamma'} \varphi_{LS}^{MM_S}(1 \cdots N-1 \mid \hat{N})\, F_{\Gamma'\Gamma}(r_N) \qquad \ldots.(2.59)$$

and

$$P_{ij}\, f(i,j) = f(j,i)$$

$F_{\Gamma'\Gamma}(r_N)$ is the $F_{ij}(r_N)/r_N$ of the previous section and

$$\Gamma\varphi_{LS}^{MM_S} = \sum_{M_\Gamma \mu_\Gamma} \varphi_{L_\Gamma S_\Gamma}^{M_\Gamma \mu_\Gamma}(1 \cdots N-1)\, Y_{\ell_\Gamma}^{M-\mu_\Gamma}(N)\, \chi_{\frac{1}{2}}^{M_S-\mu_\Gamma}(N)\, (L_\Gamma \ell_\Gamma M_\Gamma m_{\ell_\Gamma} \mid LM) \times (S_\Gamma \tfrac{1}{2} \mu_\Gamma M_S - \mu_\Gamma \mid S M_S) \qquad \ldots.(2.60)$$

The radial functions used in Φ_0 are different from those used in $\varphi_{L_\Gamma S_\Gamma}$ and will be designated by primes when a distinction must be made. We may note

$$\varphi_{L_\Gamma S_\Gamma}^{M_\Gamma \mu_\Gamma}(1 \cdots N-1) = \frac{A_{N-1}}{\sqrt{2!\,2!\,(N-1)!\,(q-1)!}}\, \varphi(1s^2 \mid 12)\, \varphi(2s^2 \mid 34) \times \varphi_{L_\Gamma S_\Gamma}^{M_\Gamma \mu_\Gamma}(2p^q \mid 5 \cdots N-1)$$

$$\Phi_{L_0 S_0}^{M_0 M_{S_0}}(1s^2 2s^2 2p^q) = \frac{A_N}{\sqrt{2!\,2!\,N!\,q!}}\, \varphi'(1s^2 \mid 12)\, \varphi'(2s^2 \mid 34) \times \varphi_{L_0 S_0}^{M_0 M_{S_0}}(2p^q \mid 5 \cdots N) \qquad \ldots.(2.61)$$

Thus

$$\Gamma\Phi_{LS}^{MM_S} = \sum_{\Gamma' M_{\Gamma'} \mu_{\Gamma'}} \frac{A_N}{\sqrt{2!\,2!\,(N-1)!\,(q-1)!}}\, \varphi(1s^2 \mid 12)\, \varphi(2s^2 \mid 34) \times \Phi_{L_{\Gamma'} S_{\Gamma'}}^{M_{\Gamma'} \mu_{\Gamma'}}(2p^{q-1} \mid 5 \cdots N-1)\, Y_{\ell_{\Gamma'}}^{M-M_{\Gamma'}}(N)\, \chi_{\frac{1}{2}}^{M_S-\mu_{\Gamma'}}(N)\, F_{\Gamma'\Gamma}(N) \times (L_{\Gamma'} \ell_{\Gamma'} M_{\Gamma'} M - M_{\Gamma'} \mid LM)(S_{\Gamma'} \tfrac{1}{2} \mu_{\Gamma'} M_S - \mu_{\Gamma'} \mid S M_S) \qquad \ldots.(2.62)$$

where we again have the antisymmetrization operator A_N of equation (2.35).

We want to evaluate matrix elements of the form

$$\xi = \langle \Phi^{M_0 M_{S_0}}_{L_0 S_0} | \theta_i^m | {}^r\Phi^{M M_S}_{LS} \rangle$$

$$= \sum_{r' M_{r'} \mu_{r'}} \frac{\sqrt{q}}{2!\,2!\,N!\,q!} (L_{r'} \ell_{r'} M_{r'} M - M_{r'} | L M)$$

$$\times (S_{r'} \tfrac{1}{2} \mu_{r'} M_S - \mu_{r'} | S M_S)\, A_N \varphi'(1s^2|12)\, \varphi'(2s'|3,4)$$

$$\times \Phi^{M_0 M_{S_0}}_{L_0 S_0}(2p^q | S \cdots N) \Big| \sum_{i=1}^{N} \theta_i^m(i) \Big| A_N \Phi(1s^2|12)\, \varphi(2s^2|34)$$

$$\times \varphi^{M_{r'} \mu_{r'}}_{L_{r'} S_{r'}}(2p^{q-1} | S \cdots N)\, Y^{M - \mu_{r'}}_{\ell_{r'}}(N)\, \chi^{M_S - \mu_{r'}}_{\frac{1}{2}}(N)\, F_{r' r}(N) ! \ldots \quad (2.63)$$

This is a sum over permutations of products of one electron integrals of the form

$$\langle n' \ell' \tfrac{1}{2} m_{\ell'} m_{s'} | n \ell \tfrac{1}{2} m_\ell m_s \rangle = \langle n' \ell' | n \ell \rangle \delta_{\ell \ell'} \delta_{m m'} \delta_{m_s m_{s'}} \quad \ldots . (2.64a)$$

and one of the type

$$\langle n' \ell' \tfrac{1}{2} m_{\ell'} m_{s'} | \theta_i^m | n \ell \tfrac{1}{2} m_\ell m_s \rangle = \delta_{m_s m_{s'}} \delta_{m_{\ell'}, m + m_\ell} \left(\frac{2\ell'+1}{2\ell+1} \right)^{\frac{1}{2}}$$

$$\times (\ell' 1 m_{\ell'} m_\ell - m_{\ell'} | \ell m_\ell)(\ell' 1 0 0 | \ell 0) \langle n' \ell' | \rho_{\ell' \ell} | n \ell \rangle \quad \ldots . (2.64b)$$

where

$$\rho_{\ell' \ell} = \frac{d}{dr} + \frac{1 - (\ell' - \ell)(2\ell+1)}{2r}$$ for

the gradient operator and

$$\rho = \sqrt{\frac{4\pi}{3}}\, r$$

for the dipole operator. The Clebsh-Gordon coefficient, $(\ell' 1 0 0 | \ell 0)$ is zero unless

$$\ell' = \ell \pm 1$$

which is the usual one electron selection rule for dipole radiation. This means that an S-electron can only couple to a

p-electron and a p-electron can only couple to an s- or a d-electron. If an s-electron from the L.H.S. of equation (2.63) couples to a p-electron on the R.H.S. there will only be three s- electrons remaining on the L.H.S., whereas there will be at least four s- electrons on the R.H.S. Such terms will vanish because they contain inner products between Y_0 's and Y_1 's . Only a p-electron from the L.H.S. can couple to the R.H.S. through the dipole operator. It can be coupled to the outgoing electron provided that

$$\ell_{r'} = 0 \quad \text{or} \quad 2$$

and it can be coupled to one of the s-electrons if $\ell_{r'} = 0$ for them there will be four uncoupled s- electrons on each side of equation (2.63). Using the facts and the properties of the antisymmetrization operator A_N and also noting that both sides are completely antisymmetric in co-ordinates S through N we obtain

$$\xi = \frac{\sqrt{9}}{2!2!} \langle 2p' | 2p \rangle \sum_{r' M_{r'} \mu_{r'}}^{9-1} (L_{r'} \ell_{r'} M_{r'} M - M_{r'} | L M)$$

$$\times (S_{r'} \tfrac{1}{2} \mu_{r'} M_S - \mu_{r'} | S M_S)(p^9 L_0 S_0 | \} p^{9-1} L_{r'} S_{r'})(L_{r'} | M_{r'} M_0 - M_{r'} | L_0 M_0)$$

$$\times (S_{r'} \tfrac{1}{2} \mu_{r'} M_{S_0} - \mu_{r'} | S_0 M_{S_0}) \varphi'(1s^2 | 12) \varphi'(2s' | 34) Y_1^{M_0 - M_{r'}}(5) \chi_{\frac{1}{2}}^{M_{S_0} - \mu_{r'}}(5)$$

$$\times R'_{2p}(5) | \theta_1^m(5) | A_5 \varphi(1s^2 | 12) \varphi(2s^2 | 34) Y_{\ell_{r'}}^{M - M_{r'}}(5) \chi_{\frac{1}{2}}^{M_S - \mu_{r'}}(5) F_{r',r}(5)$$

.... (2.65)

But

$$A_5 = (1 - P_{15} \cdots - P_{45}) A_4$$
$$= A_4 (1 - P_{15} \cdots - P_{45})$$

and

$$[A_4 , \theta_1^m(5)] = 0$$

The integral in equation (2.65) may be written

$$\langle A_4\, \varphi'(1s^2|1,2)\,\varphi'(2s^2|3,4)\,Y_{l}^{M_0-M_{\rho'}}(5)\,\chi_{\frac{1}{2}}^{M_{s_0}-\mu_{\rho'}}(5)\,R'_{2p}(5)\,|\,\theta_1^m(5)\,|$$

$$\times\,\varphi(1s^2|1,2)\,\varphi(2s^2|3,4)\,Y_{l_{\rho'}}^{M-M_{\rho'}}(5)\,\chi_{\frac{1}{2}}^{M_s-\mu_{\rho'}}(5)\,F_{\rho'\rho}(5)$$

$$-\,(P_{15}+P_{25})\,\varphi(1s^2|1,2)\,\varphi(2s^2|3,4)\,Y_{l_{\rho'}}^{M-M_{\rho'}}(5)\,\chi_{\frac{1}{2}}^{M_s-\mu_{\rho'}}(5)\,F_{\rho'\rho}(5)$$

$$-\,(P_{35}+P_{45})\,\varphi(1s^2|1,2)\,\varphi(2s^2|3,4)\,Y_{l_{\rho'}}^{M-M_{\rho'}}(5)\,\chi_{\frac{1}{2}}^{M_s-\mu_{\rho'}}(5)\,F_{\rho'\rho}(5)\rangle$$

.... (2.66)

using equation (2.64) and the fact that

$$\varphi(1s^2|1,2) = R_{1s}(1)\,R_{1s}(2)\,C(\tfrac{1}{2}\,\tfrac{1}{2}\,M\;-\mu|00)\,\chi_{\frac{1}{2}}^{M}(1)\,\chi_{\frac{1}{2}}^{-\mu}(2)\,Y_0^0(1)\,Y_0^0(2)$$

we see that equation (2.66) may be written as

$$4\,(1s'2s'|1s2s)^2\,\delta_{m\,M_0-M}\,\delta_{M_{s_0}M_s}\left(\frac{3}{2l_{\rho'}+1}\right)^{\frac{1}{2}}C(1100|l_{\rho'}0)$$

$$\times\,C(1\,M_0-M_{\rho'}\;M-M_0\,|\,l_{\rho'}\,M-M_{\rho'})\left\{\langle 2p'|\,\rho_1\,\ell_{\rho'}\,|\,F_{\rho'\rho}\rangle - \delta_{0\,l_{\rho'}}\right.$$

$$\left.\times\left[\frac{\langle 1s\,2s\,|F_{\rho'\rho}\,2s\rangle}{\langle 1s'2s'|1s\,2s\rangle}\langle 2p'|\,\rho_{10}\,|1s\rangle + \frac{\langle 1s'2s'|1sF_{\rho'\rho}\rangle}{\langle 1s'2s'|1s\,2s\rangle}\langle 2p|\rho_{10}|2s\rangle\right]\right\}$$

Therefore

$$\xi = \sqrt{9}\,\langle 1s'2s'|1s2s\rangle^2\,\langle 2p'|2p\rangle^{9-1}\,\delta_{m\,M_0-M}\,\delta_{M_{s_0}M_s}\sum_{\rho'}\left(\frac{3}{2l_{\rho'}+1}\right)^{\frac{1}{2}}$$

$$\times\,f_{\rho\rho'}\sum_{M_{\rho'}\mu_{\rho'}}(1\;1\;M_0-M_\rho\;M-M_0\,|\,l_{\rho'}0)(L_{\rho'}\,l_{\rho'}\,M_{\rho'}\,M-M_{\rho'}|LM)$$

$$\times\,(L_{\rho'}\,1\,M_{\rho'}\;M_0-M_{\rho'}|L_0M_0)(S_{\rho'}\,\tfrac{1}{2}\,\mu_{\rho'}\,M_{s_0}-\mu_{\rho'}|S_0M_{s_0})(S_{\rho'}\,\tfrac{1}{2}\,\mu_{\rho'}\,M_s-M_{\rho'}|SM_s)$$

.... (2.67)

where

$$f_{\rho'\rho} = (p^9L_0S_0|\}p^{9-1}L_{\rho'}S_{\rho'})(1100|l_{\rho'}0)\left\{\langle 2p'|\,\rho_1\,\ell_{\rho'}\,|\,F_{\rho'\rho}\rangle\right.$$

$$\left.-\,\delta_{0\,l_\rho}\left[\frac{\langle 1s'2s'|\,F_{\rho'\rho}\,2s\rangle}{\langle 1s'2s'|1s\,2s\rangle}\langle 2p'|\,\rho_{10}\,|1s\rangle + \frac{\langle 1s'2s'|1sF_{\rho'\rho}\rangle}{\langle 1s'2s'|1s\,2s\rangle}\langle 2p'|\rho_{10}|2s\rangle\right]\right\}$$

.... (2.68)

But

$$\sum_{\mu_{r'}} (S_{r'}\tfrac{1}{2}\,\mu_{r'}\,M_{s_0}-\mu_r \mid S_0 M_{s_0})(S_{r'}\tfrac{1}{2}\,\mu_{r'}\,M_s-\mu_{r'}\mid S M_s)\,\delta_{M_s M_{s_0}} = \delta_{M_s M_{s_0}}\,\delta_{S S_0}$$

and also

$$\sum_{M_{r'}} (l\,l\,M_0-M_{r'}\,M-M_0 \mid \ell_{r'}\,M-M_r)(L_{r'}\,\ell_{r'}\,M_{r'}\,M-M_{r'}\mid L M) \times (L_{r'}\,l\,M_{r'}\,M_0-M_{r'}\mid L_0\,M_0)$$

$$= (-1)^{M_0-L}\left[\frac{(2L+1)(2\ell_{r'}+1)(2L_0+1)}{3}\right]^{\frac{1}{2}} W(L L_{r'} l l : \ell_{r'} L_0) \times (L\,L_0\,-M\,M_0 \mid l\,M_0-M) \qquad \ldots.(2.69)$$

so

$$\xi = \sqrt{9}\,\langle 1s'2s' \mid 1s\,2s\rangle^2 (2p'\mid 2p)^{9-1}\,\delta_{S_0 S}\,\delta_{M_s M_{s_0}}\left[(2L+1)(2L_0+1)\right]^{\frac{1}{2}} \times (-1)^{M_0-L}(L\,L_0\,-M\,M_0\mid 1\,0)\sum_{r'} f_{r'r}\,W(L L_{r'} l l\,\ell_r L_0) \qquad \ldots(2.70)$$

Substituting back into equation 2.58 we obtain

$$P^r = \frac{1}{(2L_0+1)(2S_0+1)}\,9\,\delta_{S S_0}\left[\langle 1s'2s'\mid 1s\,2s\rangle^2\langle 2p'\mid 2p\rangle^{9-1}\right]^2 \times (2L+1)(2L_0+1)\sum_{r'r''} g_{r'r}\,A^r_{r'r''}\,g_{r''r} \times \sum_{\substack{M_s M_{s_0}\\ M\,M_0}} \delta_{M_s M_{s_0}}\,(L\,L_0\,-M\,M_0\mid l\,M_0-M)^2 \qquad \ldots.(2.71)$$

where

$$g_{r'r} = f_{r'r}\,W(L L_{r'} l l : \ell_{r'} L_0)$$

But

$$\sum \delta_{M_s M_{s_0}}\,\delta_{S S_0} = (2S_0+1)\,\delta_{S S_0}\sum_m \delta_{m,M_0-M} = 1$$

and

$$\sum_{M M_0}(L\,L_0\,-M\,M_0\mid l\,M_0-M)^2 = 3\,\Delta(L\,l\,L_0)$$

where

$$\Delta(L|L_0) = \delta_{LL_0} + \delta_{L\,L_0+1} + \delta_{L\,L_0-1}$$
$$= 0$$

unless

$$|L-1| \leq L_0 \leq (L+1)$$

so the final expression for P^Γ is

$$P^\Gamma = 3\,\delta_{SS_0}\,\Delta(L|L_0)\,q\left[\langle 1s'2s'|1s\,2s\rangle^2\langle 2p'|2p\rangle^{q-1}\right]^2 \times (2L+1)\sum_{\Gamma'\Gamma''} g_{\Gamma'} A^{\Gamma}_{\Gamma'\Gamma''} g_{\Gamma''} \quad \ldots.(2.72a)$$

with

$$g_\Gamma = \sum_{\Gamma'} (P^q L_0 S_0 | P^{q-1} L_{\Gamma'} S_{\Gamma'})\,(1\,1\,0\,0|\ell_{\Gamma'}0)\,W(L L_{\Gamma'} 1 1 : \ell_{\Gamma'} L_0) \times \left\{\langle 2p'|P_1 \ell_{\Gamma'}|F_{\Gamma'\Gamma}\rangle - \delta_{\ell_{\Gamma'}0}\left[\frac{\langle 1s'2s'|F_{\Gamma'\Gamma}\,2s\rangle}{\langle 1s'2s'|1s\,2s\rangle} \times \langle 2p'|P_{10}|1s\rangle + \frac{\langle 1s'2s'|1sF_{\Gamma'\Gamma}\rangle}{\langle 1s'2s'|1s\,2s\rangle}\langle 2p'|P_{10}|2s\rangle\right]\right\} \quad \ldots.(2.73a)$$

We now make some approximations to equation (2.73a). Since

$$\langle 1s'2s'|1s\,2s\rangle = \langle 1s'|1s\rangle\langle 2s'|2s\rangle - \langle 1s'|2s\rangle\langle 2s'|1s\rangle$$

we can neglect the second term in the above expansion since the overlap of the 1S' and 2S' radial functions of the atom with the 2S and 1S of the ion will be negligible. Also noting that the first term inside the square brackets in equation (2.73a) will have a similar factor we may write

$$g_\Gamma = \sum_{\Gamma'} (P^q L_0 S_0 | P^{q-1} L_{\Gamma'} S_{\Gamma'})\,(1\,1\,0\,0|\ell_{\Gamma'}0)\,W(L L_{\Gamma'} 1 1 : \ell_{\Gamma'} L_0) \times \left\{\langle 2p'|P_1 \ell_{\Gamma'}|F_{\Gamma'\Gamma}\rangle - \delta_{\ell_{\Gamma'}0}\langle 2s'|F_{\Gamma'\Gamma}\rangle \times \langle 2p'|P_{10}|2s\rangle\right\} \quad \ldots.(2.73b)$$

The effect of the last term in equation (2.73b), called the s-wave core relaxation term by Henry and Lipsky[41] is very small. For example we find that the photoionization cross section of nitrogen at K^2_f=.3 Rydberg equals 11.98 and 12.18 megabarn when we exclude and include the s-wave term. In view of this we have not antisymmetrized with respect to the 1s,2s, and 2p subshells in our treatment of the $(3p)^q$ configuration. For this case we write the s-wave core relaxation term as

$$\delta_{l',0} \langle 3s' | F_{l'l} \rangle \langle 3p' | P_{10} | 3s \rangle \quad \ldots\ldots (2.73c)$$

The factor containing overlap integrals of the atomic wave functions and those of the residual ion in equation (2.72) become in the $(3p)^q$ case

$$\left[\langle 3s' | 3s \rangle^2 \langle 3p' | 3p \rangle^{q-1} \right]^2 \quad \ldots\ldots (2.72b)$$

Chapter 3

In this chapter we present calculations of photoionization cross sections using equations (2.27) and (2.73) for various atoms and ions of the $(2p)^q$ and $(3p)^q$ configuration. In all previous calculations of these systems, except that of Henry[47] for atomic nitrogen, it has been assumed that the coupling between final state channels is negligible. As we have seen in Chapter I it is this coupling that give use to structures in the photoionization cross sections. Since these line shapes have been the subject of considerable theoretical and experimental investigation in recent years it is interesting to compare the line shapes predicted from perturbation theory, c.f. equation (1.76), with our ab initio calculations. We notice from the tables and graphs in this chapter that the photoionization cross sections in the dipole length and dipole velocity approximations do not agree and that the agreement is worse for the $(3p)^q$ system than the $(2p)^q$. The two approximations should agree exactly if our wave functions for the initial and final state were eigenfunctions of the same Hamiltonian-which they are not. The wave function for the initial state is obtained from a Hartree-Fock calculation and the final state wave function of course is obtained from Kohn's variational principle i.e. equation (1.47).

NI

There are three terms in this configuration i.e. $^4S, ^2D$ and ^2P. For $N(^4S)$ we consider only the transitions

$$h\nu + N(^4S) \longrightarrow [N^+(^3P) + \epsilon s]\ ^4P$$
$$h\nu + N(^4S) \longrightarrow [N^+(^3P) + \epsilon d]\ ^4P \qquad \ldots(3.1)$$

We note that both channels are open so we do not get any structure in the cross section

In Figure 3 our results are compared to the experimental results of Comes and Elzer[48,49]. Our present calculations do not reflect the resonant structure that is evident in the experimental results because we have not coupled together the ^3P and ^4S states of the ion. A Rydberg series of levels has been observed by Carrol[50] in the region 694-612°A and the have attributed the series to transitions from the ground $^4S^o$ state of the nitrogen atom to the Rydberg terms $2s(2p)^3(^5S^o)np\ ^4P$

We now consider photoionization of the $^2P^o$ term. In order to obtain the total cross section for this term we need the contributions from three partial waves ($^2S^e$, $^2P^e$, $^2D^e$).

In Figure 4 we show the contribution of the $^2S^e$ partial wave.

$$h\nu + N(^2P) \rightarrow {}^2S \rightarrow \begin{matrix} N^+(^1D) + \epsilon d \\ N^+(^1S) + \epsilon s \end{matrix} \quad \ldots.(3.2)$$

If we decoupled these two channels we would get the usual Rydberg series converging on the ^1S threshold. With coupling these states show up as resonances corresponding to excited states of the atom $(1s^2)(2s^2)(2p)^2(^1S)ns\ ^2S$. These states have a very short life time as they decay into the adjacent continuum. From equation (1.75) we see that at the resonant energy the cross section takes the form

$$\sigma = \sigma_a \frac{(q+\epsilon)^2}{1+\epsilon^2} \qquad \epsilon = \frac{E - E_r}{\Gamma/2} \qquad \ldots(3.3)$$

The cross section has a zero minimum at $q=\epsilon$ as is evident from the graph. Of course experimenters measure photo transmission and do not see this zero as they only see the total cross

section.

The excess transition probability due to the discreet state is simply

$$f = \int_{-\infty}^{\infty} \sigma_a \left[\frac{(q+\epsilon)^2}{1+\epsilon^2} - 1 \right] dE$$

$$= \frac{\Gamma}{2} \int_{-\infty}^{\infty} \sigma_a \left[\frac{q^2 + 2q\epsilon - 1}{1+\epsilon^2} \right] d\epsilon$$

$$= \frac{\Gamma}{2} \int_{-\infty}^{\infty} \frac{q^2-1}{1+\epsilon^2} d\epsilon = \frac{\Gamma}{2} \pi \sigma_a (q^2-1) \quad \ldots.(3.4)$$

where we subtract of the background contribution and neglect $2q\epsilon$ as it is an odd function.

We now discuss the case

$$h\nu + N(^2P) \longrightarrow {}^2P \longrightarrow \begin{matrix} N^+(^3P) + \epsilon s + \epsilon d \\ N^+(^1D) + \epsilon d \end{matrix} \quad \ldots.(3.5)$$

For sufficiently low energy the third channel is closed and we have two continuum states and one discreet state. This gives rise to a series of resonances converging on the $N^+(^1D)$ threshold. The cross section now takes the form (c.f. equation (1.76))

$$\sigma = \sigma_b + \sigma_a \left(\frac{(q+\epsilon)^2}{1+\epsilon^2} \right) \quad \ldots.(3.6)$$

This is because we can form linear combinations of the open channels such that the discreet state interacts with only one of them. The other then gives the background σ_b which is continuous. We see from Figure 5 that there is a big jump in the cross section at threshold where the ^1D channel opens up.

However if we average the oscillator strength of these transitions i.e. add the quantity $2f/(E_{n+1}-E_n)$ to the background cross section for each pair of resonances, we see that the total oscillator strength is a continuous function of energy. The dashed line in Figure 5 shows the 'smoothed out' cross section. The above remarks merely imply that our calculations are self-consistent.

The remaining partial wave we have to consider is $^2D^e$ (Figure 6).

$$h\nu + N(^2P) \longrightarrow {}^2D^e \longrightarrow \begin{cases} N^+(^3P) + \epsilon d \\ N^+(^1D) + \epsilon s \\ \quad + \epsilon d \\ \quad + \epsilon g \\ N^+(^1S) + \epsilon d \end{cases} \quad \ldots.(3.7)$$

We see that we have three Rydberg series of resonances converging on the ^1D state of N^+ and one series converging on the ^1S state. At energies below the ^1D threshold there are four series of discreet states superimposed on one continuum. Equation (3.6) does not apply in this case. Mies[29] gives the formula

$$\sigma = \sigma_b + \sigma_a\left(\sum \frac{\Gamma_n q_n}{2}/(E-E_n) + q\right), \quad q = \sum \frac{\Gamma_n}{2(E-E_n)} \quad \ldots.(3.8)$$

where the summation is over the number of interacting resonances. However we have used equation (3.6) in curve fitting our results to extract the quantities

We expect this formula to hold if the resonances are well

separated. The results are tabulated in Tables 6. We also have calculated the correlation co-efficient[27]

$$\rho^2 = \frac{\sigma_a}{\sigma_a + \sigma_l} \qquad \rho = \langle \psi_a | \psi_d \rangle \qquad \ldots.(3.9)$$

where ψ_a is the continuum state generated by autoionization and ψ_d is the continuum state generated by direct photon absorption from the ground state. Since the infinite sequences of resonances are due to the residual Coulcomb interactions in the final state their positions can be predicted to fit a Rydberg series

$$E_r = E_\infty - (n-d)^{-2} \qquad \ldots.(3.10)$$

where E_∞ is the series limit, d the quantum defect, and n the 'principle quantum number' of the autoionizing state. d is a slowly varying function of energy as can be seen from the tables.

The resonant phase shift can be parameterized in terms of E_r, Γ and the background phase shift δ_o (c.f. equation 162). The E_r and Γ that are extract from parameterizing the phase shift agree very well with those obtained by curve fitting our cross sections to equation (3.6). This provides another check on the consistency of our calculations.

Curve Fitting Procedure

We wish to minimize the quantity

$$\Delta = \sum_{i=1}^{N} \left\{ \sigma_i - \left[\sigma_a \frac{\left(q + \frac{E_i - E_r}{\Gamma/2}\right)^2}{1 + \left(\frac{E_i - E_r}{\Gamma/2}\right)^2} + \sigma_l \right] \right\}^2 \qquad \ldots.(3.11)$$

where σ_i is the cross section we calculate and E_i is the energy at which it is calculated. N is the number of points to which we wish to fit our formula for the cross section. We normally take N to be about 15 and we chose the E_i such that they well define the profile. We let

$$\gamma = (\Gamma/2)^2 + E_r$$
$$Q = 9\Gamma/2 - E_r$$

the equation

$$\sigma_i = \sigma_a \left(9 + \frac{E_i - E_r}{\Gamma/2}\right)^2 \Big/ \left\{1 + \left(\frac{E_i - E_r}{\Gamma/2}\right)^2\right\} + \sigma_b$$

becomes upon multiplying across by the denominator

$$\sigma_i E_i^2 + \sigma_i \gamma - 2E_i E_r - \sigma_a Q^2 - 2\sigma_a Q E_i - \sigma_a E_i^2 - \sigma_b \gamma - \sigma_b E_i^2 + 2\sigma_b E_i E_r$$

.....(3112)

We now make a further change of variables

$$x_1 = -\gamma \qquad x_4 = 2\sigma_a Q - 2\sigma_b E_r$$
$$x_2 = 2E_r \qquad x_5 = \sigma_a + \sigma_b$$
$$x_3 = \sigma_a Q^2 + \sigma_b \gamma$$

.....(3113)

In terms of these variables equation (3.11) becomes

$$\Delta = \sum (\sigma_i E_i^2 - \sigma_i x_1 - E_i x_2 - x_3 - E_i x_4 - E_i^2 x_5)^2$$

The extremum conditions

$$\frac{\partial \Delta}{\partial x_i} = 0 \qquad i = 1, 5$$

gives us the following matrix equation

$$\begin{bmatrix} \overline{\sigma^2} & \overline{E\sigma^2} & \overline{\sigma} & \overline{E\sigma} & \overline{E^2\sigma} \\ \overline{E\sigma^2} & \overline{E^2\sigma^2} & \overline{E\sigma} & \overline{E^2\sigma} & \overline{E^3\sigma} \\ \overline{\sigma} & \overline{E\sigma} & N & \overline{E} & \overline{E^2} \\ \overline{E\sigma} & \overline{E^2\sigma} & E & \overline{E^2} & \overline{E^3} \\ \overline{E^2\sigma} & \overline{E^3\sigma} & \overline{E^2} & \overline{E^3} & \overline{E^4} \end{bmatrix} \begin{bmatrix} x_1 \\ x_2 \\ x_3 \\ x_4 \\ x_5 \end{bmatrix} = \begin{bmatrix} \overline{E^2\sigma^2} \\ \overline{E^3\sigma^2} \\ \overline{E^2\sigma} \\ \overline{E^3\sigma} \\ \overline{E^4\sigma} \end{bmatrix}$$

.....(3.14)

where $\overline{\sigma^2} = \sum_{j=1}^{N} \sigma_j^2$ ... etc. . Equation (3.14) together with equation (3.13) gives us the parameters we require. We may improve on these first approximation parameters q_i^0 by making use of differentials.

We let

$$\sigma_i = \sigma(q_1^0 \cdots q_5^0) + \sum_j \frac{\partial \sigma}{\partial q_j} \Delta q_j \quad \ldots.(3.15)$$

where $q_1 = \sigma_a$; $q_2 = q$, $q_3 = E_r$, $q_4 = \Gamma$, $q_5 = \sigma_b$ and where the q_i^0 are obtained from equation (3.14). We now solve for the Δq_i. We have

$$\Delta = \sum_j \left\{\sigma_i - \left[\sigma(q_i^0) + \sum_{j=1}^{5} \frac{\partial \sigma}{\partial q_j} \Delta q_j\right]\right\}^2$$

$$\frac{\partial \Delta}{\partial \Delta q_K} = \sum_j \left(\sigma_i - \sigma(q_i^0) - \sum_{j=1}^{5} \frac{\partial \sigma}{\partial q_j} \Delta q_j\right) \frac{\partial \sigma}{\partial q_K} \quad \ldots.(3.16)$$

which gives us a system of linear equations for the Δq_i .

This method works very well in most cases i.e. we can obtain three place agreement between the calculated cross section and our parameterized cross section. The position E_Γ, and width Γ, of the resonance is also obtained by parameterizing the phase shift according to equation (1.60), and they agree very well with those given by the above method.

In figures 7, 8 and 9 we present the $^2P^e$, $^2D^e$ and $^2F^e$ partial wave contributions to the photoionization cross section of the ^2D state of nitrogen. The parameters for the resonances shown in these graphs are tabulated in Table 7. We note from figure 9

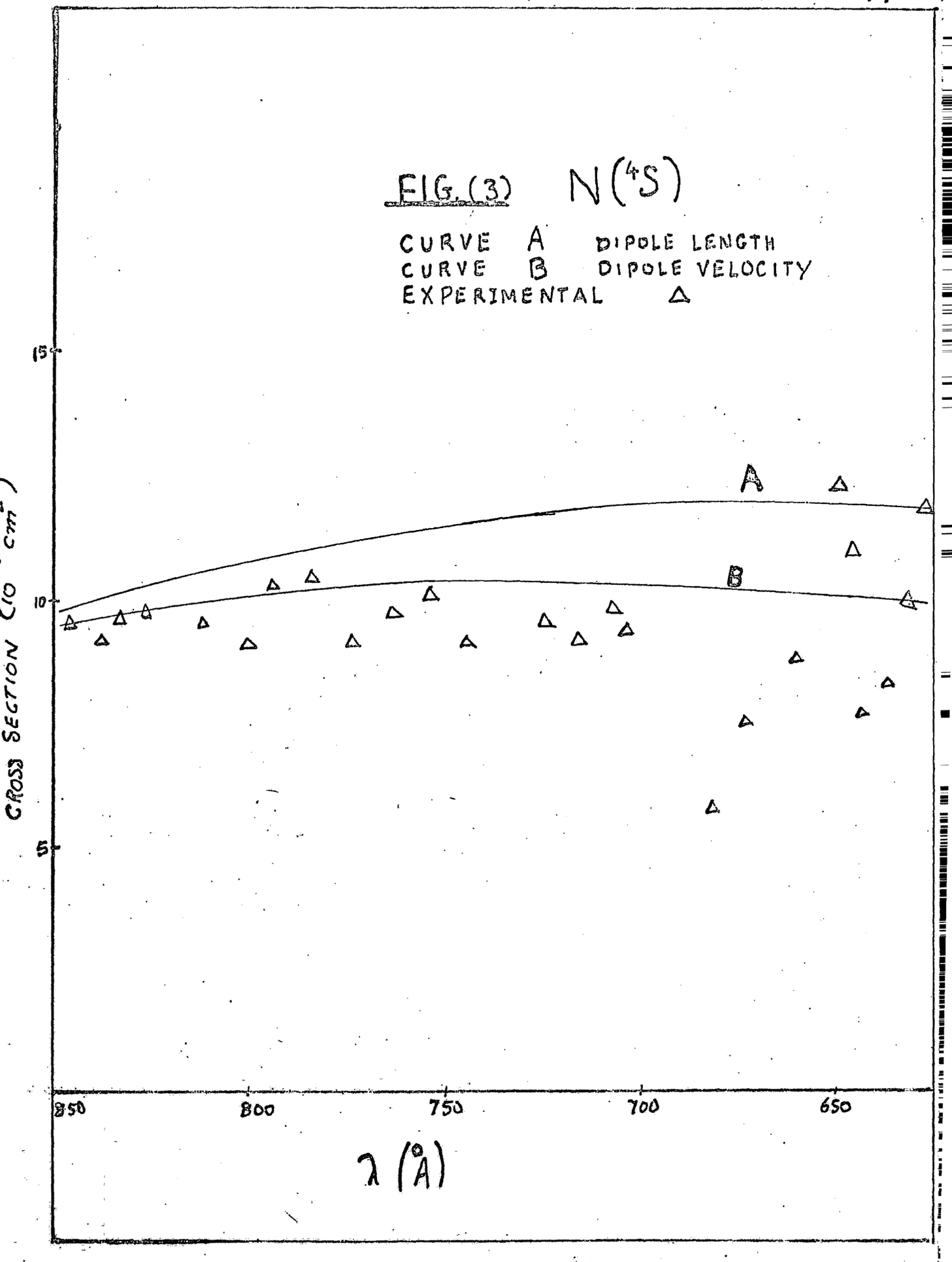
FIG.(3) N(⁴S)
CURVE A DIPOLE LENGTH
CURVE B DIPOLE VELOCITY
EXPERIMENTAL △
A
B
15
10
5
CROSS SECTION (10⁻¹⁸ cm²)
850
800
750
700
650
λ (Å)

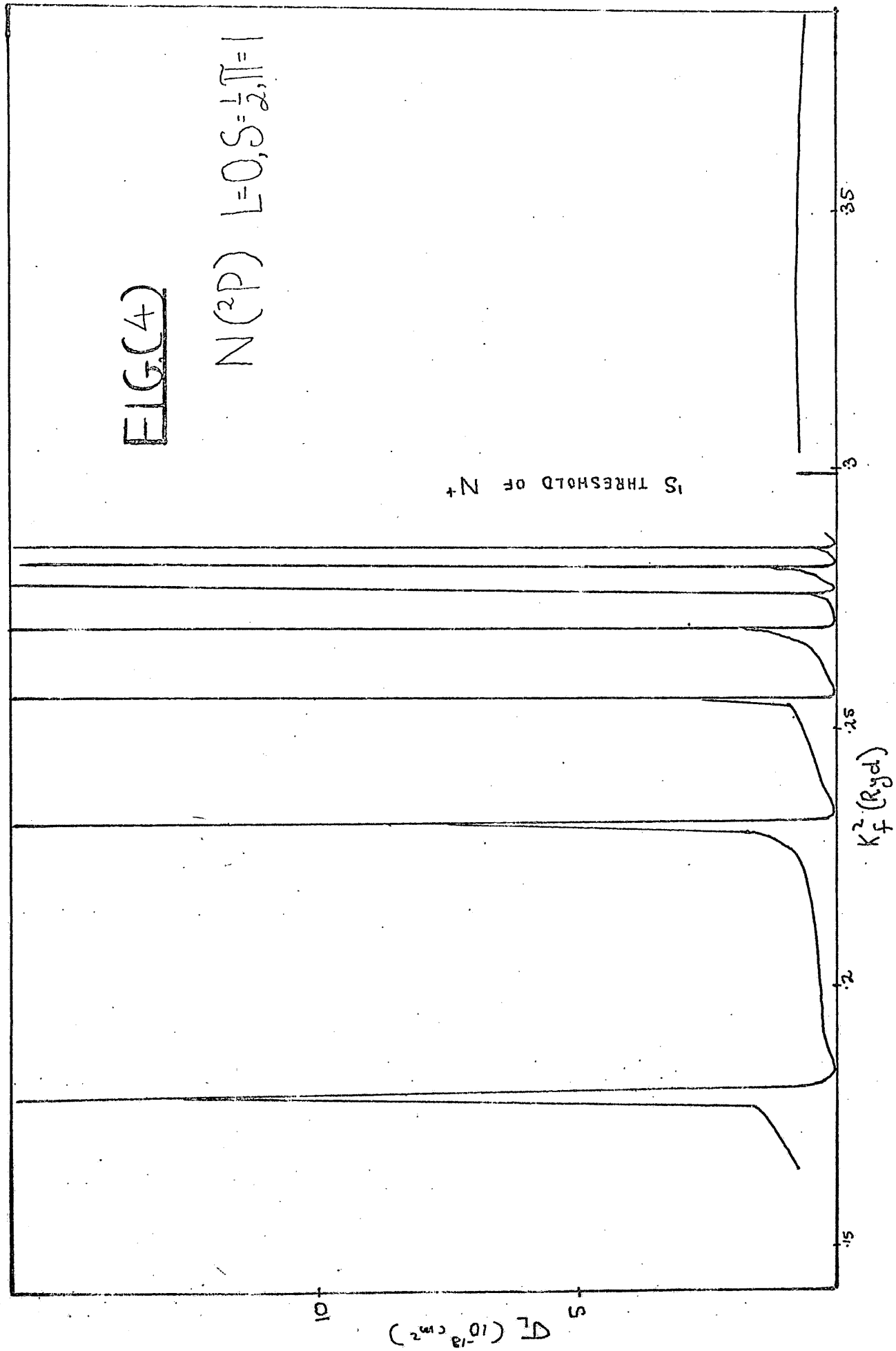
FIG.(4)
N(²P) L=0, S=½, π=1
¹S THRESHOLD OF N+
.35
.3
.25
.2
.15
K_f^2 (Ryd)
0
5
σ_L (10^{-18} cm²)

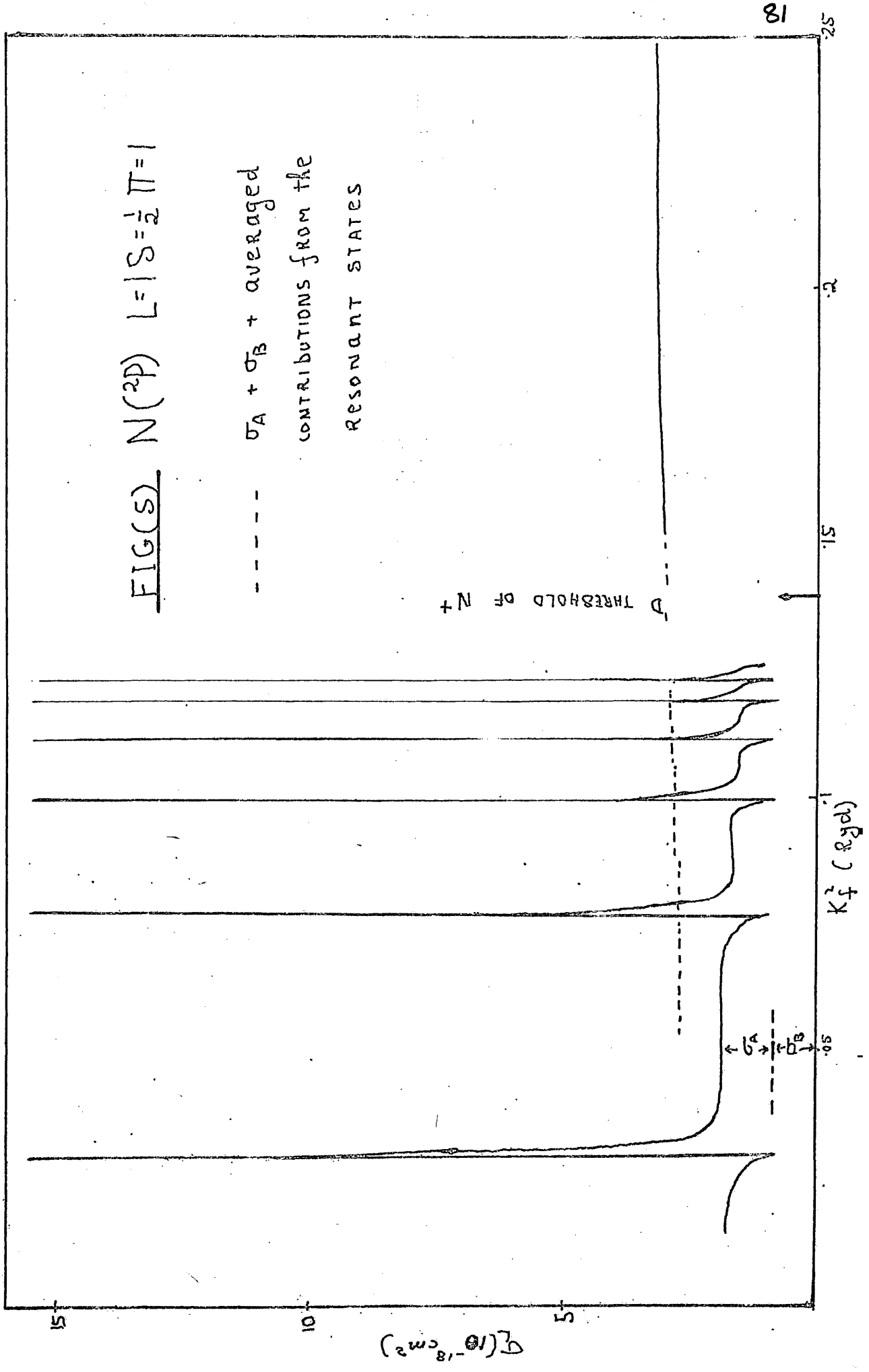
FIG(5) N(2P) L=1 S=½ IT=1
---- σA + σB + averaged contributions from the Resonant states
THRESHOLD OF N+
σ(10⁻¹⁸ cm²)
K²f (fm⁻²)
15
10
5
.25
.2
.15
.1
.05
σA
σB

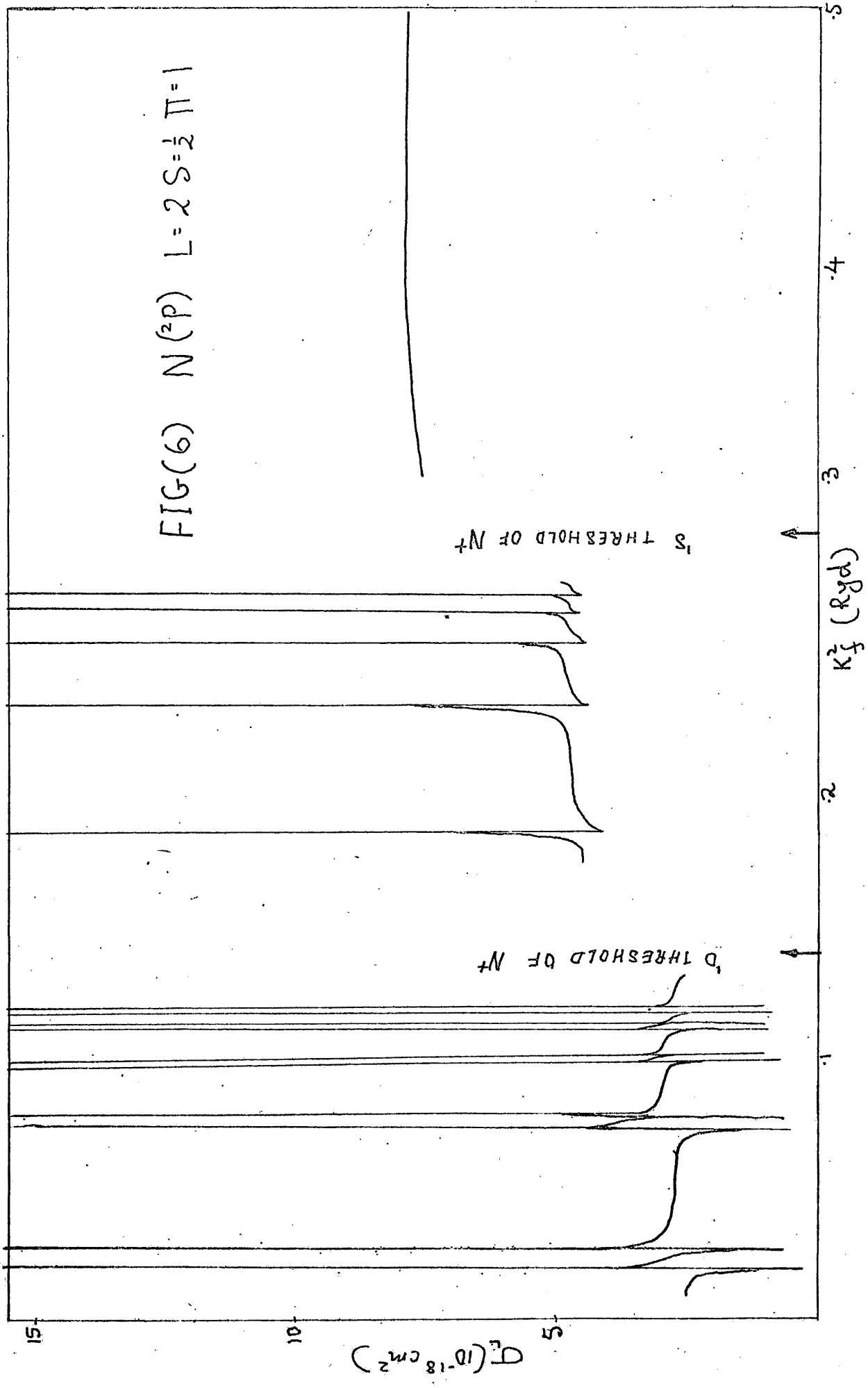
FIG(6) N(²P) L=2 S=½ Π=1
¹S THRESHOLD OF N+
¹D THRESHOLD OF N+
K_f^2 (Ryd)
$\sigma_L(10^{-18}\,cm^2)$
15
10
5
.1
.2
.3
.4
.5

EIG(2) N(2D) L=1 S=1/2 Π=1
D THRESHOLD OF N+
σ_L (10^{-18} cm^2)
15
10
5
0
.25
.2
.15
.1
.05
k^2 (Ryd)

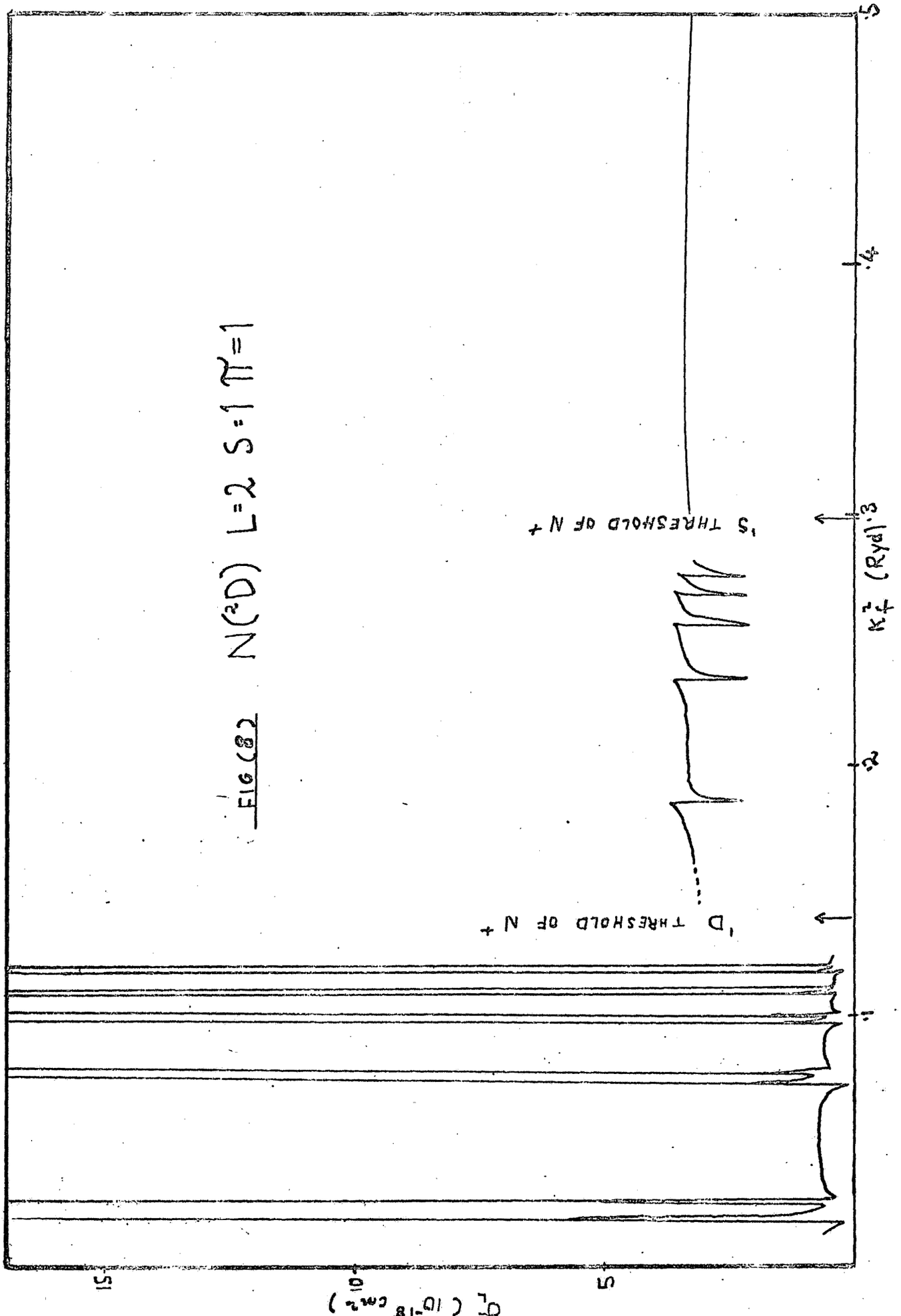

FIG (8) $N(^2D)$ L=2 S=1 Π=1

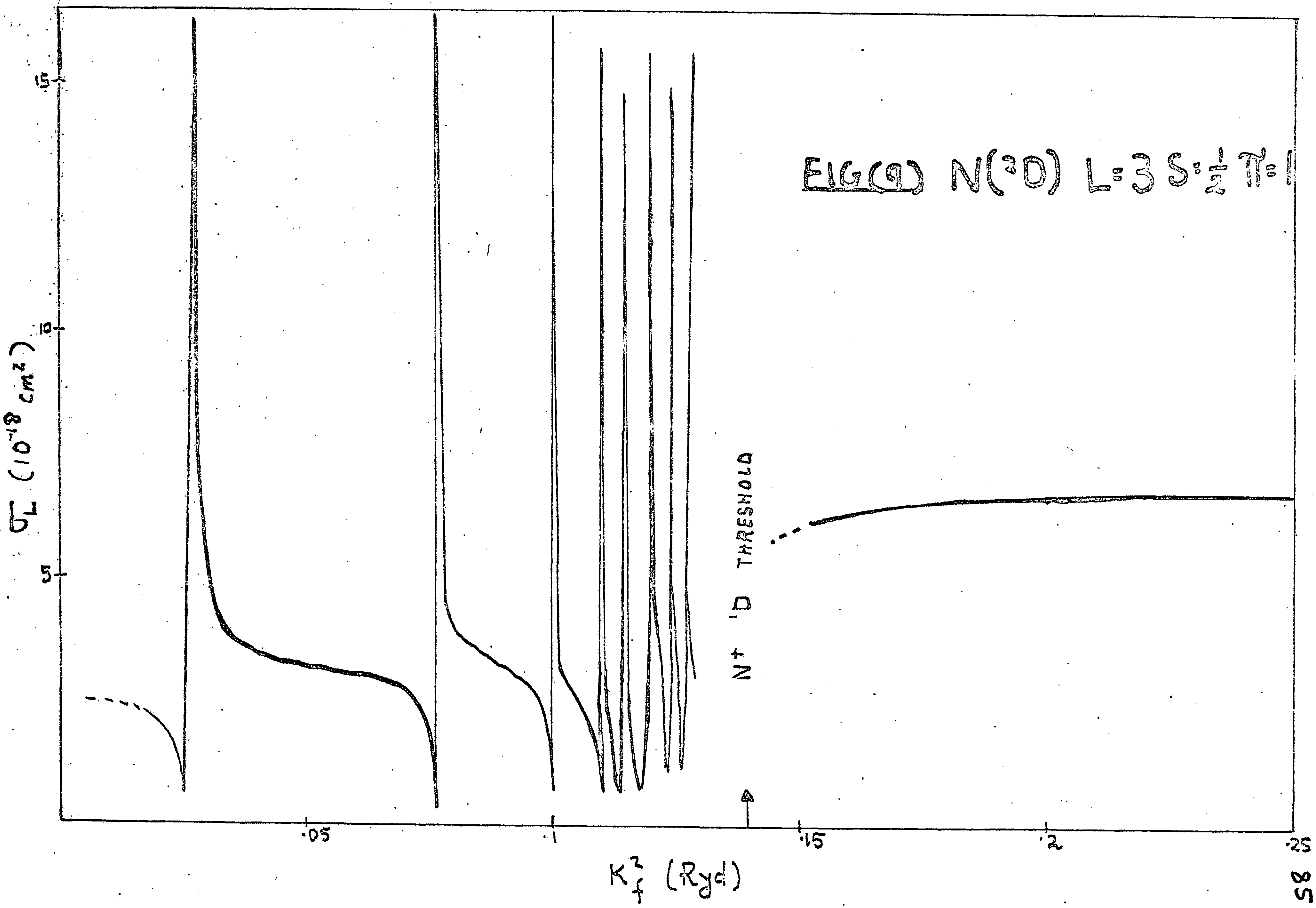

FIG(9) $N(^2D)$ $L=3$ $S=\frac{1}{2}$ $\pi=1$

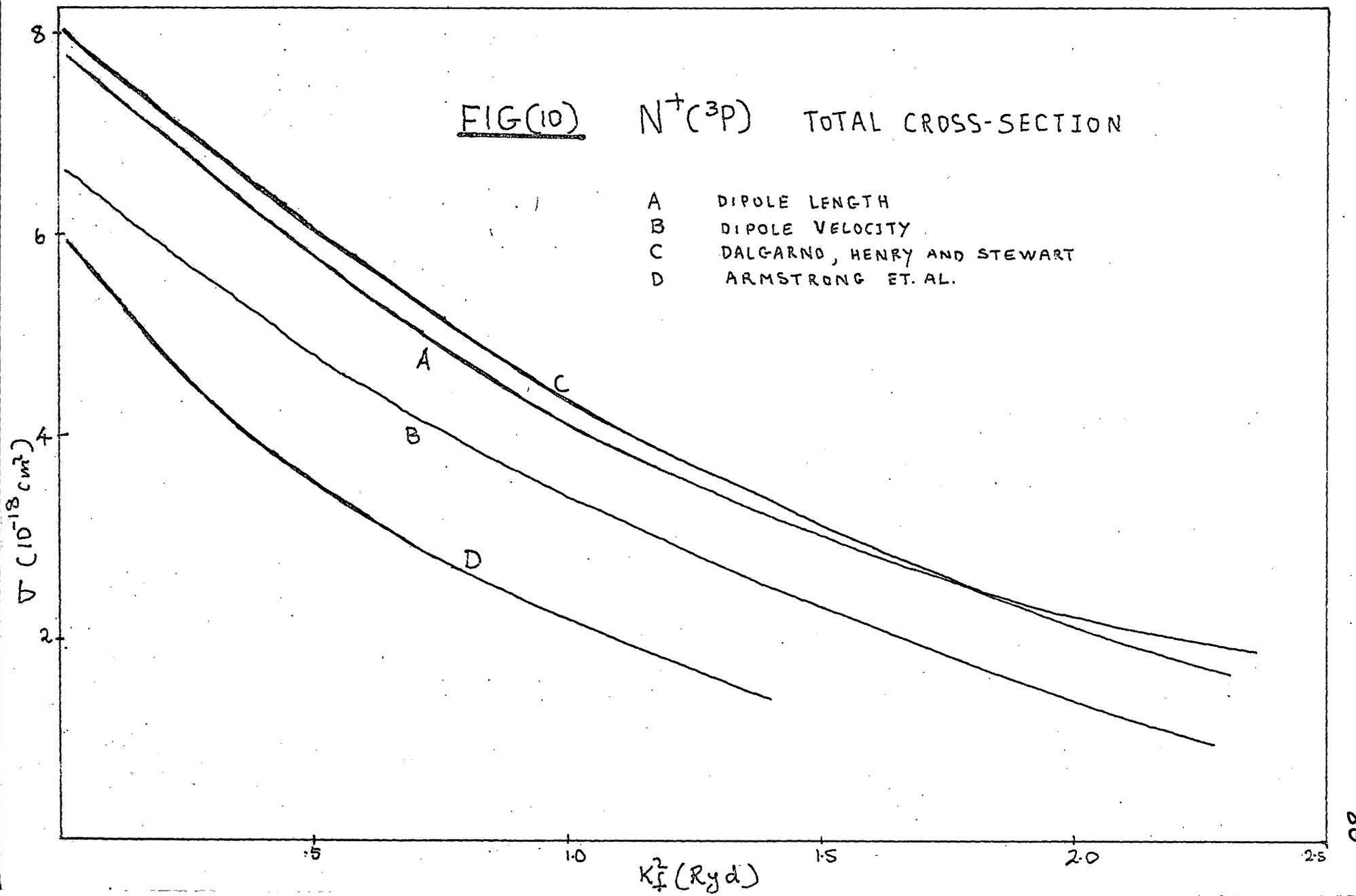
FIG(10) $N^+(^3P)$ TOTAL CROSS-SECTION
A DIPOLE LENGTH
B DIPOLE VELOCITY
C DALGARNO, HENRY AND STEWART
D ARMSTRONG ET. AL.
A
B
C
D
8
6
4
2
σ (10^{-18} cm^2)
·5
1·0
1·5
2·0
2·5
K_i^2 (Ryd)

that the series $(2p)^2\,(^1D)\,ng\ ^2F$ is missing or is too narrow to show up in our calculation. The partial wave contributions to the photoionization cross section of nitrogen above all thresholds are tabulated in Table 8.

N^+

No experimental results have been reported for photoionization cross sections for N^+, so it is not possible to evaluate the accuracy of our results as we have done in for $N(^4S)$ in figure 3. However in figure 10 we compare our results to a similiar calculation by Dalgarno[51] et al and to a calculation by Armstrong[52] et al who used a modified Burgess-Seation approximation.

The cross sections in tabular form are given in table 9.

P

Atomic phosphorus has the same configuration as atomic nitrogen so it is intersting toccompare our results for the two systems. In figure 11 we compare the results for $N(^4S)$ and $P(^4S)$. We note the phosphorus cross sections are approximately four times larger than those for nitrogen. This is because the atoms are larger. Using hydrogenic functions we see

$$\frac{\bar{r}_{2p}}{\bar{r}_{3p}} \sim \frac{2^2}{3^2} \sim \frac{1}{2}$$

where $\bar{r}$ denote the average distance from the nucleus. Furthermore we note that the slope of nitrogen in figure 11 is more gentle than that of phosphorus. This can be explained qualita-

FIG(11) $N(2P)^3\,{}^4S$, $P(3P)^3\,{}^4S$

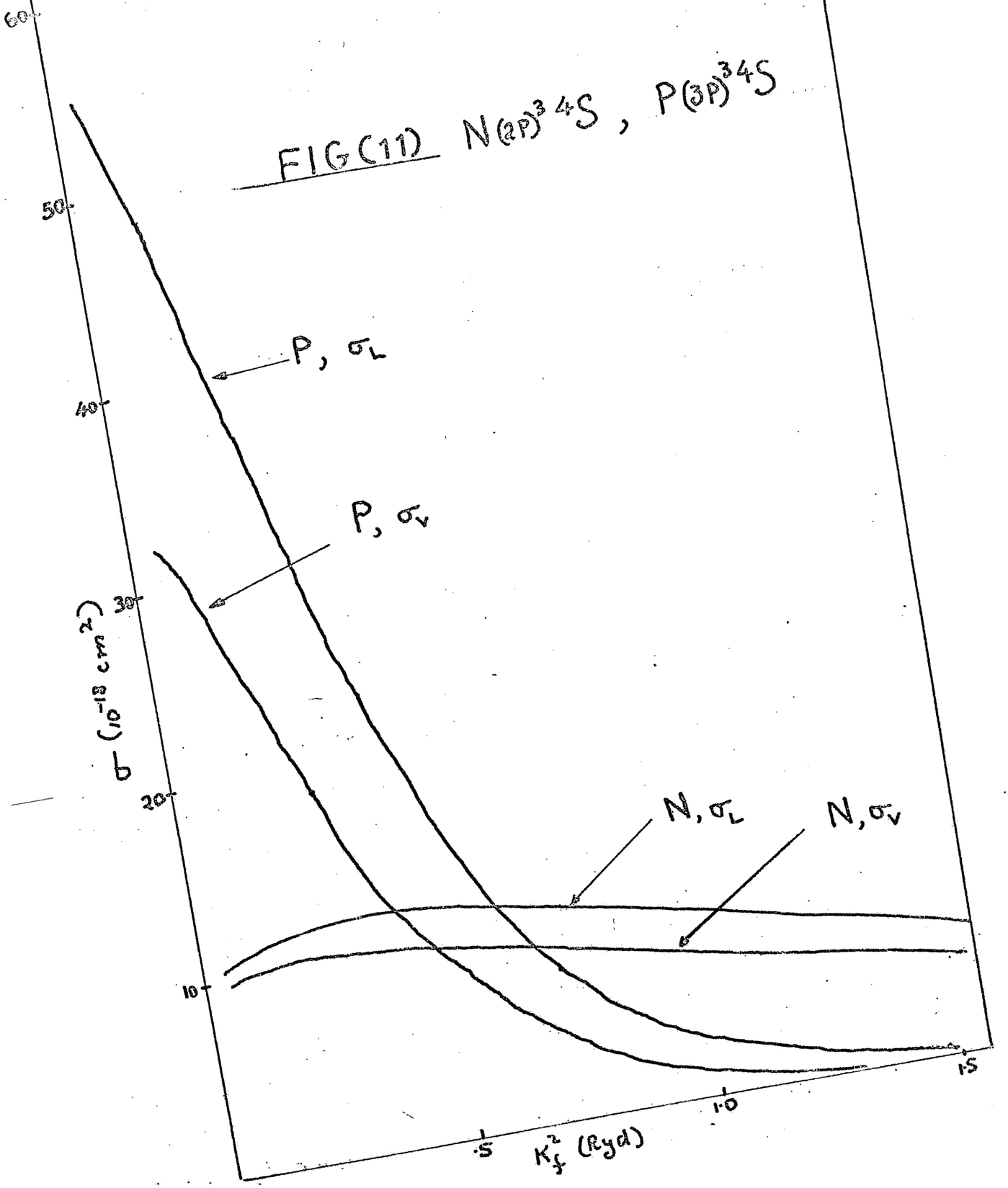

tively in the following way. The cross section apart from geometrical factors will depend on matrix elements of the type $\langle P_{2p}|r|\epsilon d\rangle$ and $\langle P_{3p}|r|\epsilon d\rangle$. We draw the functions in the following diagram

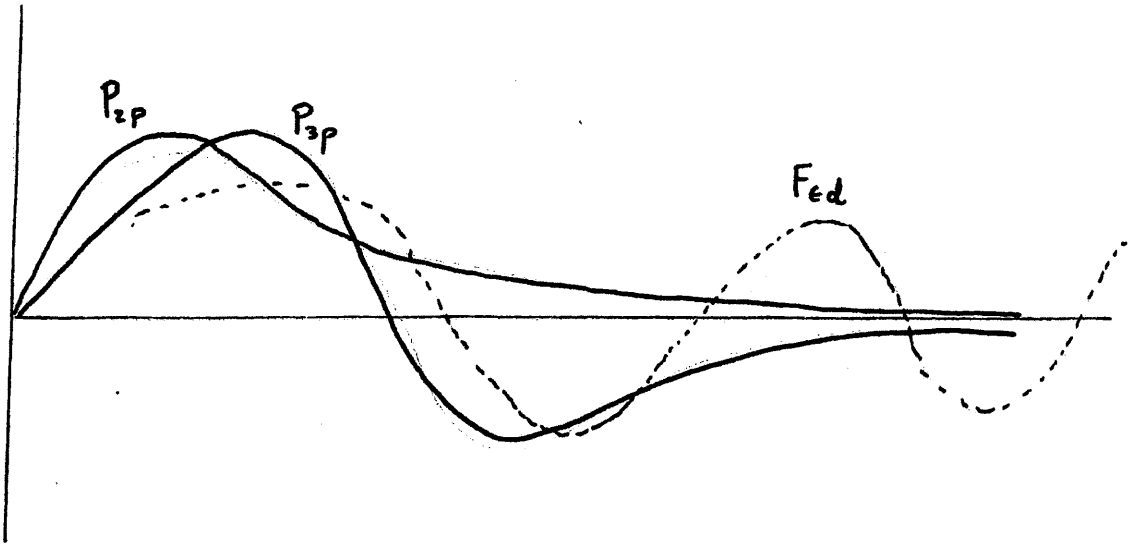

As the energy of $F_{\epsilon d}$ increases i.e. the wave length decreases, we see that the P_{3p} wave function cancels out faster than P_{2p}. This explains the difference in the graph.

The $^2S^e$, $^2P^e$, and $^2D^e$ partial wave contribution to photoionization cross sections of P (^2P) are given in figures 12, 13 and 14, and the parameters for the resonances shown in these graphs are given in table 10. The corresponding figures and graphs for nitrogen are figures 4, 5 and 6 and table 6. The various quantum numbers involved in a photoionization process for an atomic system with initial configuration P^3 have been tabulated by Smith[60], The results for photoionization of P(^2D) are given in figures 15, 16 and 17 and table 11. We note

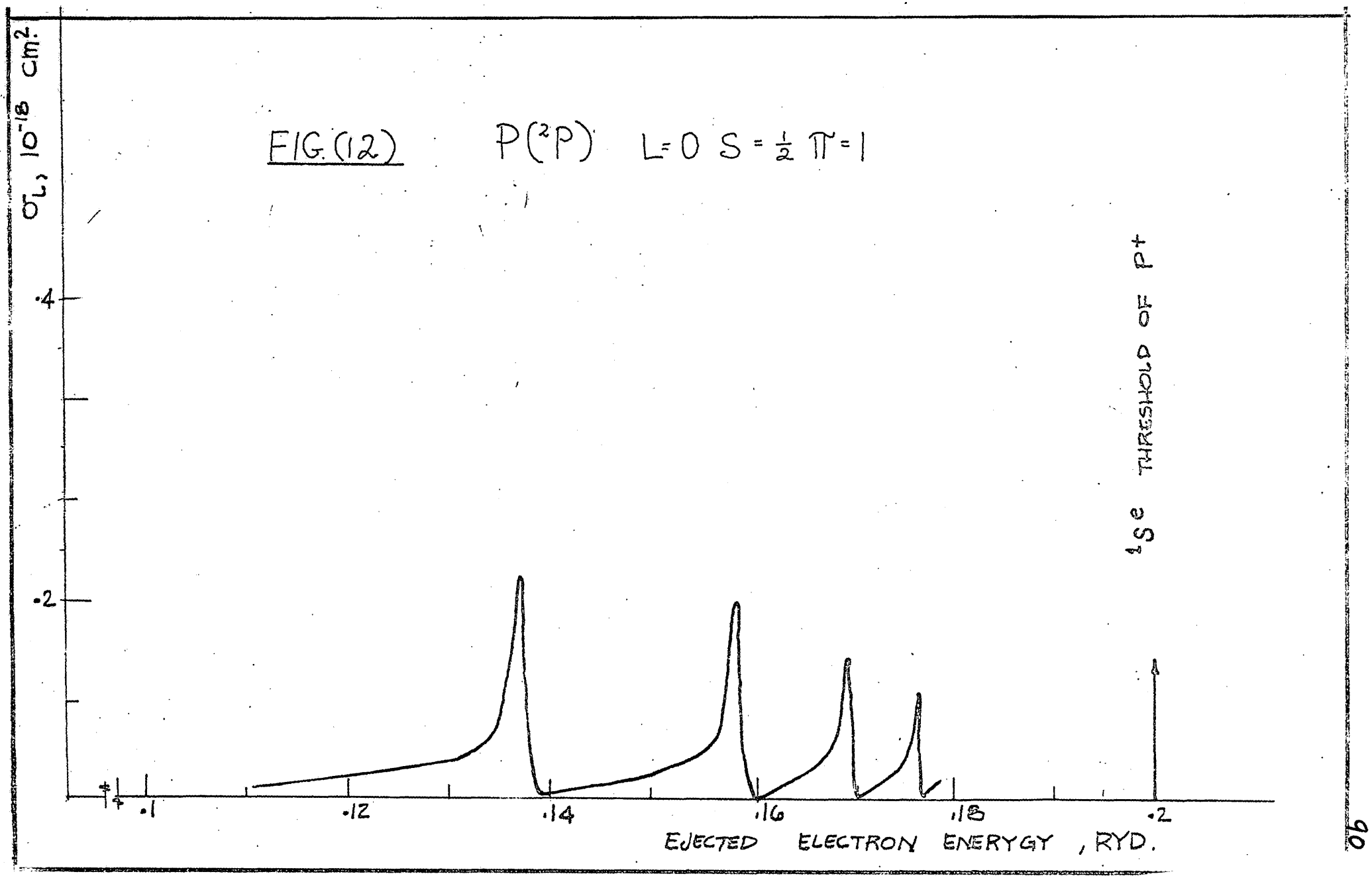
FIG. (12) P(²P) L=0 S=½ Π=1
σL, 10⁻¹⁸ cm²
·4
·2
·1
·12
·14
·16
·18
·2
EJECTED ELECTRON ENERYGY, RYD.
1Se THRESHOLD OF P+

FIG. (13) $P(^2P)$ $L=1$ $S=\frac{1}{2}$ $\pi=1$

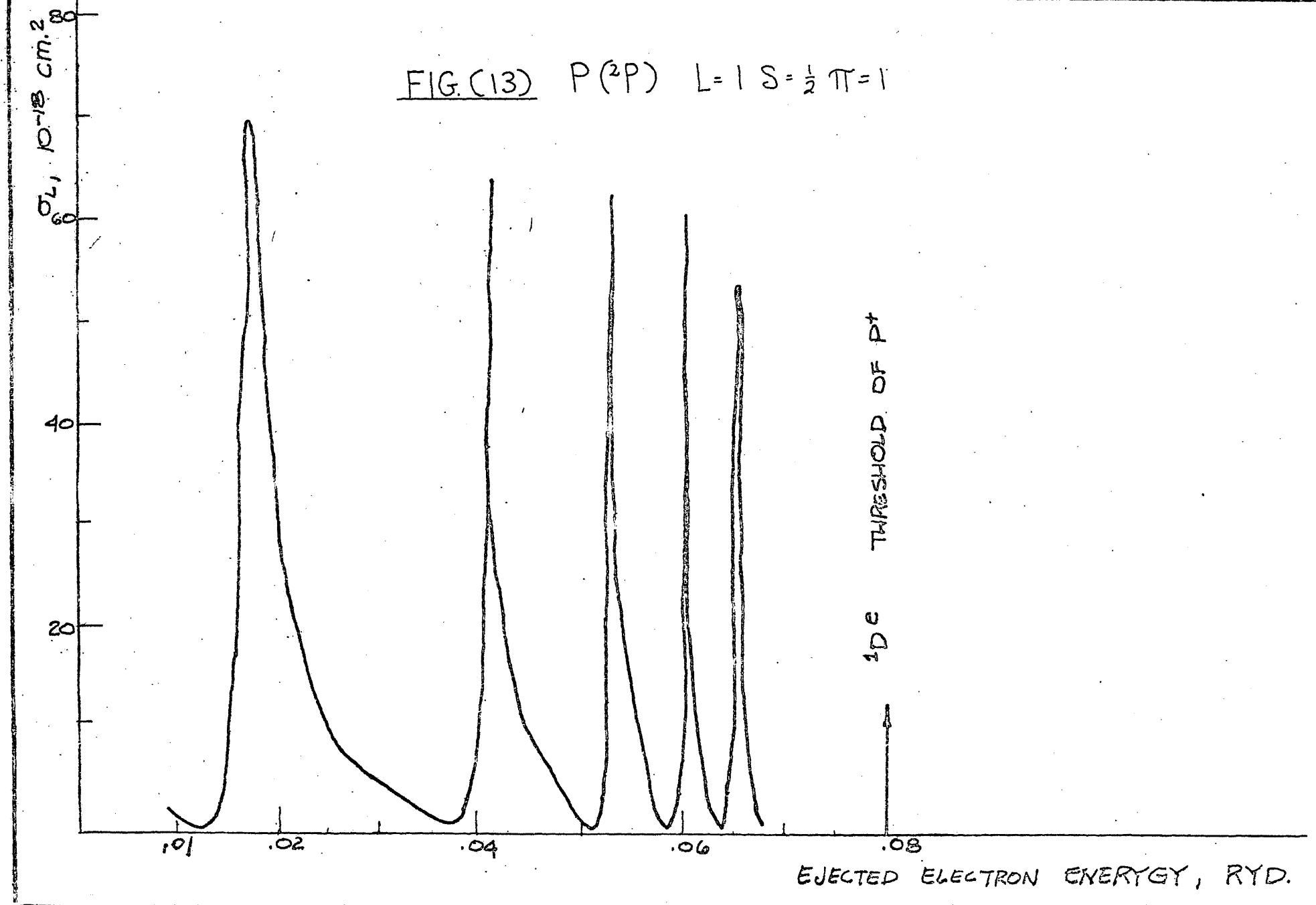

16

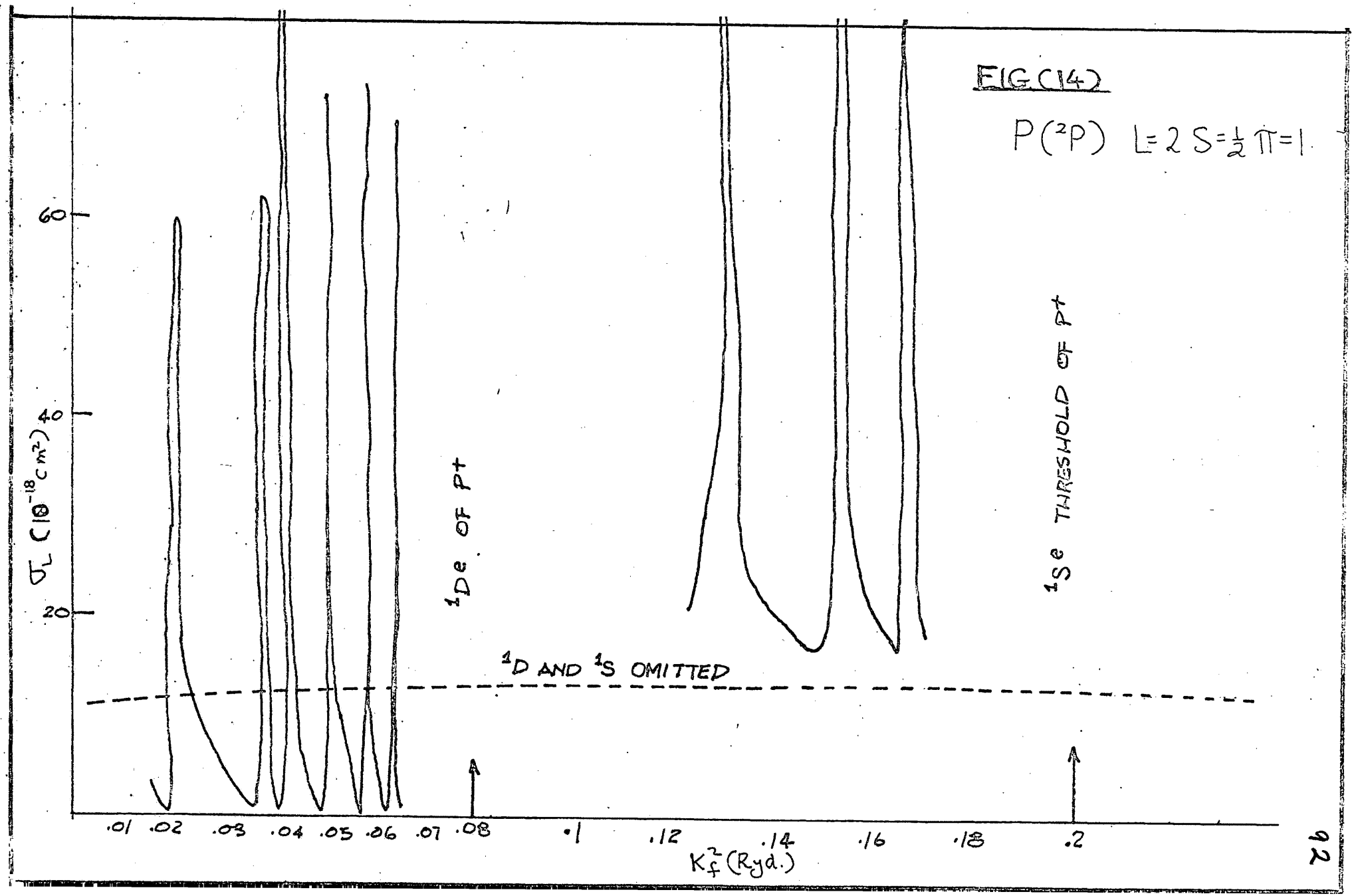
FIG (14)
P(²P) L=2 S=½ π=1
60
40
20
σL (10⁻¹⁸ cm²)
¹De OF Pt
¹Se THRESHOLD OF Pt
¹D AND ¹S OMITTED
.01 .02 .03 .04 .05 .06 .07 .08 .1 .12 .14 .16 .18 .2
K²f (Ryd.)

FIG. (15)

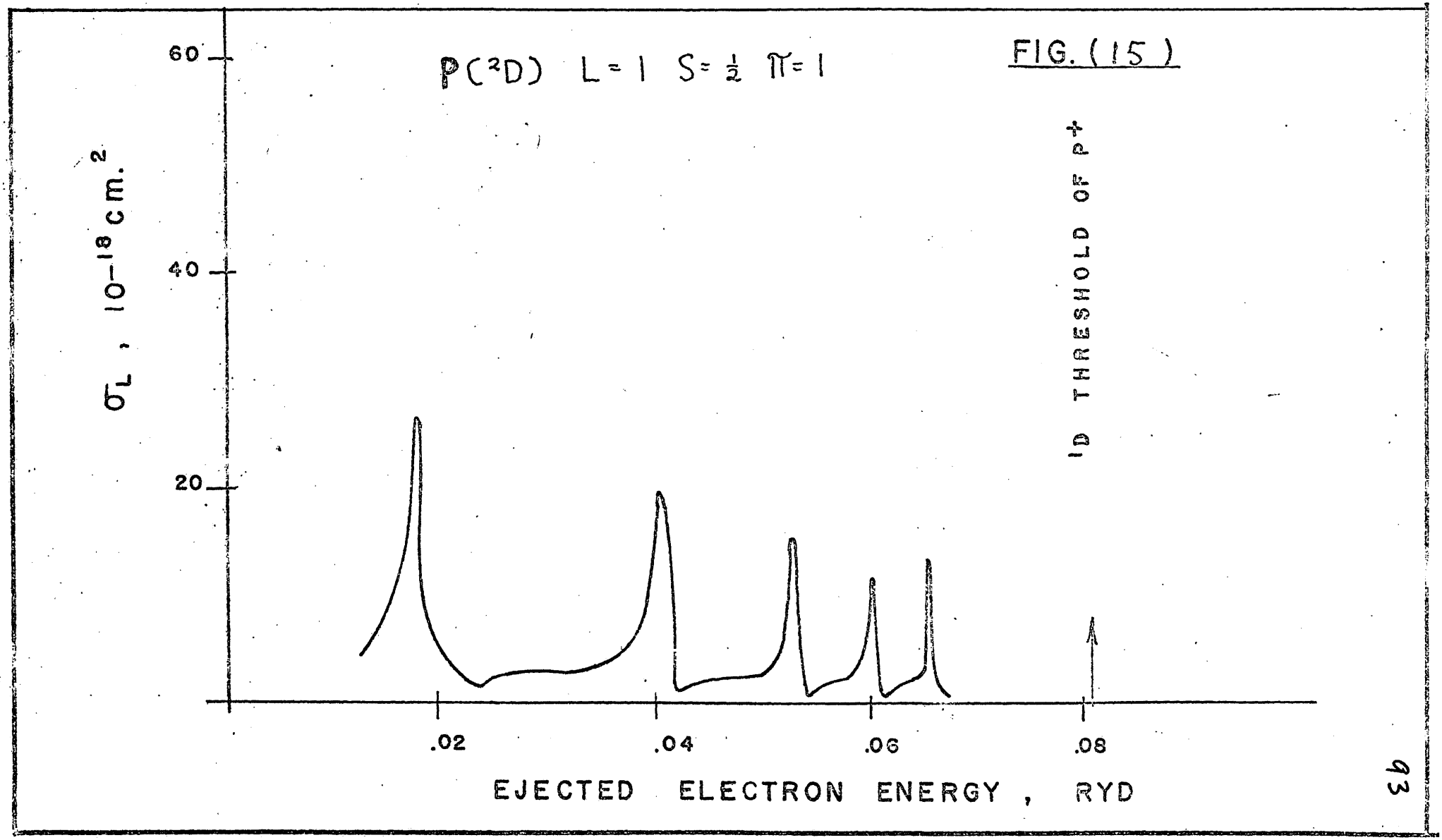
P(²D) L = 1 S = ½ π = 1
60
40
20
σ_L , 10^{-18} cm.²
¹D THRESHOLD OF P⁺
.02
.04
.06
.08
EJECTED ELECTRON ENERGY , RYD

FIG. (16)

$P(^2D)$ $L=2$ $S=\frac{1}{2}$ $\Pi=1$.

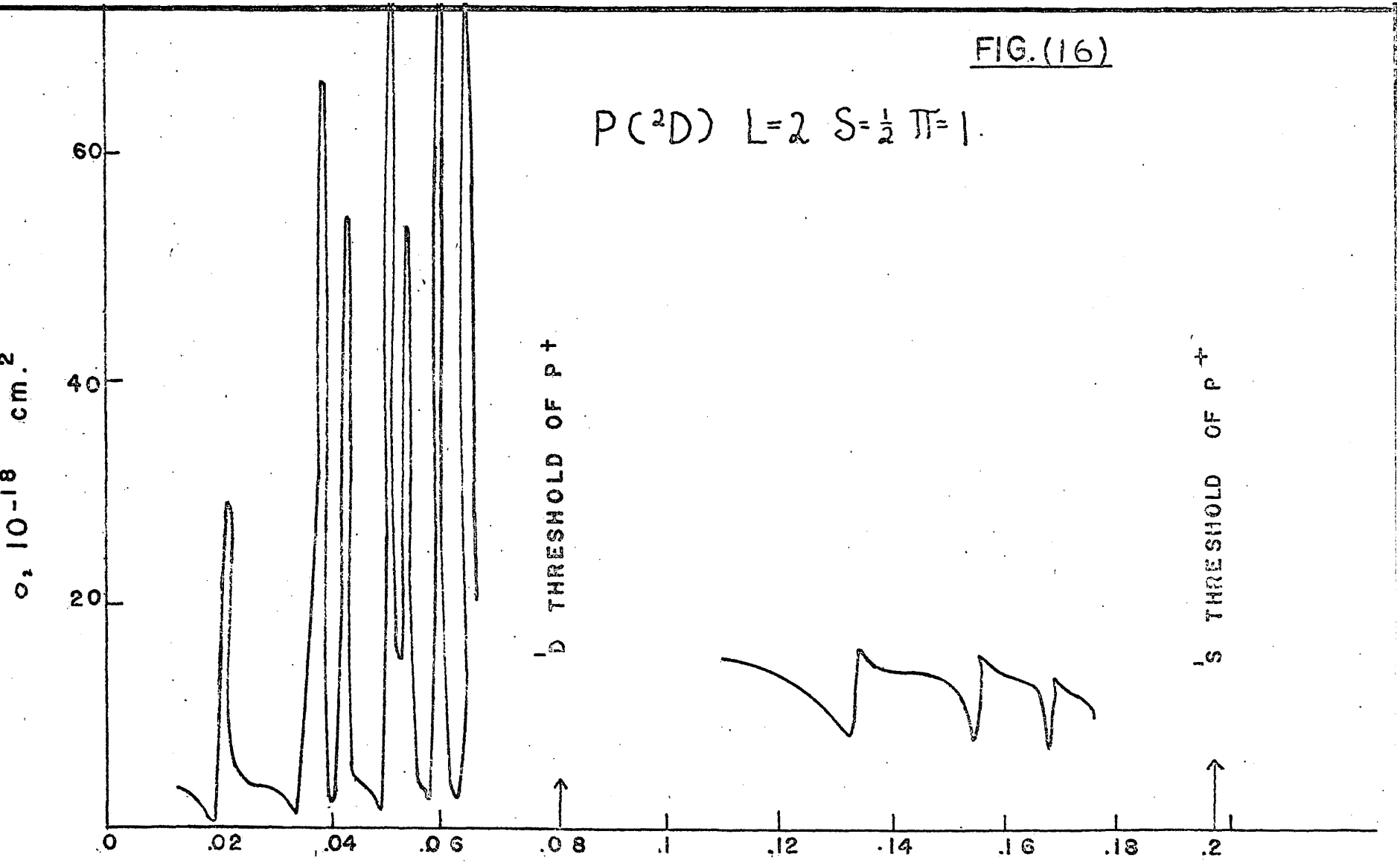

FIG. (17)

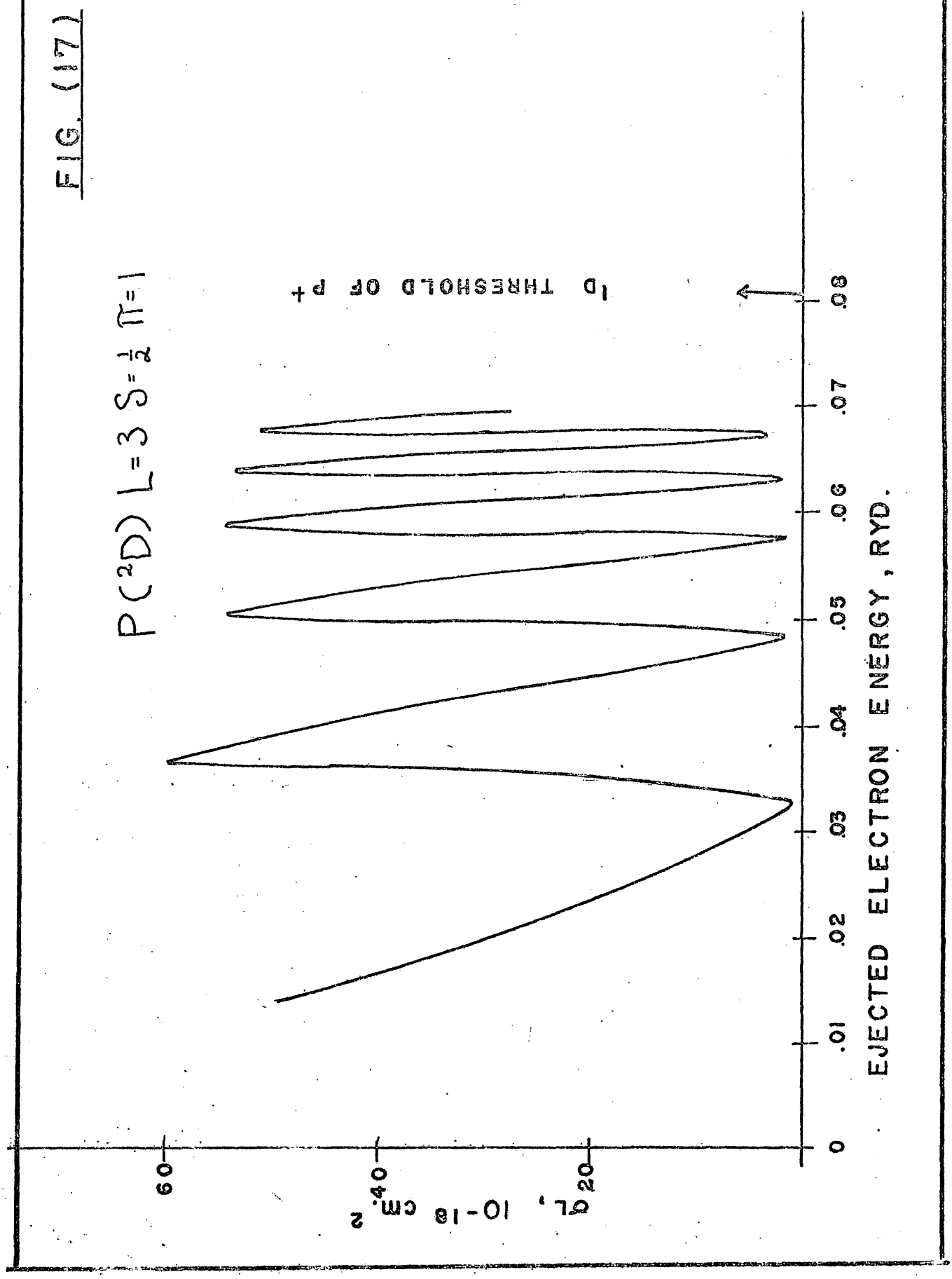
$P(^2D)\ L=3\ S=\frac{1}{2}\ \Pi=1$
^1D THRESHOLD OF P^+
σ_L, 10^{-18} cm.^{2}
60
40
20
0
.01
.02
.03
.04
.05
.06
.07
.08
EJECTED ELECTRON ENERGY, RYD.

that the widths of the resonances in phosphorus are greater than those in nitrogen. This is because the coupling between the channels is greater in the $(3p)^2$ case. In table 12 we give the partial wave contributions to the photoionization cross sections of phosphorus above all thresholds.

Al

Total absorption cross sections have been measured by Kozlov et al.[53], while calculations have been carried out by Vainshtein and Norman[54], Burgess et al.[55], Peach[56] and Manson and Cooper[57]. According to Peach, the absorption of radiation by aluminum in the ground state ep $^2P^o$ may be the cause of the abrupt change in the solar continuum radiation at 2085 ^oA. In figure 18 we compare our computation of the photoionization cross sections for the 3p $^2P^o$ level with the results of Peach and Burgess et al. We recall that whereas our model is the full Hartree-Fock treatment for a single configuration, the other models involve extrapolating measured quantum defects into the energy region of interest in the collision problem, as well as employing the Coulombic asymptotic form of the free electron orbital in the matrix element for all Γ. Within our model the $^2P^o$ state of aluminum can photoionize into two final states $^2S^e$ and $^2D^e$ with the ejected electron having angular momentum 0 and 2 respectively, with the residual ion having the configuration of magnesium.

At energies just above the photoionization threshold the algorithm[46] used to compute the asymptotic solution to the close coupling equations breas down. From figure 18 we see that the

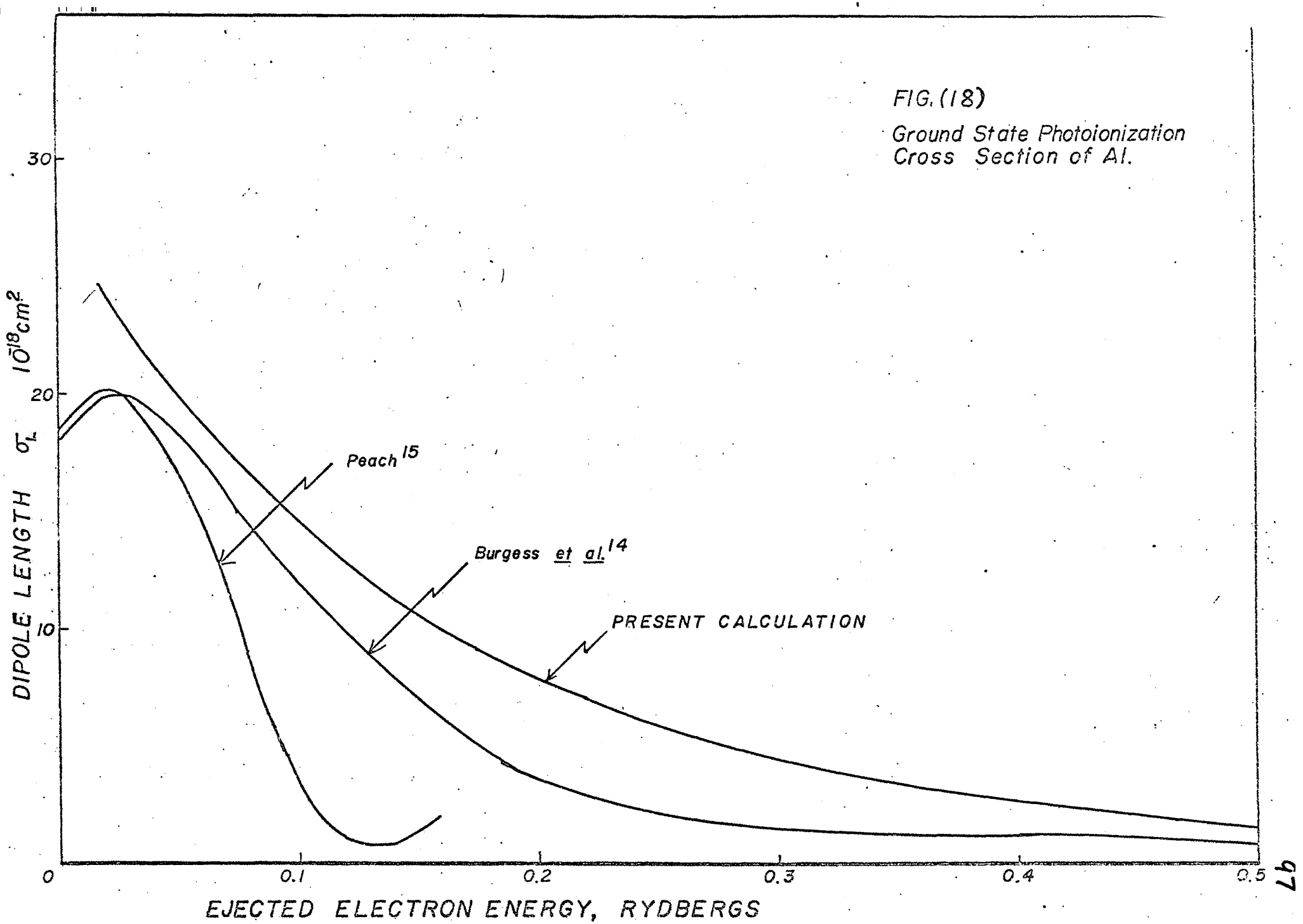
FIG. (18)
Ground State Photoionization Cross Section of Al.
30
20
10
0
DIPOLE LENGTH σ_L $10^{-18}cm^2$
Peach[15]
Burgess et al.[14]
PRESENT CALCULATION
0.1
0.2
0.3
0.4
0.5
EJECTED ELECTRON ENERGY, RYDBERGS

maximum predicted by the quantum defect method, if it existed at all in the close-coupling approach. In the neighborhood of 0.05 Ryd. the three calcuations are in reasonable agreement. At higher energies, one would expect the quantum defect method to become unreliable due to it being an extrapolation procedure and therefore the long tail of the close-coupling approximation at about twice the previous calculated values should be the better values. The Peach minimum at 0.125 Ryd. is probably due to severe cancellation of the matrix elements as previously discussed. In table 13 we present the cross sections in tabular form.

Si

Photionization cross sections for the $^3P^e$ and the excited $^1D^e$ terms of the ground state configuration have been measured by Rich. In figure 19 we compare the measured photoionization cross sections of the ^3P level of Si with our calculations. Previous calculations have been performed in either a hydrogenic approximation or using the quantum defect method of Burgess and Seaton[59] (who calculated 3p→es and 3p→ed amplitudes in Si^+). As remarked by Rich one would expect the quantum defect method to be inaccurate since it requires extrapolation of poorly behaved experimentally observed quantum defects of bound levels, the extrapolation naturally getting worse the further one goes beyond the ionization threshold.

From figure 19 we see that there is excellent agreement between the observations of Rich and the calculations from first

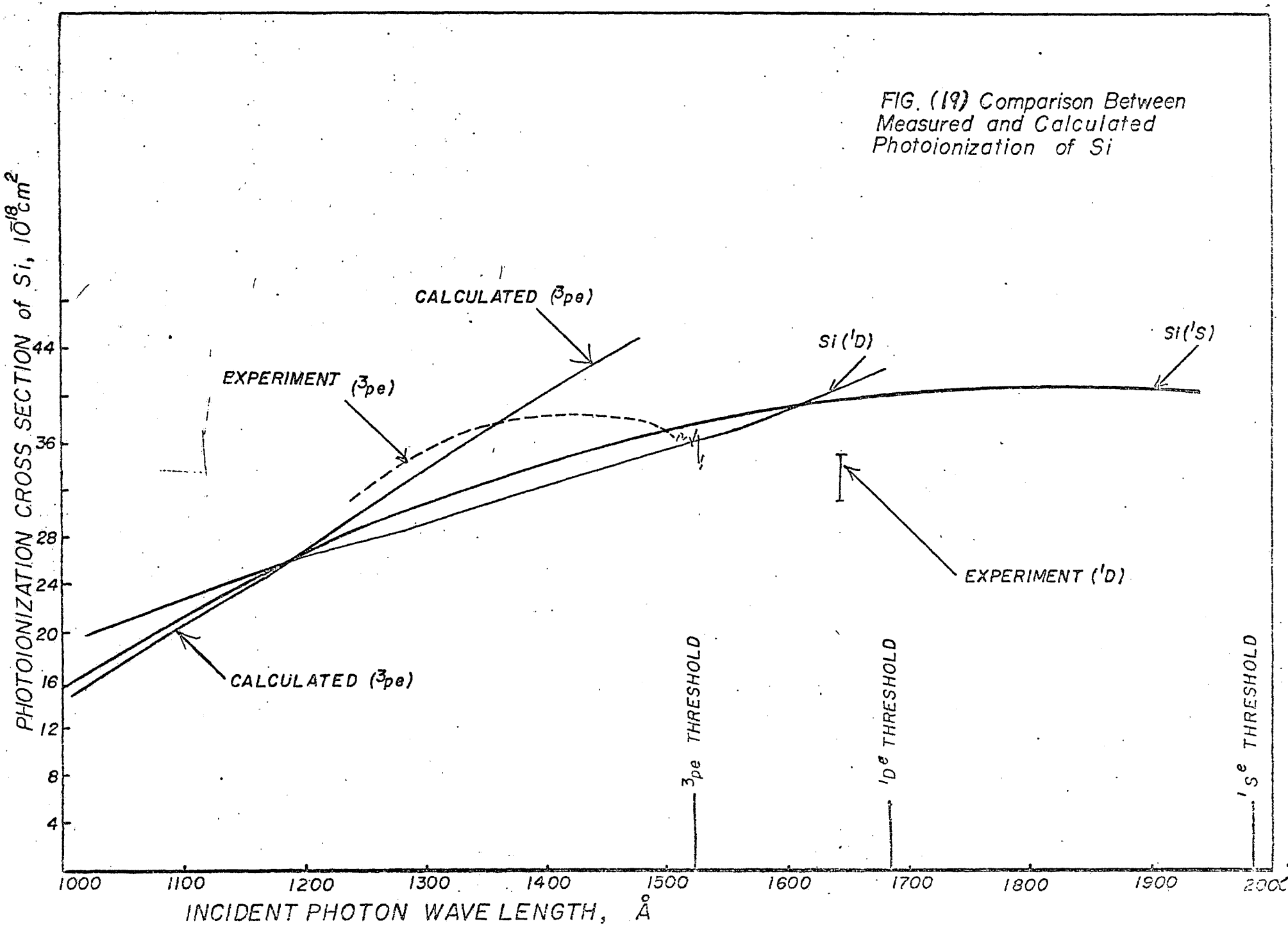
FIG. (19) Comparison Between Measured and Calculated Photoionization of Si
PHOTOIONIZATION CROSS SECTION of Si, $10^{-18} cm^2$
CALCULATED (^{3}pe)
EXPERIMENT (^{3}pe)
Si (^{1}D)
Si (^{1}S)
EXPERIMENT (^{1}D)
CALCULATED (^{3}pe)
^{3}pe THRESHOLD
^{1}D^e THRESHOLD
^{1}S^e THRESHOLD
4
8
12
16
20
24
28
36
44
1000
1100
1200
1300
1400
1500
1600
1700
1800
1900
2000
INCIDENT PHOTON WAVE LENGTH, Å

principles as carried out in the close-coupling approximation for photoionization from the $^3P^e$ ground state of silicon. Just above threshold as previously mentioned, we have also plotted Rich's single energy point for photoionization from the first excited state $^1D^e$, which is about 10% below the value predicted by our calculations. Finally we present the cross section for photoionization from the $^1S^e$ excited term of Si ground configuration for which we have nothing to compare with. The importance of figure 19 must be stressed in view of the very few laboratory experiments carried out on these reasonably complex structures. It is clear evidence of the quantitative correctness of the close-coupling results presented in this paper. In table 14 we have tabulated the partial wave contribution to the photoionization cross sections above all thresholds.

S

In order to compute the photoionization cross section of the $^3P^e$ state of sulphur we need three partial wave contributions ($^3S^o$, $^3P^o$ and $^3D^o$). The residual ion having configuration P^3 has three states that give rise to structures in the photoionization cross sections. In figures 20 to 22 where we present the individual partial wave contributions to the photoionization cross section of $S(^3P)$ we demonstrate the profound influence the excited states of the residual ion have on the cross sections by comparing with the results obtained when those states are neglected (represented by dashed lines on the graphs). In figure 27 we have attempted to sum the three partial wave contributing to photoionization from the ground state. The parameters for the various series of resonances in each partial

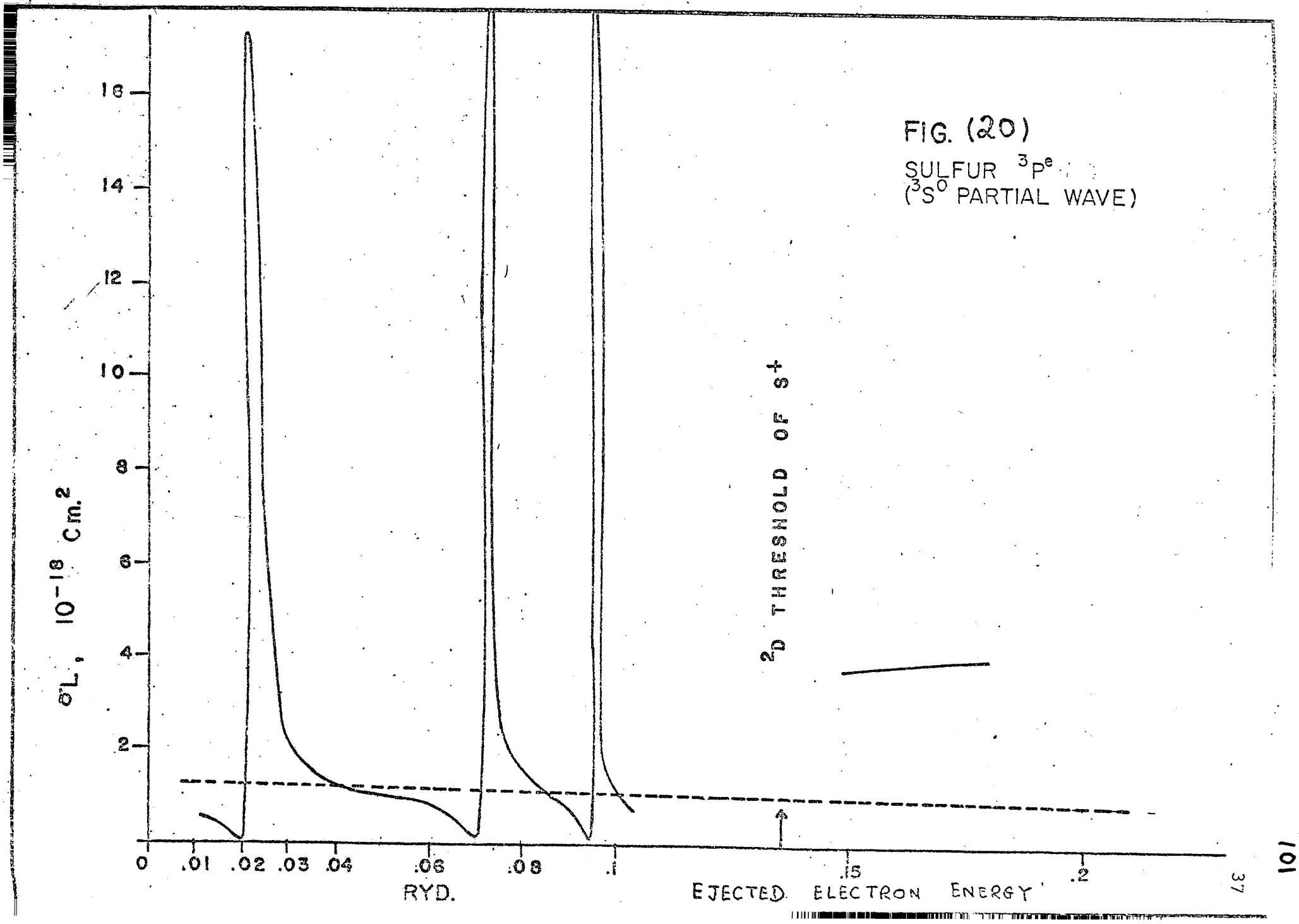
FIG. (20)
SULFUR $^3P^e$
($^3S^o$ PARTIAL WAVE)
σ_L, 10^{-18} Cm.^{2}
16
14
12
10
8
6
4
2
^2D THRESHOLD OF S^+
0
.01
.02
.03
.04
.06
.08
.1
.15
.2
RYD.
EJECTED ELECTRON ENERGY
37
101

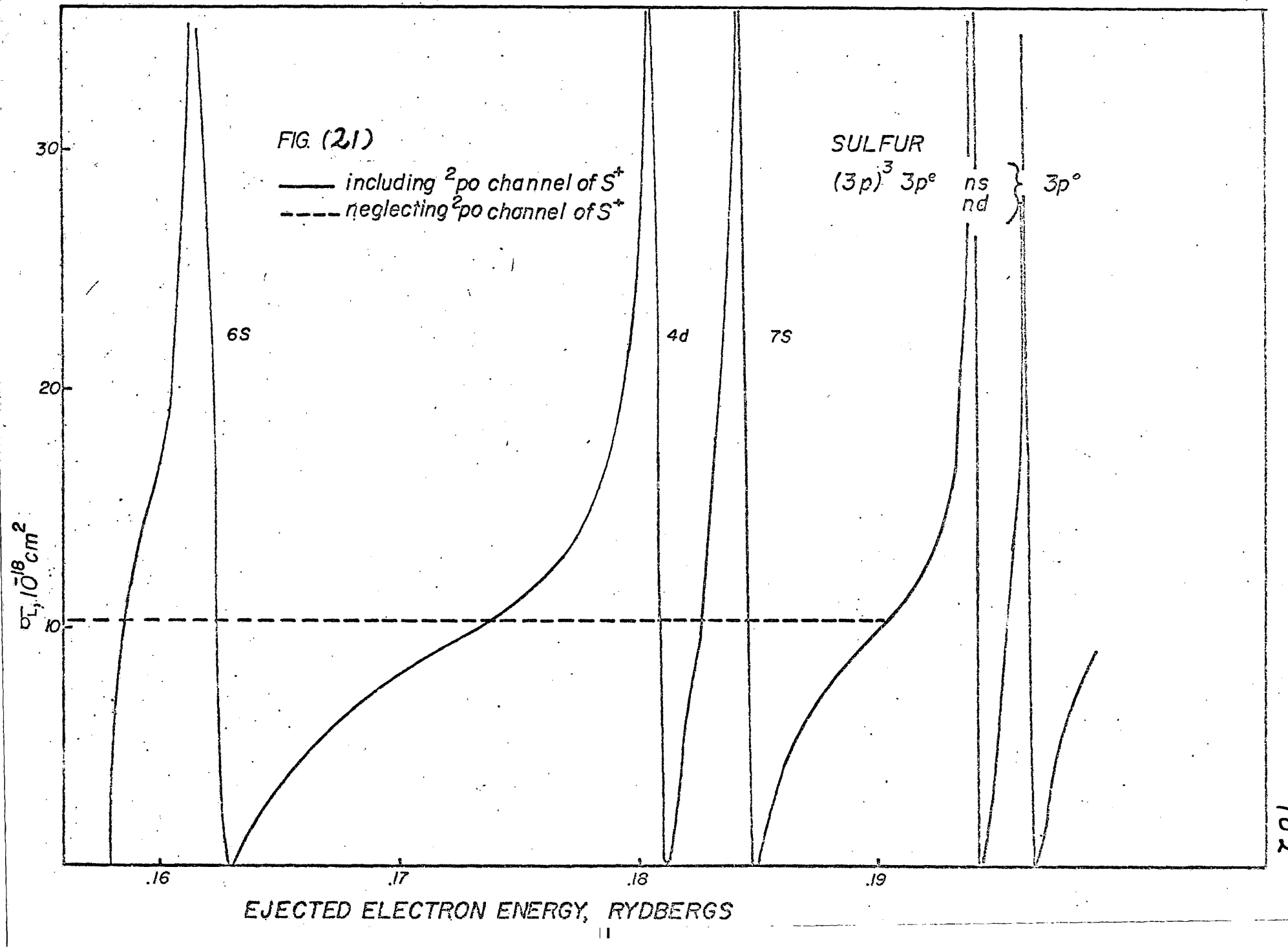
FIG. (21)
including ^{2}po channel of S^+
neglecting ^{2}po channel of S^+
SULFUR
$(3p)^3\ 3p^e$ ns nd 3p°
6S
4d
7S
30
20
10
$\sigma_L, 10^{-18} cm^2$
.16
.17
.18
.19
EJECTED ELECTRON ENERGY, RYDBERGS

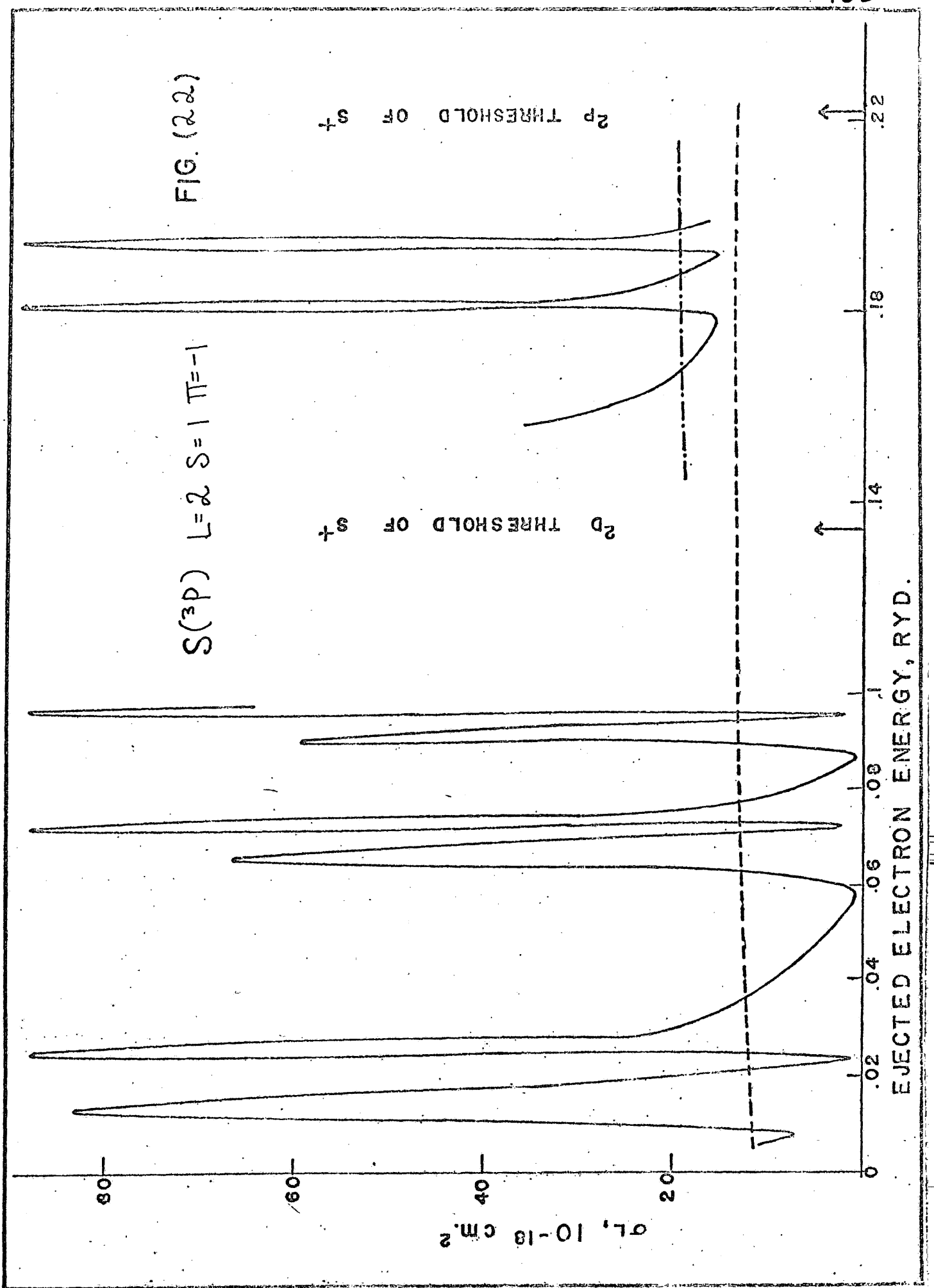
FIG. (22)
$S(^3P)$ $L=2$ $S=1$ $\Pi=-1$
^2P THRESHOLD OF S^+
^2D THRESHOLD OF S^+
σ_L, 10^{-18} cm.^{2}
EJECTED ELECTRON ENERGY, RYD.
0
20
40
60
80
.02
.04
.06
.08
.1
.14
.18
.22

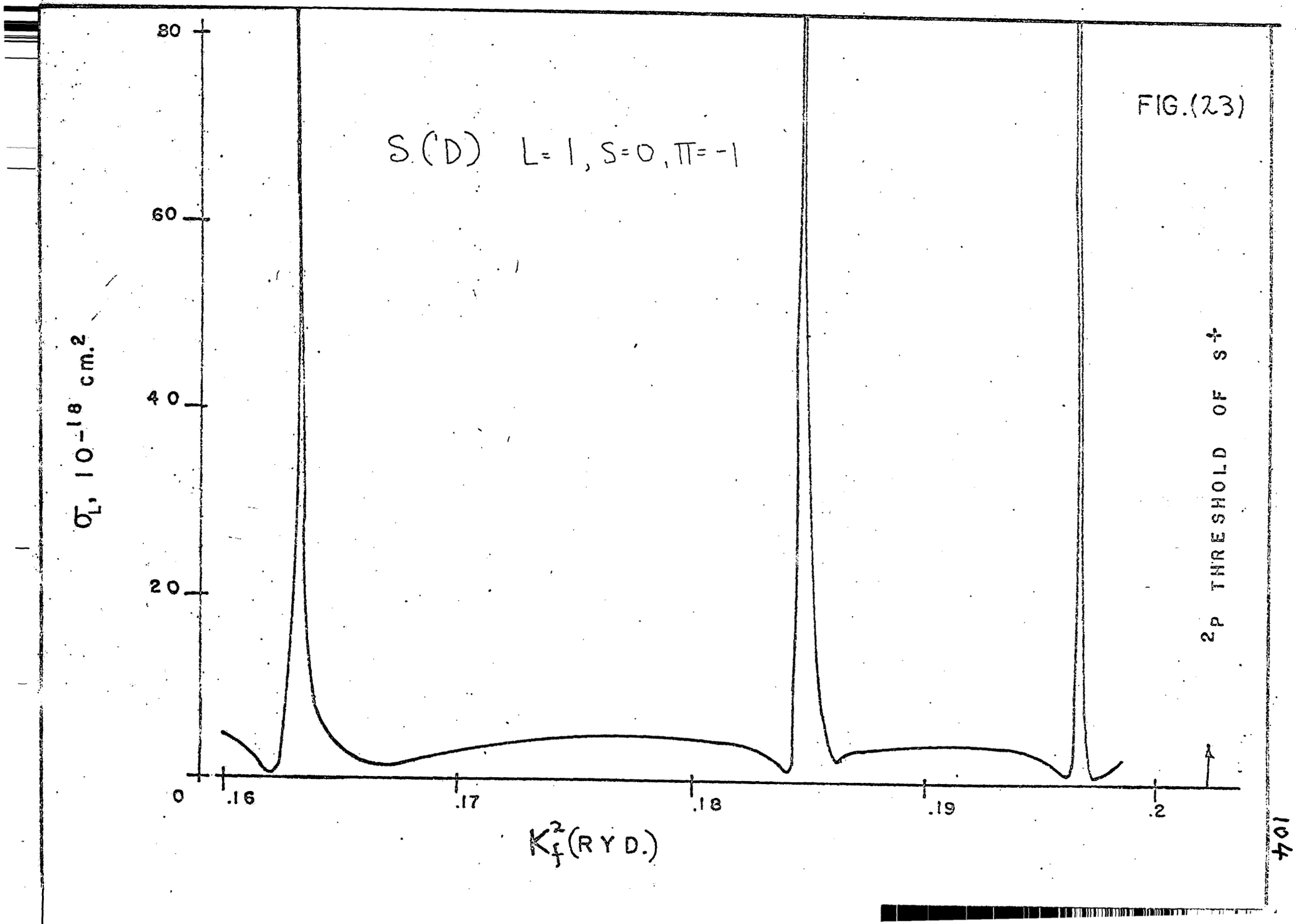
FIG.(23)
S('D) L=1, S=0, π=-1
σ_L, 10^{-18} cm.^{2}
80
60
40
20
0
.16
.17
.18
.19
.2
K_f^2(RYD.)
^2P THRESHOLD OF S^+

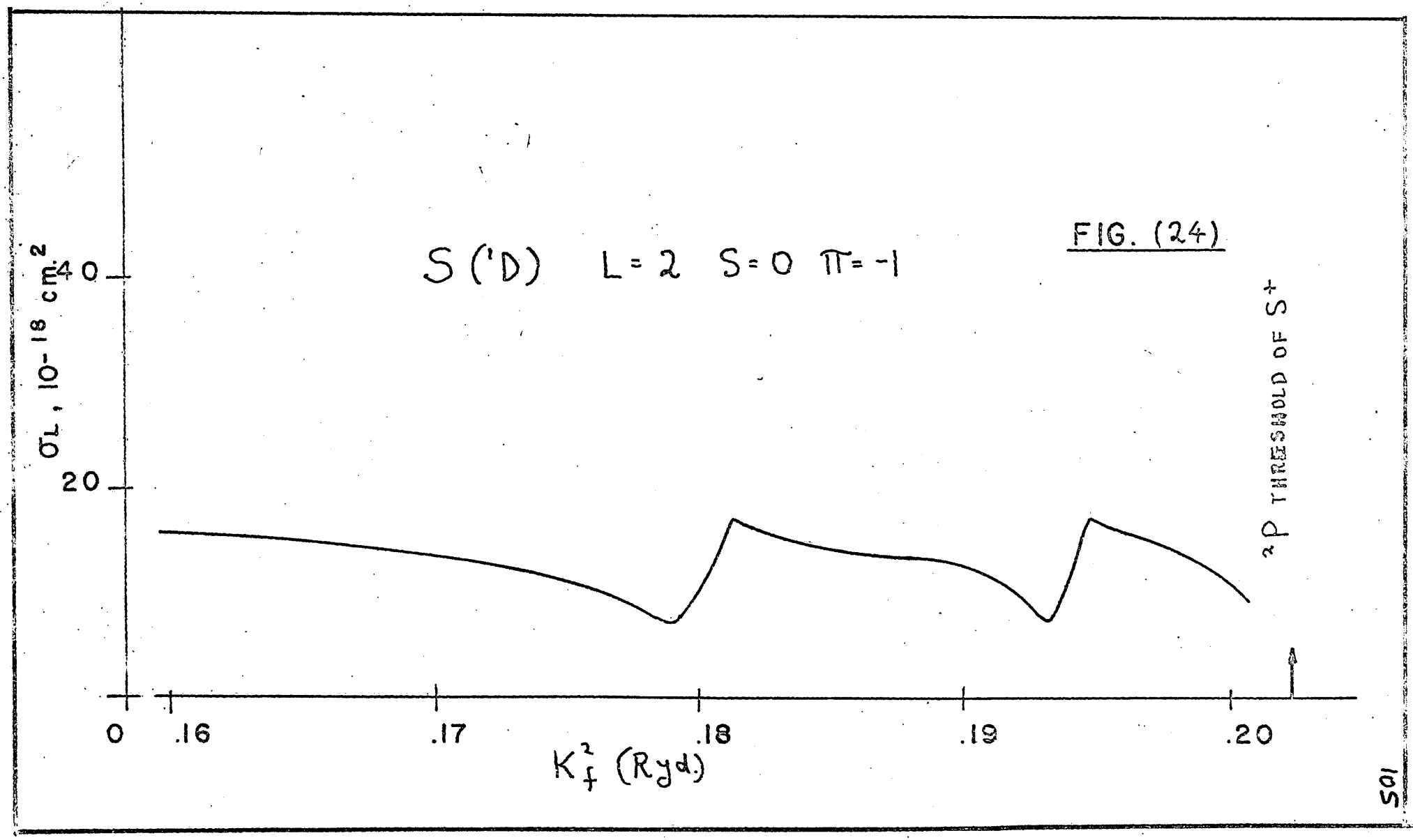
S ('D) L = 2 S = 0 π = -1
FIG. (24)
σL, 10-18 cm2
40
20
0
.16
.17
.18
.19
.20
K2f (Ryd.)
2P THRESHOLD OF S+
501

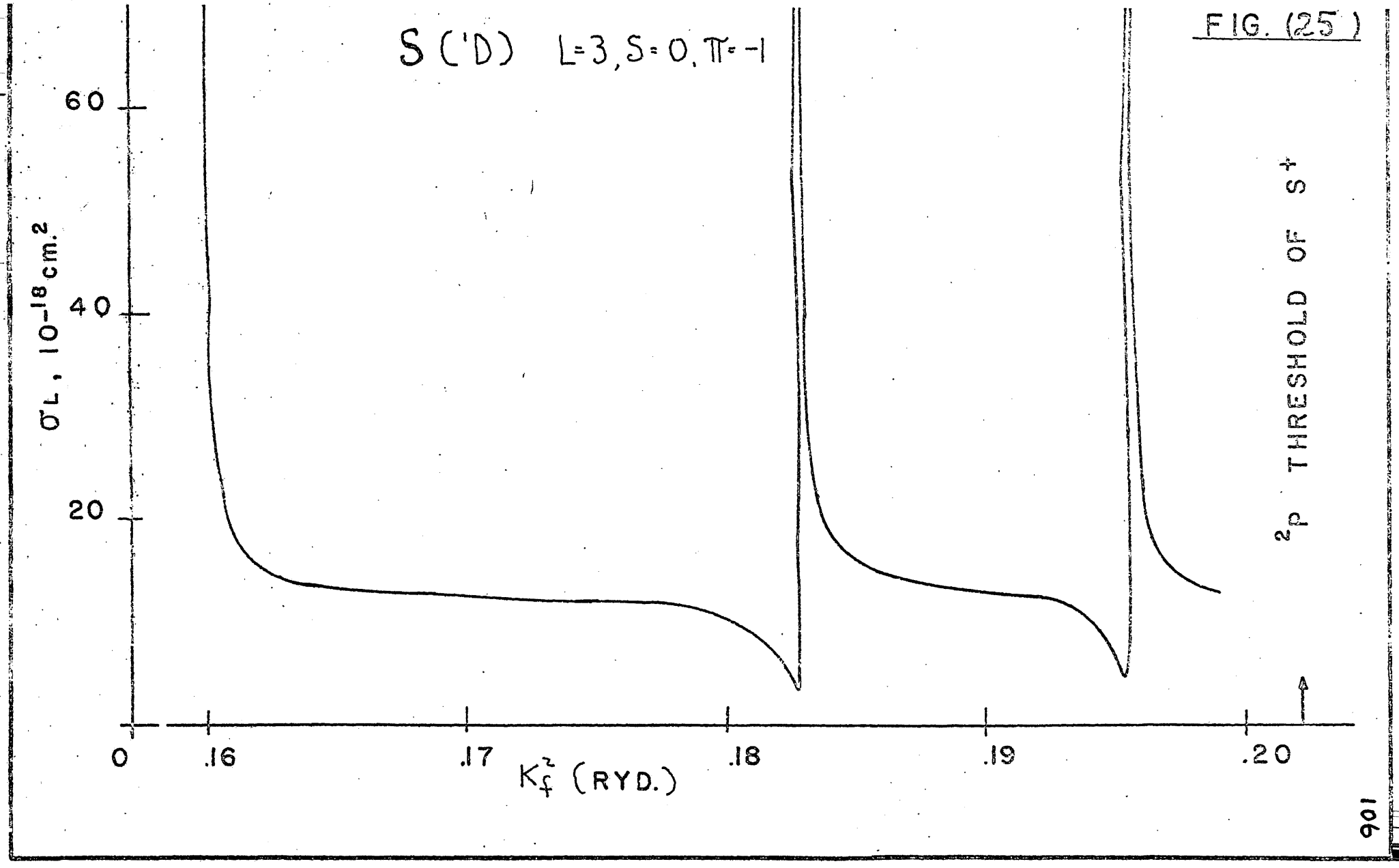
S ('D) L=3, S=0, π=-1
FIG. (25)
60
40
20
σ_L, 10^{-18} cm.^{2}
0
.16
.17
.18
.19
.20
K_f^2 (RYD.)
^2P THRESHOLD OF S^+
901

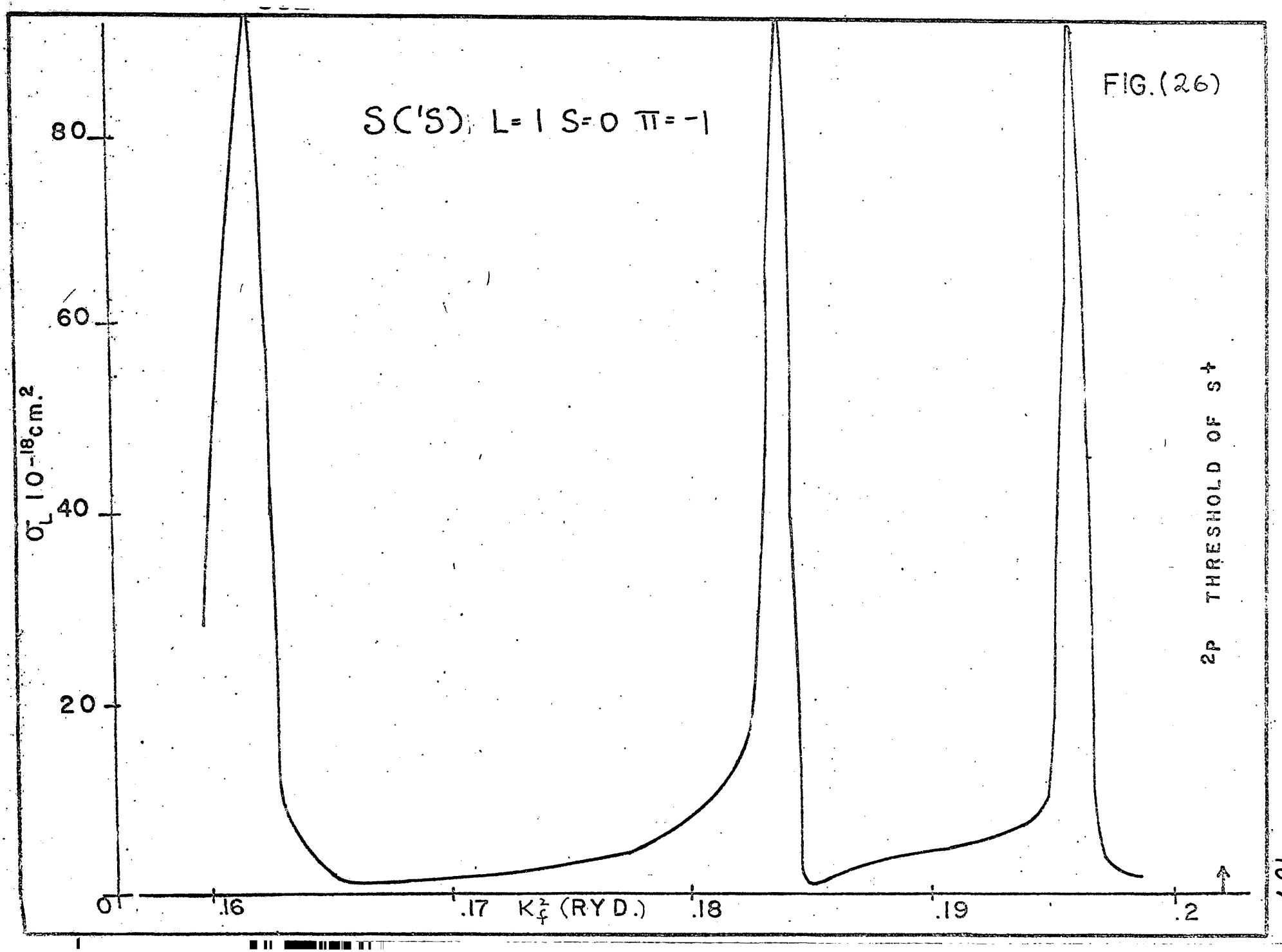
FIG.(26)
S('S); L=1 S=0 π=-1
80
60
40
20
0
σ_L 10^{-18}cm.^{2}
.16
.17
K_f^2 (RYD.)
.18
.19
.2
2P THRESHOLD OF S^+

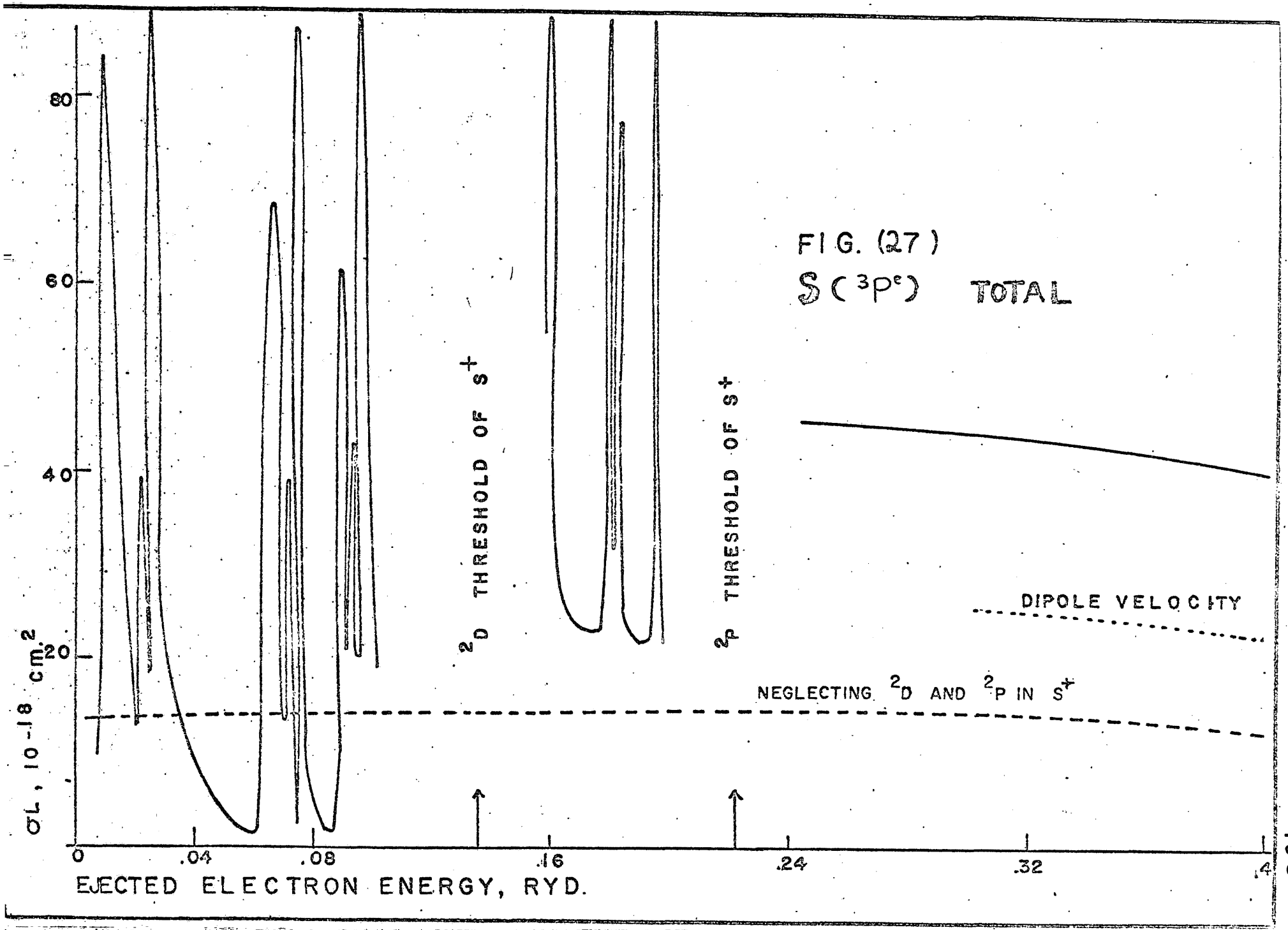
FIG. (27)
S (3Pe) TOTAL
2D THRESHOLD OF S+
2P THRESHOLD OF S+
DIPOLE VELOCITY
NEGLECTING 2D AND 2P IN S+
σL , 10-18 cm2
80
60
40
20
0
.04
.08
.16
.24
.32
.4
EJECTED ELECTRON ENERGY, RYD.

wave are tabulated in table 15.

The results for the ^1D state of sulphur are similar and are presented in figures 23 to 25, and in table 16. We note that the $^1P^o$ partial wave which also contributes to the photoionization of S (^1S) has only one series of resonances whereas we expect two series converging on the S^+ (^2P) threshold since

$$h\nu + S(^1D) \longrightarrow {}^1P \longrightarrow \begin{matrix} S^+(3p)^3\ {}^2D + \epsilon d \\ S^+(3p)^3\ {}^2P + \epsilon s \\ \qquad\qquad + \epsilon d \end{matrix}$$

The results for $S(^1S)$ are presented in figure 26 and table 17. The partial wave contributions to the photoionization cross sections above all thresholds for the three terms of sulphur are given in table 18.

Cl

Recently new Rydberg series of Chlorine have been observed in absorption in the 600-1500 ^oA region by Huffman et al[61]. The series are due to transitions from the $^2P^o$ ground state to $(3p)^4$ ns and $(^3P)^4$ nd and converge to the $(^3P)^4$ states ^3P, ^1D and ^1S. In figures 28 to 30 and in table 19 we present graphs and tables of resonance series converging on the excited ^1D and ^1S states of Cl^+. Unfortunately ref. (61) was a preliminary report so we cannot compare the observed positions of these resonances with our calculated values, as we have done for oxygen[37]. Line shape parameters, namely on q-values, have been determined theoretically and experimentally only for simple systems such as Helium[27]. It is hoped that the values presented

FIG. (28) $CL(^2P)$ $L=0$, $S=\frac{1}{2}$, $\Pi=1$

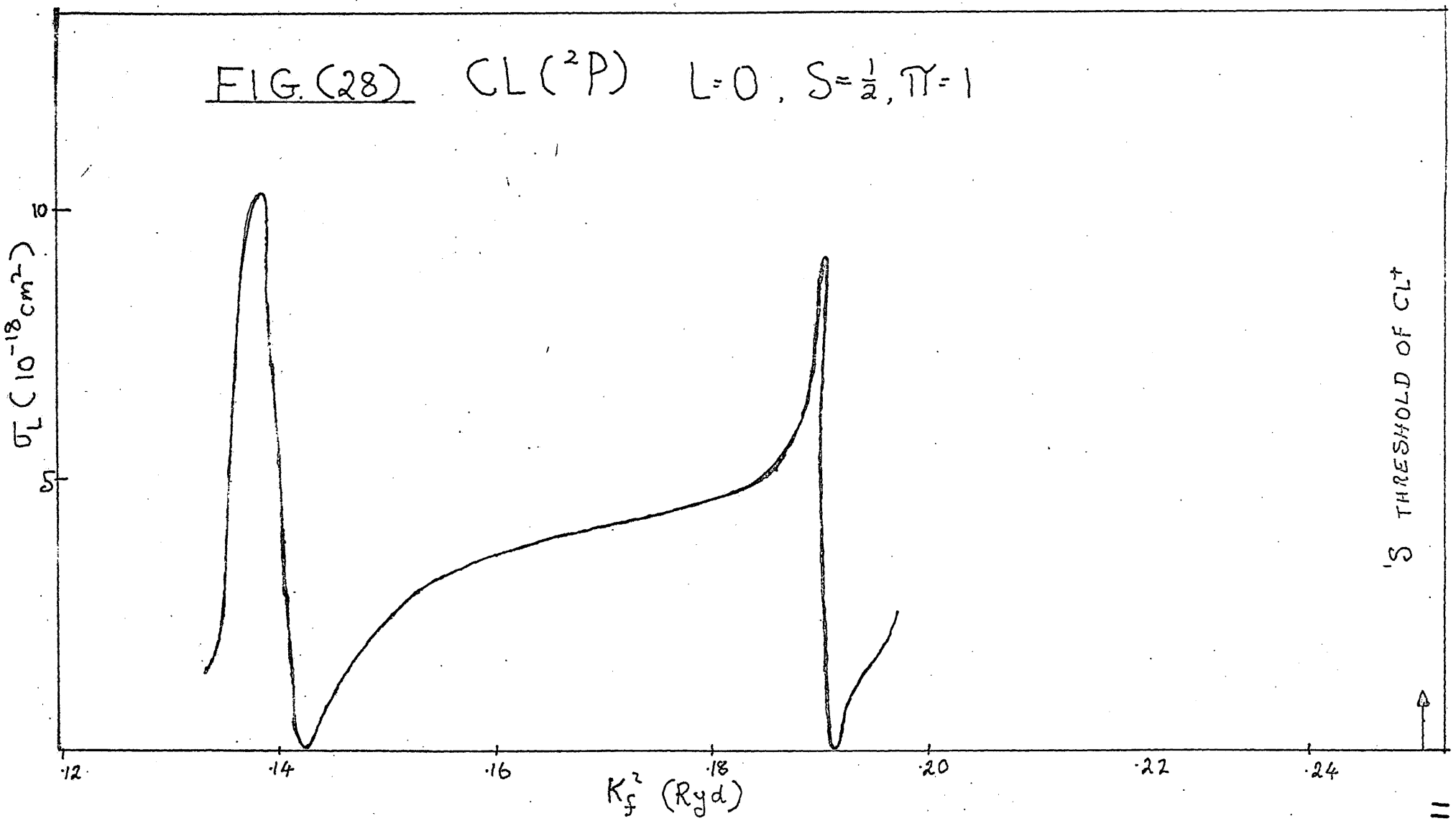

FIG (29) CL (^{2}P) L = 1 S = $\frac{1}{2}$ Π = 1

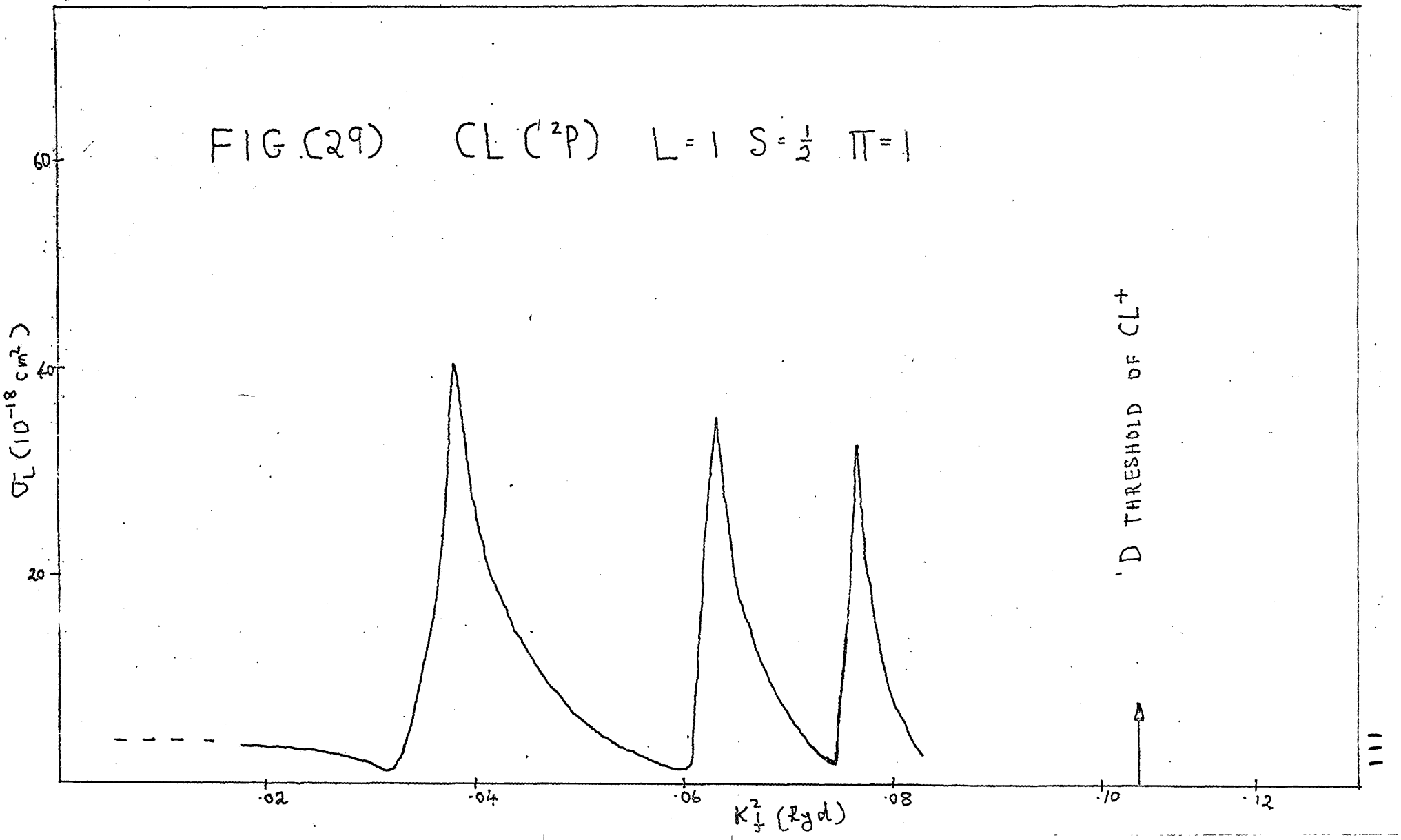

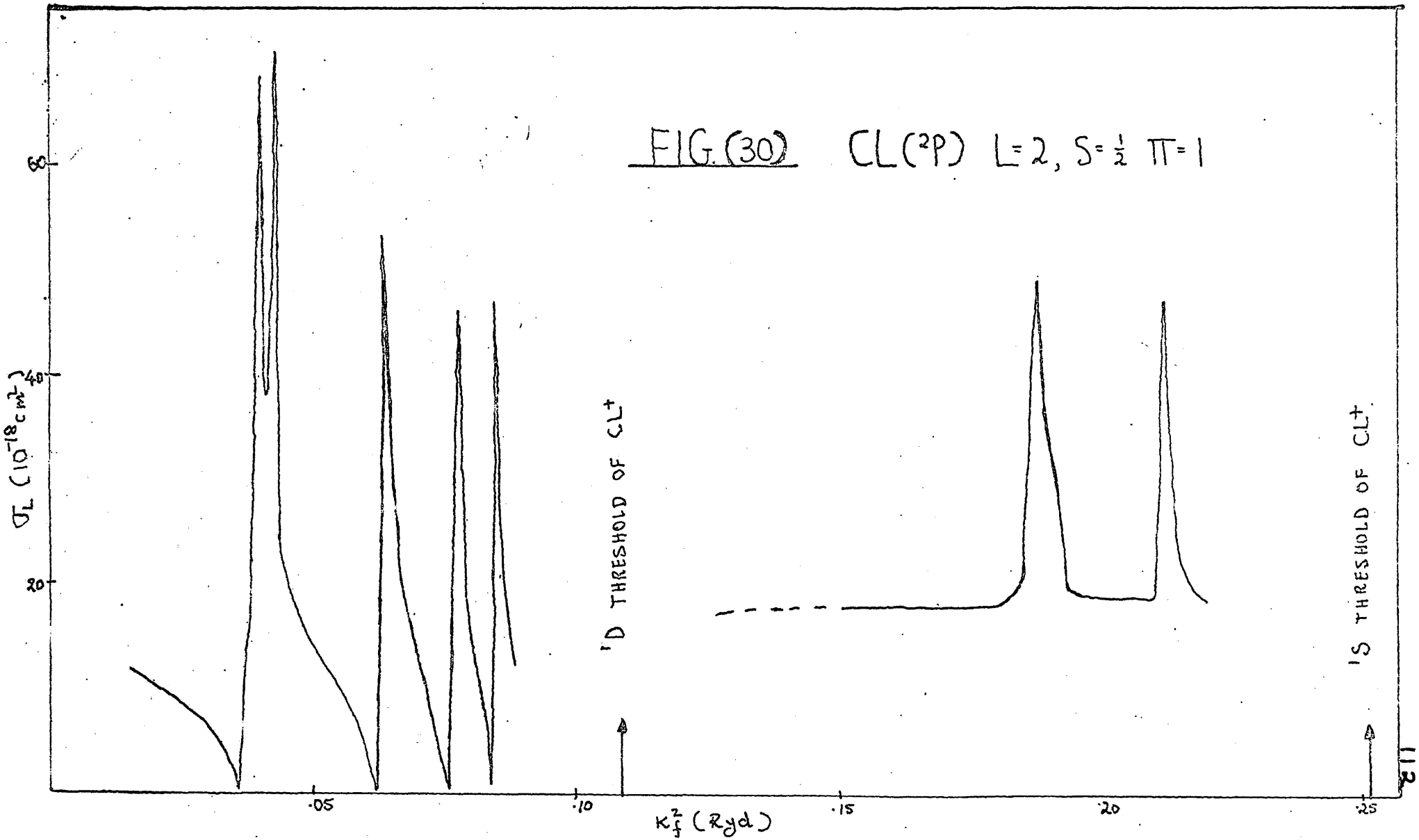
FIG. (30) CL(²P) L=2, S=½ π=1
σL (10⁻¹⁸ cm²)
60
40
20
.05
.10
.15
.20
.25
k²f (Ryd)
¹D THRESHOLD OF CL⁺
¹S THRESHOLD OF CL⁺

here should serve as a guide to experimenters on what to expect in more complicated systems such as the ones we have considered. In table 19 we present the partial wave contributions to the photoionization cross sections of $C\ell\ ^2P$ above all thresholds.

The Negative Ions

The photodetachment cross sections of electrons from the negative ions of silicon, sulphur and chlorine have been calculated by Robinson and Geltman whose tabulated values we compare with the present calculations in figures 31, 32 and 33. These authors use a central-field model i.e. a single radial equation, in which a parameter is adjusted in the potential to yield the observed binding energies of the negative ions. In other words the method is somewhat empirical, like the quantum defect method, in which experimental observations are used to impose constraints on the model. On the other hand the close-coupling approach is strictly an *ab initio* calculation. Consequently it is remarkable that the two techniques are in close agreement for photodetachment from the $^4S^o$ ground state of silicon (figure 31).

We have also computed photodetachment cross sections for S^- and $C\ell^-$, and we compare them with those given by Robinson and Geltman in figures 32 and 33. Calculations on $C\ell^-$ have also been reported by Moskvin[63] and Cooper[64]. We note that our agreement with reference (62) is poor for $C\ell^-$. Berry *et al*[65] gives a value of $15.5 \times 10^{-18} cm^2$ for the photodetachment cross

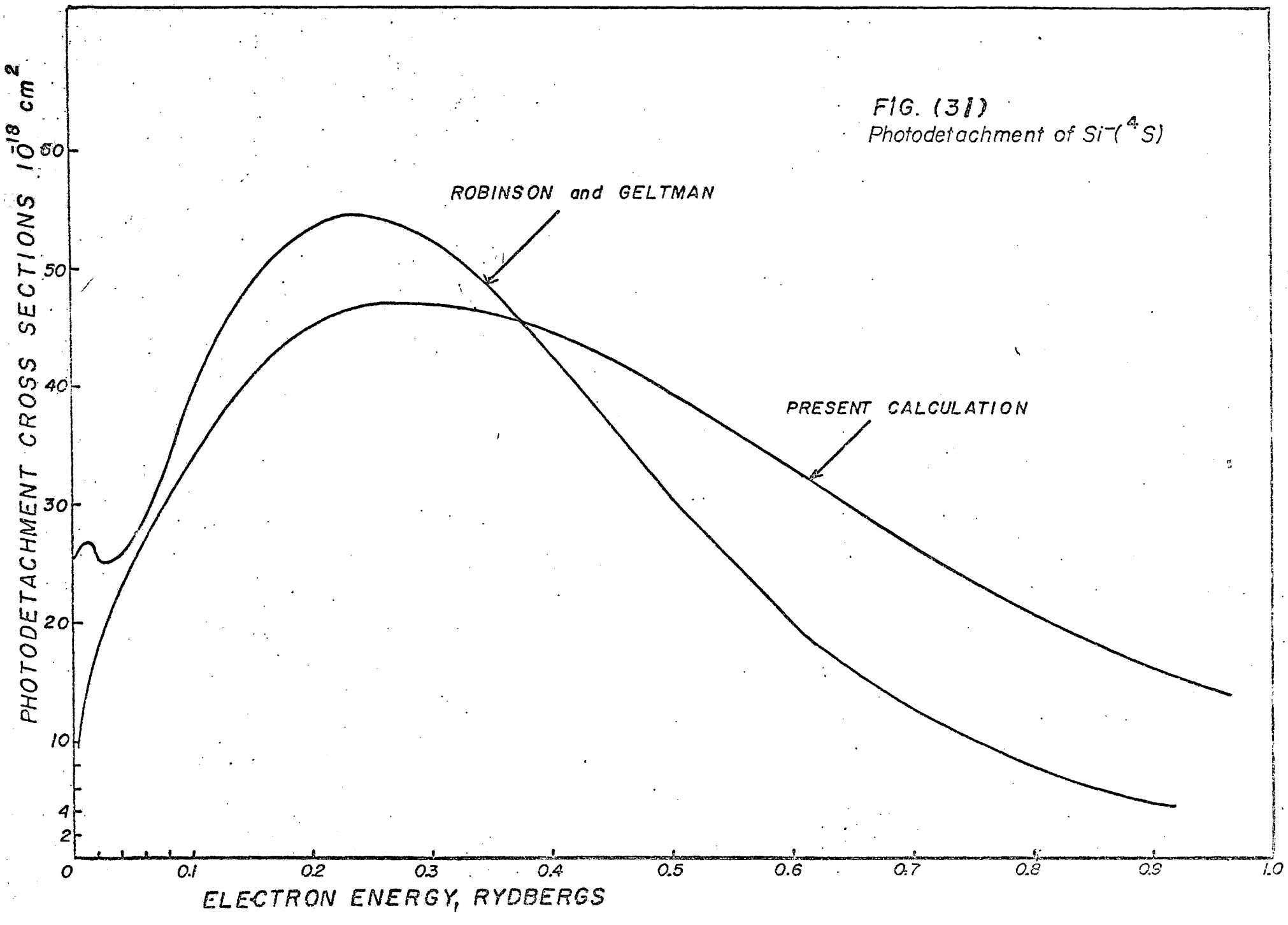
FIG. (31)
Photodetachment of $Si^-(^4S)$
ROBINSON and GELTMAN
PRESENT CALCULATION
PHOTODETACHMENT CROSS SECTIONS 10^{-18} cm^2
60
50
40
30
20
10
4
2
0
0.1
0.2
0.3
0.4
0.5
0.6
0.7
0.8
0.9
1.0
ELECTRON ENERGY, RYDBERGS

FIG. (32)

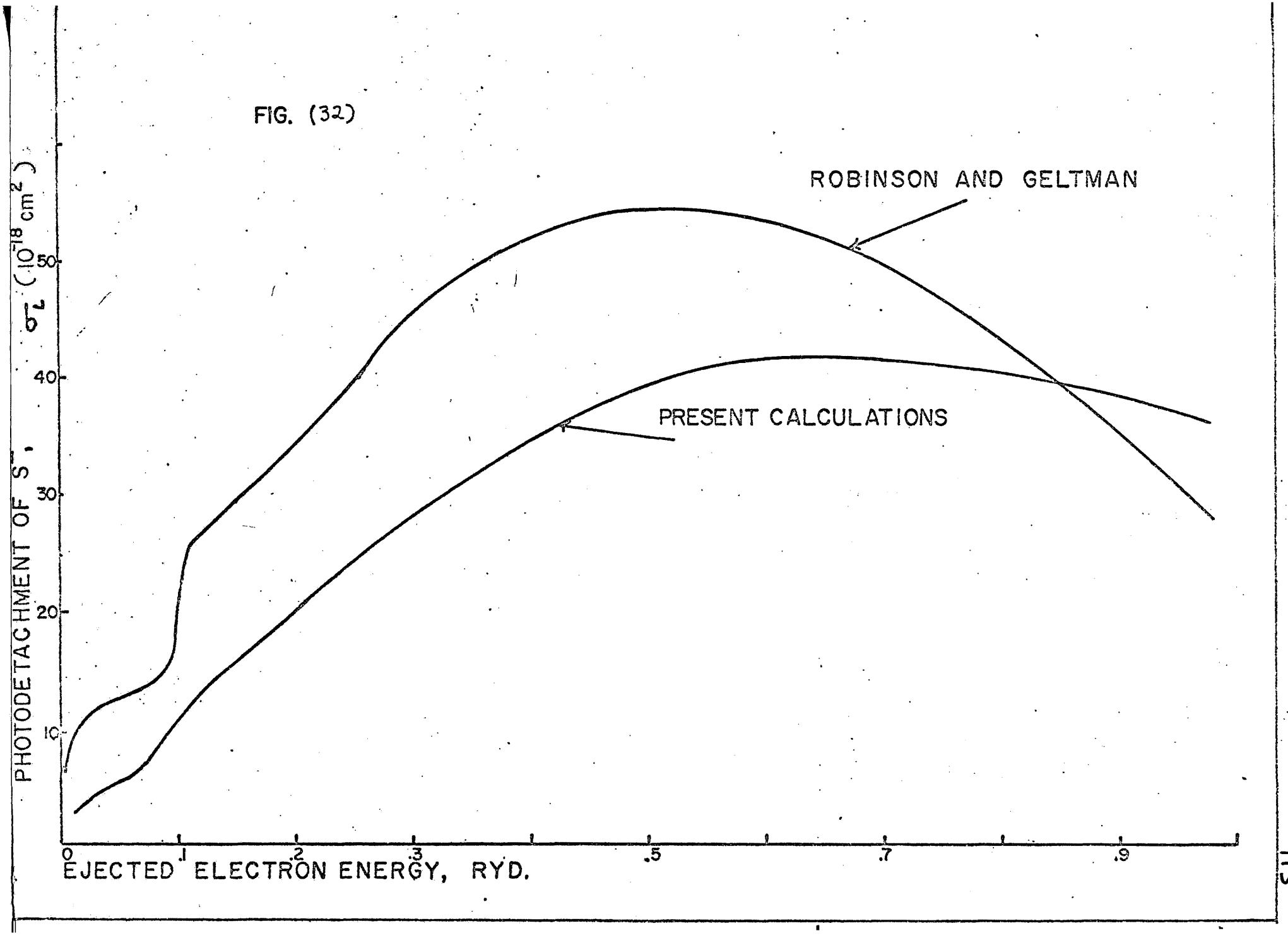
ROBINSON AND GELTMAN
PRESENT CALCULATIONS
PHOTODETACHMENT OF S⁻, σ_L (10⁻¹⁸ cm²)
10
20
30
40
50
0
.1
.2
.3
.5
.7
.9
EJECTED ELECTRON ENERGY, RYD.

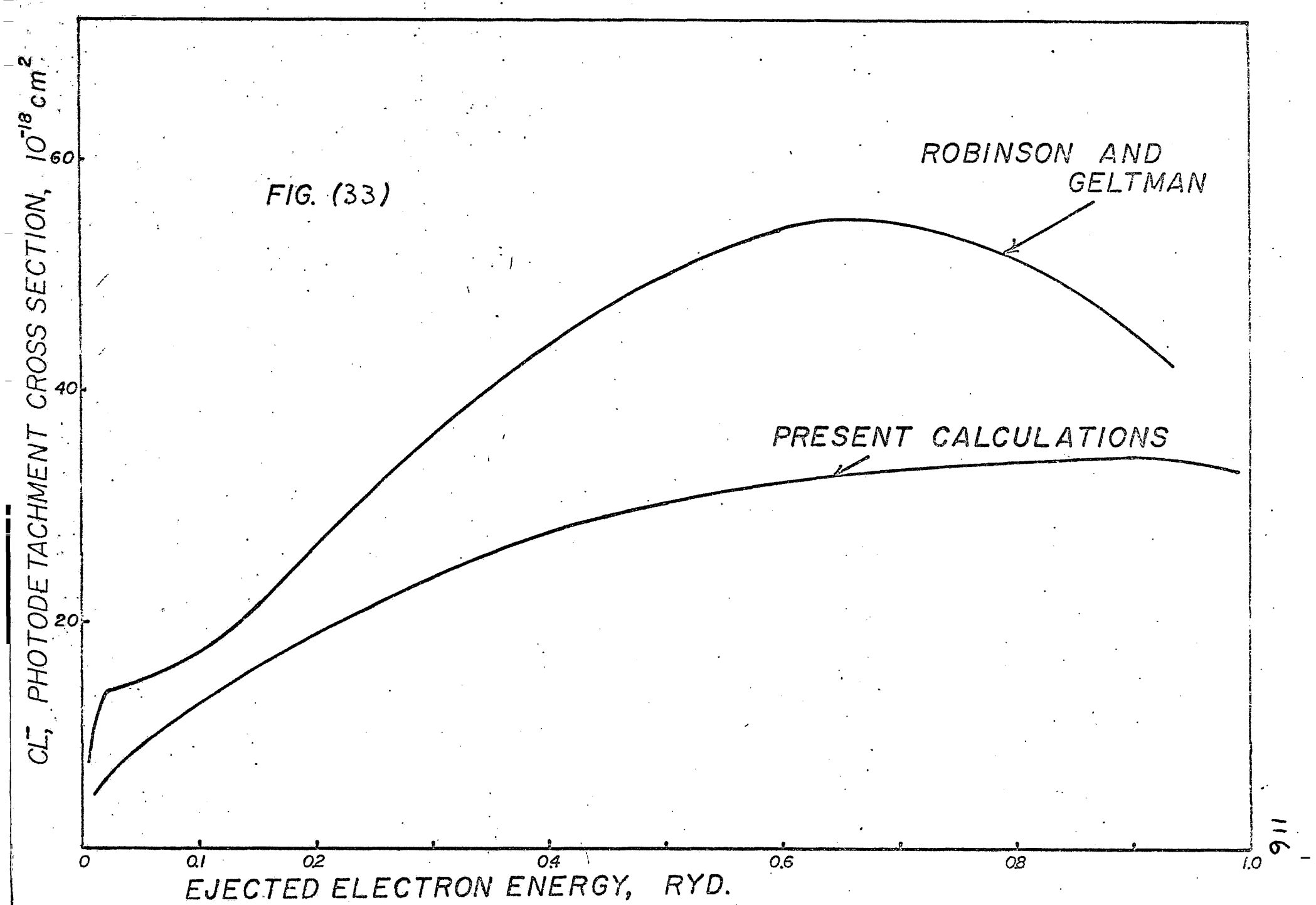
FIG. (33)
ROBINSON AND GELTMAN
PRESENT CALCULATIONS
Cl^-, PHOTODETACHMENT CROSS SECTION, 10^{-18} cm^2
60
40
20
0
0.1
0.2
0.4
0.6
0.8
1.0
EJECTED ELECTRON ENERGY, RYD.

section at $K^2=.0064$ ad we see from figure 33 that our values are outside the error limits of this experiment.

In the photodetachment calculations we have used the binding energies tabulated in reference (62) and we have represented our initial states by analytic Hartree-Fock wave function given by Clementi[36]. It is possible that our results could be improved by using wave functions other than the Hartree-Fock type to represent our initial states, since for negative ions these wave functions are overdamped asymptotically.

TABLE VI(a) Photoionization of Nitrogen (^2P)

$$h\nu + N(^2P) \rightarrow {}^2S^e \rightarrow N^+(^1D) + e\ d$$
$$\rightarrow N^+(^1S) + e\ s$$

n	E_r	Γ	q	σ_a	σ_b	$\sigma_a \frac{\pi}{2} \Gamma(q^2-1)\frac{\sigma_a}{\sigma_a+\sigma_b}$		Quantum Defect	δ_o
3d	.1784	1.281×10^{-3}	-7.42	.495	0	5.395×10^{-2}	1	.1064	-0.1066
4d	.2320	5.022×10^{-4}	-7.03	.498	0	1.901×10^{-2}	1	.0906	-0.0803
5d	.2562	2.531×10^{-4}	-7.05	.467	0	9.055×10^{-3}	1	.0993	-0.0987
6d	.2691	1.445×10^{-4}	-6.70	.498	0	4.960×10^{-3}	1	.0977	-0.0974
7d	.2768	9.001×10^{-5}	-6.51	.510	0	2.988×10^{-3}	1	.0978	-0.0942
8d	.2818	6.024×10^{-5}	-6.47	.510	0	1.974×10^{-3}	1	.0970	-0.0932
9d	.2852	4.005×10^{-5}	-6.80	.509	0	1.449×10^{-3}	1	.0979	-0.1007

TABLE VI (b) Photoionization of Nitrogen (^2P)

$$h\nu + N\ (^2P) \rightarrow {}^2P \rightarrow N^+\ (^3P) + e\ s$$
$$N^+\ (^1D) + e\ d$$

n	E_r	Γ	q	σ_a	σ_b	$\sigma_a \frac{\pi}{2}\Gamma(q^2-1)$	$\frac{\sigma_a}{\sigma_a+\sigma_b}$	Quantum Defect	δ_o
4dd	.0297	3.611×10^{-5}	23.60	1.727	.104	5.445×10^{-2}	.943	.982	2.985
5d	.0775	2.468×10^{-5}	21.27	1.748	.112	3.059×10^{-2}	.940	.985	.2944
6d	.0997	1.440×10^{-5}	20.27	1.753	.116	1.625×10^{-2}	.938	.986	.2943
7d	.1119	8.975×10^{-6}	19.78	1.755	.119	9.656×10^{-3}	.936	.987	.2933
8d	.1192	5.901×10^{-6}	19.51	1.756	.121	6.179×10^{-3}	.935	.987	.2928
9d	.1239	4.110×10^{-6}	19.31	1.756	.122	4.216×10^{-3}	.935	.987	.2927

TABLE VI (c) Photoionization of Nitrogen (^2P)

$$h\nu + N(^2P) \rightarrow {}^2P \rightarrow N^+ (^3P) + e\ d$$

$$N^+ (^1D) + e\ s$$
$$+ e\ d$$
$$+ e\ g$$

$$N^+ (^1S) + e\ d$$

n	E_r	Γ	q	σ_a	σ_b	$\sigma_a \frac{\pi}{2}\Gamma(q^2-1)$	$\frac{\sigma_a}{\sigma_a+\sigma_b}$	Quantum Defect	δ_o
4s	.0201	6.948×10^{-6}	35.61	2.518	0	3.480×10^{-2}	1	1.1063	-0.06936
5d	.0274	4.577×10^{-6}	4.81	2.801	0	4.465×10^{-4}	1	2.0093	-0.06982
5s	.0737	2.798×10^{-6}	25.17	2.74	0	7.617×10^{-3}	1	1.1017	-0.06791
6d	.0765	3.359×10^{-6}	10.60	2.97	0	1.745×10^{-3}	1	2.0150	-0.06877
6s	.0979	1.348×10^{-6}	22.33	2.76	0	2.909×10^{-3}	1	1.0999	-0.06710
7d	.0993	2.097×10^{-6}	21.66	3.04	0	4.688×10^{-3}	1	2.0160	-0.06825
7s	.1108	7.608×10^{-7}	7.19	2.87	0	1.739×10^{-4}	1	1.0987	-0.06663
8d	.1116	1.360×10^{-6}	47.02	3.07	0	1.449×10^{-2}	1	2.0163	-0.06798
8s	.1185	4.658×10^{-7}	2.53	2.74	0	1.083×10^{-5}	1	1.0953	-0.06629
9d	.1190	9.162×10^{-7}	26.31	3.08	0	3.064×10^{-3}	1	2.0162	-0.06773
			converging on ^1S Threshold						
5d	.1859	4.397×10^{-4}	-21.12	.431	4.636	1.325×10^{-1}	.085	2.0094	.2705
6d	.2349	2.021×10^{-4}	-24.24	.365	4.779	6.796×10^{-2}	.071	2.0132	.2636
7d	.2575	1.070×10^{-4}	-26.61	.311	4.861	3.695×10^{-2}	.060	2.0151	.2604
8d	.2699	6.348×10^{-4}	-26.90	.307	4.637	2.212×10^{-2}	.062	2.0164	.2587
9d	.2773	3.971×10^{-4}	-28.80	.276	4.929	1.426×10^{-2}	.053	2.0174	.2578

TABLE VII (a) Photoionization of $N(^2D)$

$$h\nu + N(^2D) \rightarrow {}^2P \rightarrow \begin{matrix} N^+(^3P) + e_s \\ N^+(^1D) + e_d \end{matrix}$$

n	E_r	Γ	q	σ_a	σ_b	$\sigma_a \frac{\pi}{2}\Gamma(q^2-1)$	$\frac{\sigma_a}{\sigma_a + \sigma_b}$	Quantum Defect	δ_o
4d	.0297	3.611×10^{-5}	14.71	.599	.726	7.320×10^{-3}	.452	.982	.2985
5d	.0775	2.468×10^{-5}	15.01	.589	.693	5.121×10^{-3}	.459	.985	.2944
6d	.0997	1.1440×10^{-5}	14.27	.563	.675	2.580×10^{-3}	.455	.986	.2943
7d	.1119	8.975×10^{-6}	13.92	.577	.668	1.568×10^{-3}	.463	.987	.2933
8d	.1192	5.901×10^{-6}	13.83	.506	.662	8.926×10^{-4}	.433	.987	.2928
9d	.1239	4.110×10^{-6}	13.69	.488	.641	6.046×10^{-4}	.432	.987	.2927

TABLE VII (b) Photoionization of Nitrogen (^2D)

$$h\nu + N(^2D) \rightarrow {}^2D^e \rightarrow \begin{matrix} N^+(^3P) + ed_{es} \\ N^+(^1D) + ed_{eg} \\ N^+(^1S) + ed \end{matrix}$$

n	E_r	Γ	q	σ_a	σ_b	$\sigma_a \frac{\pi}{2}\Gamma(q^2-1)$	$\frac{\sigma_a}{\sigma_a + \sigma_b}$	Quantum Defect	δ_o
4s	.0201	6.948×10^{-6}	34.05	.644	0.0	8.140×10^{-3}	1	1.1063	-0.06936
5d	.0274	4.577×10^{-6}	-53.09	.671	0	1.359×10^{-2}	1	2.0093	-0.06982
5s	.0737	2.798×10^{-6}	42.10	.691	0	5.379×10^{-3}	1	1.1017	-0.06791
6d	.0765	3.359×10^{-6}	-19.05	.737	0	1.408×10^{-3}	1	2.0150	-0.06877
6s	.0979	1.348×10^{-6}	26.24	.767	0	1.117×10^{-3}	1	1.0999	-0.06710
7d	.0993	2.097×10^{-6}	-65.40	.765	0	1.078×10^{-2}	1	2.0160	-0.06825
7s	.1108	7.608×10^{-7}	17.85	.773	0	2.934×10^{-4}	1	1.0987	-0.06663
8d	.1116	1.360×10^{-6}	-25.01	.775	0	1.034×10^{-3}	1	2.0163	-0.06798
8s	.1185	4.658×10^{-7}	12.39	.793	0	8.850×10^{-5}	1	1.0953	-0.06629
9d	.1190	9.162×10^{-7}	-16.89	.805	0	3.293×10^{-4}	1	2.0162	-0.06773
converging on ^1S Threshold									
5d	.1859	4.397×10^{-4}	-0.5528	1.153	2.2158	5.530×10^{-4}	.3422	2.0094	.2705
6d	.2349	2.021×10^{-4}	-0.4947	1.338	2.091	2.941×10^{-4}	.3902	2.0132	.2636
7d	.2575	1.070×10^{-4}	-0.4696	1.400	2.045	1.834×10^{-4}	.4063	2.0151	.2604
8d	.2773	3.971×10^{-4}	-0.4546	1.426	2.023	1.128×10^{-4}	.4134	2.0164	.2587
9d	.2773	3.971×10^{-4}	-0.4360	1.459	1.991	7.371×10^{-5}	.4228	2.0174	.2578

TABLE VII(c) Photoionization of Nitrogen (^2D)

$$h\nu + N(^2D) \rightarrow {}^2F^e \rightarrow \begin{matrix} N^+(^3P) + e\ d \\ \quad\quad\quad + e\ g \\ N^+(^1D) + e\ d \\ \quad\quad\quad + e\ g \end{matrix}$$

n	E_r	Γ	q	σ_a	σ_b	$\sigma_a \frac{\pi}{2} \Gamma(q^2-1)$	$\frac{\sigma_a}{\sigma_a + \sigma_b}$	Quantum Defect	δ_o
4d	.0245	9.416×10^{-5}	18.45	2.979	.0608	1.495×10^{-1}	.980	1.0392	.05215
5d	.075691	6.545×10^{-5}	14.69	3.331	.002	7.355×10^{-2}	.999	1.0422	.0576
6d	.09883	4.215×10^{-5}	13.24	3.349	.002	3.865×10^{-2}	.999	1.0423	.0585
7d	.11134	2.350×10^{-5}	13.99	3.475	.005	2.498×10^{-2}	.998	1.0440	.0617
8d	.11882	1.641×10^{-5}	13.01	3.497	.0035	1.517×10^{-2}	.999	1.0440	.0628
9d	.12373	1.131×10^{-5}	12.84	3.518	.004	1.024×10^{-2}	.999	1.0438	.0633

TABLE VIII

Partial wave contributions to the photoionization cross sections of N (^4S, ^2D, ^2P)

$L_o S_o$	K_f^2	Dipole Velocity $^4P^e$	Dipole Length $^4P^e$
$^4S^o$	.025	9.799	10.318
	.05	9.967	10.631
	.1	10.205	11.142
	.15	10.330	11.512
	.2	10.365	11.914
	.25	10.332	11.914
	.3	10.243	11.982
	.35	10.112	11.982
	.4	9.949	11.924
	.5	9.553	11.676
	.6	9.103	11.304
	.8	8.148	10.360
	1.0	7.221	9.327
	1.5	5.269	6.959
	2.0	3.865	5.163

		Dipole Velocity			Dipole Length		
		$^2P^e$	$^2D^e$	$^2F^e$	$^2P^e$	$^2D^e$	$^2F^e$
$^2D^o$	.15	1.030	0.000	5.291	1.063	0.000	6.264
	.20	1.019	0.000	5.468	1.078	0.000	6.645
	.25	.996	0.000	5.534	1.075	0.000	6.878
	.30	.971	4.159	5.550	1.067	3.313	7.038
	.35	.944	2.963	5.528	1.053	3.436	7.138

TABLE VIII

(continued)

	$^2P^e$	$^2D^e$	$^2F^e$	$^2P^e$	$^2D^e$	$^2F^e$
.40	.916	2.910	5.479	1.034	3.409	7.189
.50	.857	2.780	5.322	.989	3.312	7.179
.60	.799	2.632	5.120	.936	3.177	7.068
.80	.687	2.324	.664	.822	2.856	6.668
1.0	.589	2.032	4.208	.712	2.525	6.173
1.5	.403	1.442	3.227	.490	1.818	4.938
2.0	.284	1.039	2.489	.343	1.318	3.916
$^2P^o$	$^2S^e$	$^2P^e$	$^2D^e$	$^2S^e$	$^2P^e$	$^2D^e$
.15	0.000	2.948	0.000	0.000	3.012	0.000
.20	0.000	2.976	0.000	0.000	3.137	0.000
.25	0.000	2.958	0.000	0.000	3.200	0.000
.30	.784	2.921	6.086	.973	3.233	7.761
.35	.765	2.871	6.088	.950	3.241	7.835
.40	.696	2.811	6.057	.921	3.229	7.923
.50	.696	2.675	5.899	.863	3.161	7.918
.60	.651	2.527	5.666	.808	3.053	7.753
.80	.566	2.231	5.116	.705	2.779	7.187
1.0	.492	1.957	3.402	.435	1.829	4.985
2.0	.250	1.031	2.568	.315	1.347	3.829

TABLE IX

Partial wave contributions to the photoionization cross sections of $N^+(^3P, ^1D, ^1S)$

L_oS_o	K_f^2	Dipole Velocity			Dipole Length		
		$^3P^o$	$^3D^o$		$^3P^o$	$^3D^o$	
^3P	.025	1.923	4.537		2.146	5.443	
	.05	1.928	4.557		2.157	5.478	
	.10	1.862	4.453		2.082	5.326	
	.15	1.797	4.276		2.023	5.174	
	.20	1.733	4.139		1.956	5.002	
	.30	1.612	3.875		1.829	4.726	
	.40	1.499	3.625		1.707	4.440	
	.50	1.394	3.389		1.591	4.167	
	.60	1.296	3.169		1.483	3.909	
	.80	1.123	2.773		1.289	3.438	
	1.0	.976	2.432		1.123	3.025	
	1.5	.700	1.774		.805	2.218	
	2.0	.516	1.321		.592	1.655	
		$^1P^o$	$^1D^o$	$^1F^o$	$^1P^o$	$^1D^o$	$^1F^o$
^1D	.025	.397	1.088	4.482	.442	1.088	5.827
	.05	.396	1.085	4.519	.442	1.086	5.892
	.10	.378	1.039	4.402	.443	1.041	5.769
	.15	.362	.994	4.285	.406	.997	5.643
	.20	.347	.952	4.169	.389	.954	5.515
	.30	.319	.872	3.943	.358	.875	5.259

TABLE IX

(continued)

.40	.294	.799	2.725	.331	.803	5.005
.50	.271	.734	3.516	.305	.736	4.756
.60	.251	.675	3.319	.283	.676	4.516
.80	.217	.573	2.956	.243	.573	4.063
1.0	.188	.489	2.635	.211	.488	3.653
1.5	.137	.340	1.992	.151	.336	2.807
2.0	.103	.245	1.527	.112	.241	2.177

l_s	$l_p o$	$l_p o$
.025	6.459	7.812
.05	6.489	7.859
.10	6.274	7.619
.15	6.063	7.381
.20	5.858	7.146
.30	5.467	6.692
.40	5.101	6.259
.50	4.759	5.852
.60	4.443	5.471
.80	3.879	4.784
1.0	3.398	4.192
1.5	2.480	3.055
2.0	1.852	2.275

TABLE X (a) Photoionization of Phosphorus (^2P)

$$h\nu + P\ (^2P) \rightarrow {}^2S \rightarrow P^+\ (^1D) + ed$$
$$P^+\ (^1S) + es$$

n	E_r	Γ	q	σ_a	σ_b	$\sigma_a \frac{\pi\Gamma}{2}(q^2-1)$	$\frac{\sigma_a}{\sigma_a \pm \sigma_b}$	Quantum Defect	δ_o
5s	.1369	1.36×10^{-3}	-2.49	.272	0.0	3.02×10^{-2}	1	.908	.024
6s	.1580	6.46×10^{-4}	-2.77	2.44	0.0	1.65×10^{-2}	1	.911	.039
7s	.1696	3.42×10^{-4}	-2.12	2.44	0.0	4.59×10^{-3}	1	.915	.059
8s	.1768	2.10×10^{-4}	-2.33	3.04	0.0	4.44×10^{-3}	1	.896	.062

TABLE X (b)

$$h\nu + P\ (^2P) \rightarrow {}^2P \rightarrow P^+\ (^3P) + e\ s + e\ d$$
$$P^+\ (^1D) + e\ d$$

4d	.0178	2.95×10^{-3}	3.64	3.25	.22	1.85×10^{-1}	.936	.024	.431
5d	.0404	1.51×10^{-3}	3.68	3.68	.55	1.26×10^{-1}	.869	.034	.433
6d	.0528	9.21×10^{-4}	3.48	4.91	.84	7.91×10^{-2}	.805	.039	.431
7d	.0603	5.96×10^{-4}	3.89	4.45	1.22	5.87×10^{-2}	.785	.042	.426
8d	.0652	3.97×10^{-4}	3.10	4.62	1.64	2.48×10^{-3}	.738	.031	.454

TABLE X (c) Photoionization of Phosphrous (^2P)

$$h\nu + P(^2P) \rightarrow {}^2D \rightarrow \begin{cases} P^+ (^3P) + e\ d \\ P^+ (^1D) + e\ s \\ \qquad\quad e\ d \\ \qquad\quad e\ g \\ P^+ (^1S) + e\ d \end{cases}$$

n	E_r	Γ	q	σ_a	σ_b	$\sigma_a \frac{\pi}{2}\Gamma(q^2-1)$	$\frac{\sigma_a}{\sigma_a+\sigma_b}$	Quantum Defect	δ_o
5s	.0213	7.09×10^{-4}	2.57	7.00	0	4.37×10^{-2}	1	.905	-0.071
5d	.0386	2.62×10^{-4}	11.12	3.20	0	1.76×10^{-1}	1	.140	-0.023
6s	.0426	2.45×10^{-4}	8.15	4.00	0	1.01×10^{-1}	1	.893	-0.027
6d	.0517	1.67×10^{-4}	7.78	2.86	0	4.46×10^{-2}	1	.152	-0.004
7s	.0542	8.97×10^{-5}	5.25	1.54	0	5.76×10^{-3}	1	.885	-0.032
8s	.0608	1.39×10^{-4}	4.92	.76	0	3.85×10^{-3}	1	.954	.040
				converging on ^1S Threshold					
7d	.1283	1.75×10^{-3}	13.17	1.81	13.15	8.58×10^{-1}	.121	.174	.133
8d	.1583	1.51×10^{-3}	9.23	1.15	16.20	2.29×10^{-1}	.066	.167	.098
9d	.1671	8.60×10^{-4}	8.33	1.39	16.19	1.28×10^{-1}	.079	.179	.096

TABLE XI (a) Photoionization of Phosphorus (^2D)

$$h\nu + P\ (^2D) \rightarrow {}^2P \rightarrow P^+\ (^3P) + e\ s$$
$$+ e\ d$$
$$P^+\ (^1P) + e\ d$$

n	E_r	Γ	q	σ_a	σ_b	$\sigma_a \frac{\pi}{2} \Gamma (q^2-1)$	$\frac{\sigma_a}{\sigma_{a+}\sigma_b}$	Quantum Defect	δ_o
4d	.0178	2.95×10^{-3}	- 9.32	.22	1.57	8.76×10^{-2}	.123	.024	.431
5d	.0404	1.51×10^{-3}	-10.51	.16	1.85	4.14×10^{-2}	.079	.034	.433
6d	.0528	9.21×10^{-4}	-11.36	.13	1.76	2.40×10^{-2}	.069	.039	.431
7d	.0603	5.96×10^{-4}	-12.60	.11	1.73	1.63×10^{-2}	.060	.042	.426
8d	.0652	3.97×10^{-4}	-12.69	.10	1.77	9.97×10^{-3}	.053	.031	.452

TABLE XI (b) Photoionization of Phosphorus (^2D)

$$h\nu + P\,(^3P)\quad {}^2D \rightarrow {}^2F \rightarrow P^+(^3P)^2\ {}^3P + e\ d + e\ g$$

$$\rightarrow P^+(^3P)^2\ {}^1D + e\ d + e\ g$$

n	E_r	Γ	q	σ_a	σ_b	$\sigma_a \frac{\pi}{2}\Gamma(q^2-1)$	$\frac{\sigma_a}{\sigma_a + \sigma_b}$	Quantum Defect	δ_o
5	.0352	4.38×10^{-2}	1.36	18.33	.79	1.07×10^{-1}	.959	.325	.347
6	.0507	2.94×10^{-3}	2.63	6.99	1.44	1.91×10^{-2}	.829	.246	.337
7	.0593	2.46×10^{-3}	3.23	5.53	1.32	2.01×10^{-2}	.807	.218	.620
8	.0630	6.33×10^{-4}	1.46	10.54	1.29	1.19×10^{-2}	.891	.362	.632
9	.0676	5.87×10^{-4}	1.09	25.72	1.13	4.45×10^{-3}	.958	.342	.372

TABLE XI (c) Photoionization of Phosphorus (^2D)

$$h\nu + P\ (^2D) \rightarrow {}^2D \rightarrow \begin{cases} P^+\ (^3P) + e\ d \\ P^+\ (^1D) + e\ s \\ \qquad\qquad e\ d \\ \qquad\qquad e\ g \\ P^+\ (^1S) + e\ d \end{cases}$$

n	E_r	Γ	q	σ_a	σ_b	$\frac{\sigma_a}{2}\pi\Gamma(q^2-1)$	$\frac{\sigma_a}{\sigma_a+\sigma_b}$	Quantum Defect	δ_o
5s	.0213	7.09×10^{-4}	5.69	2.80	0.0	9.77×10^{-2}	1	.905	-0.071
5d	.0386	2.62×10^{-4}	2.69	6.67	0.0	1.71×10^{-2}	1	.140	-0.023
6s	.0426	2.45×10^{-4}	6.30	1.66	0.0	2.47×10^{-2}	1	.893	-0.027
6d	.0517	1.67×10^{-4}	3.03	4.61	0.0	9.91×10^{-3}	1	.152	-0.004
7s	.0542	8.97×10^{-5}	4.41	3.98	0.0	1.03×10^{-2}	1	.885	-0.032
8s	.0608	1.39×10^{-4}	1.62	5.58	0.0	1.98×10^{-3}	1	.954	.040
				converging on ^1S threshold					
4d	.1283	1.75×10^{-3}	.18	8.16	3.21	-2.17×10^{-2}	.72	.174	.133
5d	.1538	1.51×10^{-3}	.20	8.76	4.93	-2.00×10^{-2}	.64	.167	.098
6d	.1671	8.60×10^{-4}	.22	9.53	3.74	-1.23×10^{-2}	.72	.179	.096

TABLE XII

Partial wave contributions to the photoionization cross section of P (^4S, ^2D, ^2P)

L_oS_o	K_f^2	Dipole Velocity ^4P	Dipole Length ^4P
	.015	32.019	54.352
	.1	29.114	50.462
	.15	25.994	45.874
	.2	22.875	41.016
	.3	17.149	31.546
	.4	12.439	23.457
	.6	6.204	12.198
	.8	2.996	6.122
	1.0	1.451	3.047
	2.0	.284	.289

^2D		^2P	^2D	^2F	^2P	^2D	^2F
	.3	1.488	5.226	11.161	2.721	9.136	24.960
	.4	1.167	3.816	9.702	2.176	6.865	22.788
	.6	.733	2.011	6.822	1.345	3.802	17.524
	.8	.476	1.082	4.281	.825	2.129	12.085
	1.0	.326	.603	2.357	.528	1.209	7.477
	2.0	.113	.121	.007	.169	.159	.213

^2P		^2S	^2P	^2D	^2S	^2P	^2D
	.3	1.574	5.632	12.828	2.701	10.895	26.937
	.4	1.193	4.558	10.817	2.109	9.182	24.047

TABLE XII

(continued)

	^2S	^2P	^2D	^2S	^2P	^2D
.6	.650	2.700	7.333	1.193	5.711	17.946
.8	.359	1.467	4.563	.664	3.174	12.164
1.0	.211	.770	2.541	.381	1.677	7.444
2.0	.049	.112	.066	.059	.200	.235

TABLE XIII

Partial wave contribution to the photoionization cross sections of Al(^{2}P)

		Dipole Velocity		Dipole Length	
L_oS_o	K_f^2	$^2S^e$	$^2D^e$	$^2S^e$	$^2D^e$
$^2P^o$	.01	.849	14.373	1.805	21.992
	.02	.609	14.236	2.159	21.833
	.03	.582	13.301	2.065	20.439
	.04	.557	12.427	1.978	19.132
	.05	.534	11.669	1.892	18.216
	.075	.482	9.808	1.717	15.183
	.10	.438	8.295	1.565	12.891
	.15	.370	5.959	1.324	9.353
	.20	.318	4.307	1.142	6.847
	.30	.246	2.280	.879	3.734
	.40	.197	1.215	.691	2.038
	.50	.163	.643	.548	1.099
	.60	.137	.332	.442	.586
	.70	.117	.163	.365	.312
	.80	.102	.073	.311	.164
	.90	.089	.027	.272	.082

TABLE XIV

Partial wave contributions to the photoionization cross sections of S_i (^3P, ^1D, ^1S)

		Dipole Velocity		Dipole Length	
L_oS_o	K_f^2	$^3P^o$	$^3D^o$	$^3P^o$	$^3D^o$
$^3P^e$	.01	8.989	18.867	13.035	29.587
	.02	9.193	19.636	13.404	30.964
	.03	8.841	19.124	12.936	30.315
	.04	8.495	18.335	12.469	29.212
	.05	8.156	17.698	12.006	28.334
	.06	7.826	17.072	11.551	27.460
	.08	7.195	15.858	10.667	26.734
	.10	6.604	14.697	9.829	24.053
	.15	5.313	12.056	7.965	20.125
	.20	4.373	9.808	6.454	16.779
	.30	2.805	6.342	4.258	11.245
	.60	.939	1.523	1.381	3.075
	.80	.530	.522	.753	1.225
	1.0	.339	.145	.464	.444

		$^1P^o$	$^1D^o$	$^1F^o$	$^1P^o$	$^1D^o$	$^1F^o$
$^1D^e$	.01	2.020	3.756	14.701	3.327	3.882	27.185
	.02	2.133	3.850	16.419	3.553	3.966	30.609
	.03	2.070	3.641	16.139	3.460	3.740	30.315
	.04	2.010	3.348	15.855	3.369	3.424	29.995

TABLE XIV

(continued)

	$^1P^o$	$^1D^o$	$^1F^o$	$^1P^o$	$^1D^o$	$^1F^o$
.05	1.952	2.803	15.566	3.280	3.182	29.651
.075	1.818	2.637	14.836	3.071	2.685	28.705
.10	1.699	2.233	14.106	2.876	2.223	27.676
.15	1.492	1.618	12.676	2.529	1.575	25.505
.2	1.324	1.193	11.335	2.292	1.161	23.567
.3	1.062	.659	8.890	1.793	.617	19.455
.6	.570	.119	3.617	.871	.103	9.395
.8	.403	.034	1.690	.579	.029	5.095
1.0	.300	.006	.684	.422	.005	2.579

l_{Se}	$^1P^o$	$^1P^o$
.01	25.653	38.353
.02	26.713	40.726
.03	26.227	40.749
.04	25.761	40.864
.05	25.243	40.747
.075	23.912	40.214
.10	22.556	39.336
.15	19.864	36.904
.2	17.301	34.866
.3	12.775	27.278
.6	4.309	10.275
.8	1.912	3.659
1.0	.819	1.918

TABLE XV (a) Photoionization of Sulfur (^3P)

(a) $h\nu + S\ (^3p)^4\ ^3P^e \rightarrow {}^3S^o \rightarrow S^+\ (3p)^3\ {}^4S^o + e\ (s)$

$\rightarrow S^+\ (3p)^3\ {}^2D^o + e\ (d)$

n	E_r	Γ	q	σ_a	σ_b	$\frac{\sigma_a}{\sigma_a + \sigma_b}$	$\sigma_a \frac{\pi}{2} \Gamma (q^2-1)$	Quantum Defect	δ_o
3d	.0231	5.39×10^{-4}	9.36	1.11	0	1	.082	.019	-0.272
4d	.0727	1.46×10^{-4}	9.14	0.92	0	1	.017	.014	-0.290
5d	.0956	1.19×10^{-4}	10.08	0.720	0	1	.022	.017	-0.298

(b) $h\nu + S\ (3p)^4\ ^3P^e \rightarrow {}^3P^o \rightarrow S^+\ (3p)^3\ {}^2D^o + e(d)$

$\rightarrow S^+\ (3p)^3\ {}^2P^o + e(s)$

$+ e(d)$

n	E_r	Γ	q	σ_a	σ_b	$\frac{\sigma_a}{\sigma_a + \sigma_b}$	$\sigma_a \frac{\pi}{2} \Gamma (q^2-1)$	Quantum Defect	δ_o
6s	.1618	7.29×10^{-3}	-2.62	7.72	0	1	5.18×10^{-1}	1.987	.257
4d	.1803	4.99×10^{-4}	-1.77	10.02	0	1	1.67×10^{-2}	-0.789	.310
7s	.1842	4.31×10^{-4}	-2.81	5.62	0	1	2.62×10^{-2}	1.982	.284
5d	.1941	4.05×10^{-4}	-2.85	7.81	0	1	3.54×10^{-2}	-0.796	.299
8s	.1963	1.57×10^{-4}	-3.63	5.45	0	1	1.60×10^{-2}	1.992	.267

TABLE XV (b) Photoionization of Sulfur (^3P)

$$h\nu + S\ (3p)^4\ {}^3P^e \rightarrow {}^3D^o \rightarrow S^+\ (3p)^3\ {}^4S^e + e(d)$$
$$\rightarrow S^+\ (3p)^3\ {}^2D^o + e(s) + e(d) + e(g)$$
$$\rightarrow S^+\ (3p)^3\ {}^2P^o + e(d)$$

n	E_r	Γ	q	σ_a	σ_b	$\frac{\sigma_a}{\sigma_a+\sigma_b}$	$\sigma_a\frac{\pi\Gamma}{2}(q^2-1)$	Quantum Defect	δ_o
4d	.0138	6.60×10^{-3}	9.93	6.66	0.0	1	6.806	0.1349	.234
6s	.0252	9.33×10^{-4}	6.01	7.15	0.0	1	.365	0.991	.276
5d	.0660	5.31×10^{-3}	3.70	3.39	0.0	1	.231	0.210	.341
7s	.0746	1.75×10^{-4}	7.20	6.81	0.0	1	.095	0.952	.362
6d	.0897	1.12×10^{-3}	5.02	3.54	0.0	1	..004	0.334	.401
8s	.0958	3.01×10^{-4}	6.82	3.97	0.0	1	.074	1.989	.364
converging on ^2P threshold									
6d	.1819	5.26×10^{-4}	9.32	1.85	16.24	.102	.131	1.122	1.213
7d	.1949	4.62×10^{-4}	8.92	1.36	16.21	.077	.077	1.130	1.152

TABLE XVI. Photoionization of Sulfur (^1D)

$$h\nu + S\ (3p)^4\ {}^1D \rightarrow {}^1D \rightarrow \begin{cases} S^+\ (3p)^3\ {}^2D + e\ d \\ S^+\ (3p)^3\ {}^2P + e\ s \\ \qquad\qquad + e\ d \end{cases}$$

n	E_r	Γ	q	σ_a	σ_b	$\sigma_a \frac{\pi\Gamma}{2}(q^2-1)$	$\frac{\sigma_a}{\sigma_a+\sigma_b}$	Quantum Defect	δ_o
4s	.1631	2.73×10^{-4}	-9.12	13.82	0.0	4.86×10^{-1}	1	-0.054	.156
5s	.1848	1.49×10^{-4}	-7.21	14.78	0.0	1.75×10^{-1}	1	-0.058	.186
6s	.1967	8.12×10^{-5}	-4.54	15.88	0.0	3.97×10^{-2}	1	-0.061	.146

$$h\nu + S\ (3p)^4\ {}^1D \rightarrow {}^1D \rightarrow \begin{cases} S^+(3p)^3\ {}^2D + e\ s \\ \qquad\qquad + e\ d \\ \qquad\qquad + e\ g \\ S^+(3p)^3\ {}^2P + e\ d \end{cases}$$

5d	.1803	2.48×10^{-3}	.908	5.38	7.33	-3.68×10^{-3}	.423	.212	.0127
6d	.1939	1.68×10^{-3}	.965	5.14	7.41	$-.30 \times 10^{-4}$	.409	.248	.0192

TABLE XVI (c). Photoionization of Sulfur (^1D)

$$h\nu + S\ (3P)^4\ {}^1D \rightarrow {}^1F \rightarrow \begin{matrix} S^+\ (^2D) + e\ d \\ \qquad\quad + e\ g \\ S^+\ (^2P) + e\ d \\ \qquad\quad e\ g \end{matrix}$$

n	E_r	Γ	q	σ_a	σ_b	$\sigma_a \frac{\pi}{2}(q^2-1)$	$\frac{\sigma_a}{\sigma_a + \sigma_b}$	Quantum Defect	δ_o
5d	.1827	4.87×10^{-5}	6.68	8.75	4.36	2.91×10^{-2}	.667	.075	.019
6d	.1954	2.31×10^{-5}	5.07	6.95	5.49	6.23×10^{-3}	.558	.079	.022

TABLE XVII. PHOTOIONIZATION OF SULFUR (^1S)

$$h\nu + S\ (3p)^4\ {}^1S \rightarrow {}^1P \rightarrow \begin{cases} S^+\ (3p)^3\ {}^2D + e\ d \\ S^+\ (3p)^3\ {}^2P + \begin{cases} e\ s \\ e\ d \end{cases} \end{cases}$$

n	E_r	Γ	q	σ_a	σ_b	$\sigma_a \frac{\pi}{2} \Gamma(q^2-1)$	$\frac{\sigma_a}{\sigma_a + \sigma_b}$	Quantum Defect	σ_o
4s	.1631	2.73×10^{-4}	-6.31	2.74	0.0	4.55×10^{-2}	1	-0.054	.156
5s	.1848	1.49×10^{-4}	-6.51	2.43	0.0	2.34×10^{-2}	1	-0.058	.186
6s	.1957	8.12×10^{-5}	-5.12	3.59	0.0	1.16×10^{-2}	1	-0.061	.146

TABLE XVIII

Partial wave contributions to the photoionization cross sections of $S(^3P, ^1D, ^1S)$

		Dipole Velocity			Dipole Length		
L_oS_o	K_f^2	$^3S^o$	$^3P^o$	$^3D^o$	$^3S^o$	$^3P^o$	$^3D^o$
^3P	.3	2.907	8.616	14.049	5.053	13.314	26.242
	.4	2.637	7.029	13.170	4.739	11.154	25.895
	.6	1.928	4.226	10.949	3.618	7.004	23.493
	.8	1.264	2.335	8.495	2.414	4.022	19.751
	1.0	.781	1.237	6.052	1.491	2.216	15.262
	2.0	.121	.099	.286	.191	.141	1.248
		$^1P^o$	$^1D^o$	$^1F^o$	$^1P^o$	$^1D^o$	$^1F^o$
^1D	.3	2.822	8.064	11.894	3.695	14.129	22.638
	.4	2.158	7.628	11.376	3.016	14.129	22.638
	.6	1.249	6.329	9.813	1.967	12.856	21.684
	.8	.763	4.800	8.021	1.325	10.385	19.334
	1.0	.495	3.336	6.144	.919	7.554	10.080
	2.0	.103	.328	.272	.151	.698	1.681
		$^1P^o$			$^1P^o$		
^1S	.3	23.807			37.182		
	.4	22.378			38.588		
	.6	18.858			37.774		
	.8	15.138			33.748		
	1.0	11.415			27.635		
	2.0	.832			2.805		

TABLE XIX. Photoionization of Clorine (^2P)

$h\nu + CL\ (3p)^5\ ^2P \rightarrow\ ^2S \rightarrow\ CL^+(3P)^4\ ^1D + ed$

$CL^+(3P)^4\ ^1S + es$

n	E_r	Γ	q	σ_a	σ_b	$\sigma_a \frac{\pi}{2}\Gamma(q^2-1)$	$\frac{\sigma_a}{\sigma_a+\sigma_b}$	Quantum Defect	δ_o
4^4S	.1401	3.56×10^{-3}	-1.26	4.19	0	1.38×10^{-2}	1	1.042	.566
5^4S	.1908	1.19×10^{-3}	-1.24	4.07	0	4.11×10^{-3}	1	1.035	.607

$h\nu + CL\ (^3P)^5\ ^2P \rightarrow\ ^2P \rightarrow\ CL^+(3P)^4\ ^3P + es$

$\rightarrow\ CL^+(3p)^4\ ^1D + ed$

n	E_r	Γ	q	σ_a	σ_b	$\sigma_a \frac{\pi}{2}\Gamma(q^2-1)$	$\frac{\sigma_a}{\sigma_a+\sigma_b}$	Quantum Defect	δ_o
4d	.0375	5.41×10^{-3}	3.53	2.66	.459	1.37×10^{-1}	.852	.185	.306
5d	.0628	2.84×10^{-3}	3.01	3.33	1.741	1.20×10^{-1}	.656	.201	.380
6d	.0765	1.98×10^{-3}	3.92	1.90	1.474	8.47×10^{-2}	.563	.202	.395

TABLE XIX (continued)

$h\nu + CL\ (^2P)\quad ^2D$

$CL^+(^3P) + e\ d$

$CL^+(^1D) + e\ s + e\ d + e\ g$

$CL^+(^1S) + e\ d$

n	E_r	Γ	q	σ_a	σ_b	$\sigma_a \frac{\pi}{2}\Gamma(q^2-1)P^2 = \frac{\sigma_a}{\sigma_a+\sigma_b}$		Quantum Defect	δ_o
4 d	.0387	3.10×10^{-3}	1.79	13.33	0	1.43×10^{-1}	1	.152	.262
4 s	.0427	2.46×10^{-4}	5.31	13.06	0	1.37×10^{-1}	1	.033	.183
5 d	.0638	6.5×10^{-4}	3.50	10.53	0	1.22×10^{-1}	1	.146	.335
6 d	.0769	5.6×10^{-4}	2.99	10.38	0	7.26×10^{-2}	1	.161	.345
7 d	.0848	2.5×10^{-4}	3.73	11.02	0	5.60×10^{-2}	1	.170	.344
4 d	.1880	$.240 \times 10^{-3}$	25.61	.045	18.48	1.11×10^{-1}	.024	.118	1.286
5 d	.2119	1.740×10^{-3}	18.45	.090	18.19	8.19×10^{-2}	.0049	.148	1.323

TABLE XX

Partial wave contributions to the photoionization cross sections of $Cl(^2P)$

		Dipole Velocity			Dipole Length		
L_oS_o	k_f^2	^2Se	^2Pe	^2De	^2Se	^2Pe	^2De
^2P	.3	2.612	7.474	12.397	3.791	13.424	23.339
	.4	2.225	7.248	12.151	3.303	13.612	23.942
	.6	1.422	6.499	11.159	2.194	13.169	23.782
	.8	.826	5.461	9.801	1.315	11.710	22.404
	1.0	.460	4.253	8.131	.754	9.598	19.913
	2.0	.039	.476	.805	.055	1.235	3.288

TABLE 21

Photodetachment cross sections of (a) $S_i^-(^4S^o)$ and (b) $Cl^-(^1S^e)$

(a) $S_i^-(^4S^o)$, $LS\pi = {}^4P^e$

K_f^2	σ_V	σ_L	K_f^2	σ_V	σ_L
.005	10.986	7.151	.15	31.461	41.028
.01	14.745	9.867	.17	31.611	43.036
.015	18.996	13.378	.19	31.555	44.578
.02	22.987	17.667	.21	31.332	45.706
.025	24.071	20.541	.23	30.978	46.477
.03	24.871	20.541	.25	30.519	46.950
.035	25.499	21.734	.3	29.053	47.137
.04	26.021	22.836	.4	25.373	44.651
.045	26.476	23.876	.5	21.280	39.609
.05	26.887	24.875	.6	17.163	33.278
.07	28.299	28.661	.7	13.337	26.973
.09	29.476	32.248	.8	9.701	20.848
.11	30.409	35.581	.9	7.289	16.501
.13	31.069	38.535			

(b) $Cl^-(^1S^e)$, $LS\pi = {}^1P^o$

K_f^2	σ_V	σ_L	K_f^2	σ_V	σ_L
.01	5.468	4.494	.40	17.518	27.750
.02	7.294	6.204	.50	17.675	30.322
.03	8.741	7.436	.60	17.535	32.027

TABLE 21

(continued)

K_f^2	σ_y	σ_L	K_f^2	σ_y	σ_L
.05	10.010	9.294	.70	17.244	33.146
.07	11.074	10.801	.80	16.921	33.962
.09	11.927	12.162	.90	16.544	34.510
.11	12.663	13.454	1.10	15.770	35.230
.13	13.321	14.708	1.30	14.908	35.510
.15	13.918	15.936	1.50	13.822	35.230
.17	14.460	17.139	1.70	12.346	33.488
.19	14.951	18.314	1.90	10.373	30.181
.21	15.392	19.449	2.10	8.005	25.112
.23	15.784	20.545	2.30	5.573	19.013
.25	16.129	21.591	2.50	3.506	13.109
.30	16.804	23.982			

TABLE 22

Partial wave contributions to the Photodetachment cross sections of $S^-(^2P^o)$

	Dipole Velocity			Dipole Length		
K_f^2	^2Se	^2Pe	^2De	^2Se	^2Pe	^2De
.01	.000	4.462	.031	.000	2.478	.013
.02	.000	5.645	.109	.000	3.395	.068
.03	.000	6.289	.360	.000	4.024	.177
.05	.000	6.767	.916	.000	4.867	.721
.07	.000	6.811	1.778	.000	5.401	1.131
.09	.001	6.682	4.217	.001	5.753	3.782
.11	.034	6.527	6.221	.030	6.037	6.243
.13	.112	6.422	7.325	.106	6.337	7.762
.15	.222	6.371	8.118	.219	6.674	8.981
.17	.344	6.361	8.738	.351	7.046	10.047
.19	.452	6.378	9.238	.462	7.444	11.011
.21	.621	6.412	9.645	.942	7.857	11.895
.23	.867	6.426	10.007	1.493	8.486	12.759
.25	1.058	6.494	10.356	1.868	8.685	13.649
.30	1.430	6.579	11.206	2.549	9.643	15.974
.40	1.890	6.623	12.701	3.379	11.097	20.414
.50	2.103	6.519	13.739	3.755	11.923	23.729
.60	2.159	6.337	14.171	3.830	12.298	25.530
.70	2.106	6.093	13.941	3.706	12.373	25.867
.80	1.973	5.833	13.168	3.447	12.309	25.068

TABLE 22

(continued)

K_f^2	$^2S^e$	$^2P^e$	$^2D^e$	$^2S^e$	$^2P^e$	$^2D^e$
.90	1.782	5.566	11.983	3.100	12.168	23.482
1.10	1.302	5.001	9.386	2.268	11.679	19.866
1.30	.888	4.336	7.226	1.484	10.797	16.922
1.50	.491	3.534	5.562	.895	9.377	14.558
2.00	.104	1.438	2.296	.212	4.447	7.967

Chapter 4

The code can be logically divided into four sections and the transfer of control within the program may be described by the following diagram

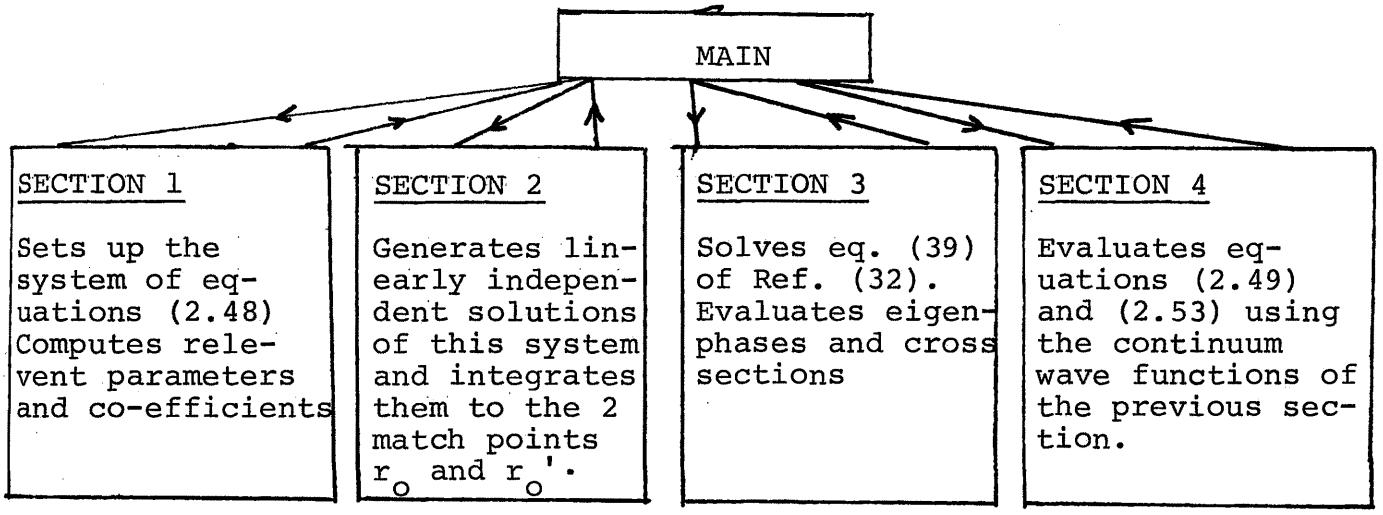

We now describe the function of each routine in the code and the COMMON variables read in or computed there.

MAIN Reads in IREAD, IWRITE the logical input and output tape numbers and calls the sections in turn.

SECTION 1

SUBROUTINE MAIN1

The remainder of the data which we now describe is read in this subroutine.

IPH { -ve call EXIT
0 implies more data cards to be read
1 implies no more data cards to be read

LRGL	Total orbital angular momentum of system
SPN	Total spin angular momentum of system
NPTY	Parity of system
W1	Energy of incident particle (in Rydbergs)
H	Basic mesh size

IDEBUG(8) {
- 0 no print out in intermediary steps in the calculation.
- 1 Prints out result of intermediary calculation

IDEBUG(8)= -1 if we require the 4th section to be entered

IPH {
- 0 Read in more data
- 1 No more data to be inputed.

IZ	Value of the nuclear charge
NST	Number of states to be included in the expansion
NELT	No. of radial equations allowed (maximum=5)
IQ	No. of electrons in np subshell of target
IP1	No. of closed subshells

The code assumes that the orbitals of the atomic electrons are accurately represented by analytic SCF functions i.e.

$$P_i(r) = \sum_{J=1}^{NBASIS} CWS(J,I)\, r^{IPWS(J,I)}\, e^{-ZETWS(J,I)\cdot r}$$

We need IP=IP1 + 1 of these for the 1s, 2S...np orbitals of the target and also 2 more such orbitals for the $(np)^{q+1}$ system, namely $P'_{np}(r)$ and $P'_{2s}(r)$ or $P'_{3s}(r)$ for the 4th section since the photoionization cross section is proportional to $|\langle \Psi_i | r | \Psi_f \rangle|^2$. The Ψ_i is merely the $(np)^{q+1}$ system

and the Ψ_f is described by the continuum wave functions that are computed in sections 1 to 3.

∴ Total number of orbitals = IP + 2 + IP2

EN (NST) Energies of the target states in atomic units

PTL Ionization potential of the $(np)^{q+1}$ L_oS_o system

IR1 Number of mesh steps in the first change in mesh size. IR1*H is also one of our matching points for the functions. The integration from the origin outwards is terminated at this point.

IR2,IR3,IR4 Number of steps from the origin to regions where the mesh size is doubled i.e. the interval size between IR1 and IR2 is 2*H etc.

IRA Number of steps from the origin to RA.

IR5 First match points=IR5*H. The IRI's satisfy the inequalities

IR5<IR1<IR2<IR3<IR4<IRA

where each IRI is at least 2 larger than the previous.

The functions are integrated from the origin as far as IR1*H. The values of the functions at IR5 and IR1 are stoed in the matrix B1. The solutions generated in the asymptotic region are integrated inwards as far as IR5*H. The values of these functions at IR1 and IR5 are also stored in B1.

ITAPE — Logical output tape number of temporary storage of the independent solutions until they are recalled in MAIN4.

LO, SO — The orbital and spin angular momentum of the $(np)^{q+1}$ system under consideration in photoionization calculations.

CNORM — $\left[(2p'|2p)^{q-1}(1s'2s'|1s2s)^2\right]^2$ where ^{1} denotes the radial wave functions of the $(np)^{q+1}$ L_oS_o system. For the $(3p)^{q+1}$ system we neglect the contribution from the $1S^1$ and only include $\left[(3p'|3p)^{q-1}(2s'3s'|2s3s)^2\right]^2$

R2SD — $\int P'_{2p}\, r\, P_{2s}\, dr$

R2SE — $\int \frac{P'_{2p}}{r} \frac{d}{dr} \frac{P_{2s}}{r} r^2\, dr$

The following variables are also computed in MAIN1

IRA1 — IRA + 1

N — Number of channels

NA — Number of open channels

NB — Number of closed channels

IFA — Number of distinct wave numbers in open channels

IFB — Number of distinct wave numbers in closed channels

NMU — Number of Lagrange multipliers needed to make F_i's orthogonal to atomic orbitals.

NMUSOL(NMU) — Number of the atomic orbitals involved in the NMUth Lagrange multiplier.

NFEQN(NMU) — Number of the radial equation involved in the NMUth Lagrange multiplier.

L2P(N), IL2(N), AL2(N) — Angular momentum of the outgoing electron in a particular channel

IL1(N) — Orbital quantum number of the target in a particular channel

SPNI(N) — Spin quantum number of the target in a particular channel

WP(N) — Wave number squared for each channel

KABOVE(N) — Number of the channel above threshold

KBELOW(N) — Number of the channel below threshold

ABOVE(N) — Distinct particle energies above threshold

BELOW(N) — Distinct particle energies below threshold

R(IRA1) — Values of the independent variable 'r' at which the functions are computed. Note: R(1)=E and R (2)=H.

RA — Value of 'r' beyond which exponential potentials are neglected.

RB — Value of 'r' at which asymptotic expansion is used.

HX(IRA) — Mesh sizes over the range of integration:

IRT(N,N) — Used to locate the potentials V_{ij} (IRA). Since V_{ij} is symmetric only $\frac{N(N+1)}{2}$ of them are stored.

EXCQ — Excess nuclear charge (=Z-number of atomic electrons)

ETAAB(NST), ETABLW(NST) — excess nuclear charge divided by distinct wave numbers

TAU(30) — Needed in subroutine CLEBSH

HF — Final mesh size (= 16*H)

NTØT=N + NE — Total number of second order differential equations.

NTØTNA=NTØT+NA

NANA=N + NA

N2TØT=2*NTØT

NIN — Number of independent solutions in the inside region

NØØT — Number of independent solutions in the outer region.

CALLS SETLSP, VIJOFR, SUBEX, GENP1.

SUBROUTINE VIJOFR

The following arrays are calculated in this subroutine.

A($\frac{N(N+1)}{2}$, IRA1) Direct potentials $\frac{l_i(l_i+1)}{r^2} - \frac{2z}{r} - k_i^2 + 2 V_{ij}(r)$

when V_{ij} is defined by equation (2.30).

AAS($\frac{N(N+1)}{2}$, 2) Co-efficient of $\frac{1}{r^3}$ of Y_λ as $r \to \infty$ for $\lambda = 2$

if such a term occurs in the direct potential, zero otherwise.

V(N,IRA1) Equation (2.41)

NV {=0 If no. V_i terms are in the equations
=1 If the equations contain a V_i term.

NVJ(N) {=0 If no. V_i terms are in a particular equation
=1 If equation has a V_i term.

CALLS YSUB, CLEBSH, RACAH.

SUBROUTINE CLEBSH

Calculates the Clebsh-Gordon co-efficient D=(ABOO/CO)

SUBROUTINE RACAH(A,B,C,D,E,F,G)

Calculates Racah co-efficient

G=W(ABCD;EF)

SUBROUTINE YSUB

Numerical evaluation of Y_K $(P_i P_j r)$

The function is stored in the array B(IRA1)

FUNCTION FG03B(A,B,C,P,Q,R,X,Y,Z)

Evaluates $\left\{ \begin{matrix} ABQ \\ CPX \\ RYZ \end{matrix} \right\}$ i.e. the Wigner 9-j symbol as defined in Ref.(39).

SUBROUTINE RSUB(I,J,K,L,X)

L=1 calculates $X=R_K(P_i P_j P_i P_j)$

L=2 calculates $X=R_K(P_i P_j P_j P_i)$

CALLS YSUB

SUBROUTINE SETLSP

Tabulated LS term values for the $(np)^q$ configuration and stored in the arrays AL(3) and ASPN(3).

SUBROUTINE CFP $(q, L_i, S_i, L_j, S_j, C)$

Tabulated values of $C = (P^q L_i S_i \| P^{q-1} L_j S_j)$ i.e. fractional parentage co-efficients for the $(np)^q$ configuration.

SUBROUTINE SUBEX

Determines the number of distinct exchangeterms and computes the following variables:

NE	Used to count the exchange terms, its final value being the number of distinct exchange terms NE.
IX1(NE)	Temporary array used in subroutine.
IX2(NE)	Value of for the NEth exchange term
IX3(NE)	The particular involved in the NEth exchange term
IX4(NE)	The particular F_i involved in the NEth exchange term.

AX1(N,NE) The co-efficients of the exchange terms

AX2(NE) $\lambda(\lambda+1)$

AX3(NE,N) $(2\lambda+1)$

CALLS CFP, RACAH, CLEBSH, FG03B.

SUBROUTINE GENP1

Calculates ENP1 = $E\{(np)^{q+1} LS\} - E$ where $E = \frac{1}{2} K1^2$ $+ E\{(np)^q L_1 S_1\}$ where $L_1 S_1$ are the quantum numbers of the lowest term and the actual expressions for the E's are obtained from equation (2.46). The wave functions of the $(np)^q$ system are used in evaluating $E\{(np)^{q+1} LS\}$.

CALLS CLEBSH, RACAH, CFP, RSUB.

SECTION 2

SUBROUTINE MAIN2

CALLS INTEGRT

SUBROUTINE INTGRT

Generates NTØT independent solutions of the system of homogeneous equations $Z'' = BZ$ where $Z = \begin{pmatrix} F_i \\ rJ_\lambda \end{pmatrix}$ is a column vector which has NTØT elements. A further (NV+NMV) independent solutions of the inhomogeneous system $Z'' = BZ + G$ where G involves the V_i terms and the Lagrange multipliers are generated by setting the co-efficients C and μ_i equal to unity in turn and the remainder equal to zero. These solutions are integrated from E to H using the Runge-Kutta method. This involves subroutines STRSL1 RUNGKT1 RUNGE and SUBG and the array, Z(N2TOT), ZPRIME (N2TOT). Knowing Z(o) and Z(H) we now can use the Numerov method

to integrate IR1 steps and we store the solutions at the points corresponding to IR5 and IR1 in the matching matrix B1.

We have

$$\frac{d^2Z}{dr^2} = \sum_j B_{ij} Z_j + G_i \qquad \ldots.(4.1)$$

$$\delta^2 Z_i = H^2 \left[\sum_j B_{ij} Z_j + G_i + \frac{1}{12} \delta^2 \left\{ \sum_j B_{ij} Z_j + G_i \right\} \right] \qquad \ldots.(4.2)$$

This gives us

$$\sum_j \left[\delta_{ij} - \frac{1}{12} H^2 B_{ij}^{(r+H)} \right] Z_j^{(r+H)}$$

$$= 2 \sum_j \left[\delta_{ij} - \frac{1}{12} H^2 B_{ij}^{(r)} \right] Z_j^{(r)}$$

$$- \sum_j \left[\delta_{ij} - \frac{1}{12} H^2 B_{ij}^{(r-H)} \right] Z_j^{(r-H)}$$

$$+ H^2 \left[B_{ij}^{(r)} Z_j^{(r)} + G_i^{(r)} + \frac{1}{12} \left\{ G_i^{(r+H)} - 2G_i^{(r)} + G_i^{(r-H)} \right\} \right] \qquad \ldots.(4.3)$$

F3 (NTØT, NTØT) $\quad \delta_{ij} - \frac{1}{12} H^2 B_{ij}^{(r+H)}$

F6 (NTØT, NIN) $\quad \left[\delta_{ij} - \frac{1}{12} H^2 B_{ij}^{(r)} \right] Z_j^{(r)}$

F7 (NTØT, NIN) $\quad \left[\delta_{ij} - \frac{1}{12} H^2 B_{ij}^{(r-H)} \right] Z_j^{(r-H)}$

F8 (NTØT, NIN) $\quad H^2 \left[B_{ij}^{(r)} Z_j^{(r)} + G_i^{(r)} + \frac{1}{12} \left\{ G_i^{(r+H)} - 2G_i^{(r)} + G_i^{(r-H)} \right\} \right]$

F1 (NTØT, NIN) $\quad Z_i^{(j)}(r) \qquad j = 1, \ldots \text{NIN}$

F2 (NTØT, NIN) $\quad Z_i^{(j)}(r-H) \qquad j = 1, \ldots \text{NIN}$

F4 (NTØT, NIN) = R.H.S. of Numerov formula

$$= 2\,F6 - F7 + F8$$

$\therefore$ F1 (NTØT, NIN) = F3 [(NTØT, NTØT)] $^{-1}$ F4 (NTØT, NIN)

The integration from the asymptotic region $r=r_B$ is now begun by calling STRSL2 in this region potentials which involve exponential terms are negligible so the equations take the form

$$\frac{d^2F_i}{dr^2} = \sum_{J=1}^{N} U_{ij} F_J \qquad i = 1, \cdots N$$

....(4.4)

where

$$U_{ij} = \left[\frac{\ell_i(\ell_i+1)}{r^2} - k_i^2 - \frac{2(z-n)}{r} + \sum_{\lambda} \frac{a_{ij}^{\lambda}}{r^{\lambda+1}} \right]$$

....(4.5)

The asymptotic form of Burke and Shey[46] for the functions F_i is assumed

$$F_i \sim \sum_{K=1}^{IFA} \left\{ \sin(k_K r + \eta_K \log 2k_K r) \sum_{P=0}^{\infty} \alpha_P^{iK} r^{-P} + \cos(k_K r + \eta_K \log 2k_K r) \sum_{P=0}^{\infty} \beta_P^{iK} r^{-P} \right\}$$

$$+ \sum_{T=1}^{IFB} \left\{ e^{[-|k_T| r - \eta_T \log 2|k_T| r]} \sum_{P=0}^{\infty} \gamma_P^{iT} r^{-P} \right\}$$

....(4.6)

Substituting these F_i's into the asymptotic form of the differential equations gives us a recurrence relation for the α_P^{iK}, β_P^{iK} and γ_P^{iT}. In order to solve these recurrence relations α_0^{ii}, β_0^{ii} and γ_0^{ii} must be specified, i.e.

2*NA + NB constants are unknown. Consequently 2*NA+NB linearly independent solutions can be generated by setting

$$\alpha_0^{NC\,NC} = 1 \text{ , all other } \alpha\ \beta\ \gamma = 0 \quad \text{for } 1 \leq NC \leq NA$$

$$\beta_0^{NC\,NC} = 1 \text{ , " " } \quad NA+1 \leq NC \leq 2.NA$$

$$\gamma_0^{NC\,NC} = 1 \text{ , " " } \quad 2.NA+1 \leq NC \leq 2.NA+NB$$

and solving the recurrence relations 2.NA+NB times (NC counts the number of solutions).

Substitution of the co-efficients α, β, γ back into equation (4.6) enables us to calculate the F_2's at r_B and (r_B-HF). These solutions of the homogeneous system of N coupled equations are integrated in wards using the Numervov method and the asymptotic form (4.5) of the potentials to the point R_A where the exchange potentials might be expected to begin contributing.

At this point the exchange potentials are explicitly taken into account. We define a further NE linearly independent solutions of the homogeneous system of NTØT coupled equations by setting the co-efficients of $r^{-\lambda}$ in the exchange terms each equal to unity in turn and the rest equal to zero. A further NV+NMU independent solutions of the inhomogeneous system are generated by setting C and the μ 's equal to unity in turn as in the inner region. These NOUT=ØNA+NB+NE+NV+MMV solutions are integrated inwards to the point corresponding to IR5. The values of the functions at the points corresponding to IR5 and IR1 are stored in the matrix B1.

Since the mesh size is halfed at the points corresponding to IR4 IR3 IR2 IR1 the following arrays are required for interpolation of F6 F7 and F8 in these regions

F9(NTOT,N2UT),F10(NTOT,NOUT),F11(NTØT,NOUT)

Subroutines called by INTGRT.

STRSL1,RNGKT1, MATINV, UFLSPR, SETF3 SETCAE, SETF8, STRSL2, SETF3A, SETDA

SUBROUTINE UFLSPR

Machine language subroutine written to supress programe interupt messages caused by underflows on the IBM 360-65.

SUBROUTINE RSTSUP

Machine language subroutine which terminates the underflow supressor programe.

SUBROUTINE STRSL1

Computes $F_i(\epsilon)$, $F_i'(\epsilon)$, $Y_\lambda(\epsilon)$, $Y_\lambda'(\epsilon)$. The results are stored in Z(N2TØT). Use is made of the fact that

$$F_i \underset{r\to 0}{\sim} r^{\ell_i+1} \qquad Y_\lambda \underset{r\to 0}{\sim} r^{\lambda+1}$$

The NIN linearly independent solutions in the inner region are generated by setting the co-efficients of the powers of equal unity in turn and setting the remainder equal to zero.

SUBROUTINE SUBG

Computes the right hand side of the differential equation at $\frac{\epsilon+H}{2}$. Result is stored in G(NTØT)

FUNCTION RUNGE

RUNGE-KUTTA formula.

SUBROUTINE RNGKT1

Converts the system of NTØT coupled second order differential equations to a system of N2TØT first order differential equations in preparation for the Runge-Kutta formula by making the transformation

$$Z_i' = Z_{i+NT\phi T}$$

$$Z'_{i+NT\phi T} = \sum_j B_{ij} Z_j + G_i \qquad \ldots.(4.7)$$

The Z_i^1 are stored in the array ZPRIME(N2TØT)

The above system may be written as

$$Z'_K = f_k(r, Z_1, \cdots Z_{N2T\phi T}) \qquad K = 1, \cdots N2T\phi T$$

$Z_i(\epsilon)$ is known from STRSL1

∴ From the Runge-Kutta formula

$$Z_i(H) = Z_i(\epsilon) + \frac{1}{6}(k_{i0} + 2k_{i1} + 2k_{i2} + k_{i3}) \qquad \ldots.(4.8)$$

where

$$k_{i0} = HM \cdot f_i(\epsilon, Z_i(\epsilon) \cdots Z^{(\epsilon)}_{N2T\phi T})$$

$$k_{i1} = HM \cdot f_i\left(\epsilon + \frac{HM}{2}, Z_1(\epsilon) + \frac{1}{2}k_{10} \cdots, Z^{(\epsilon)}_{N2T\phi T} + \frac{1}{2}k_{N2T\phi T\,0}\right)$$

$$k_{i2} = HM \cdot f_i\left(\epsilon + \frac{HM}{2}, Z_1^{(\epsilon)} + \frac{1}{2}k_{11} \cdots, Z^{(\epsilon)}_{N2T\phi T} + \frac{1}{2}k_{N2T\phi T\,1}\right)$$

$$k_{i3} = HM \cdot f_i(\epsilon + HM, Z_1^{(\epsilon)} + k_{12} \cdots, Z^{(\epsilon)}_{N2T\phi T} + k_{N2T\phi T\,2})$$

where HM=H-C

CALLS SUBG, RUNGE

SUBROUTINE SETF3(IA,HA)

Computes the NTØT X NTØT array F3 at the point R(IA+1) with H=HA .

SUBROUTINE SETF8 (IA, HI, JA, K)

Computes the array F8 at the point R(IA+1) with H=Hi.

K=0 implies that the integration is in the 'inner' region i.e. number of solutions = NIN

K=1 implies that the integration is being performed in the outer region i.e. number of solutions = NØUT

JA=0 implies that the mesh size is uniform in the region of integration

JA=2 } means that we are preparing to decrease the step size by a factor of 2.

SUBROUTINE MATINV (A,N,B,M,DETERM)

M=0 inverts the NXN matrix A

M=1 computes $A^{-1}B$

DETERM= det |A|

SUBROUTINE SETF3A

Computes the NXN matrix F3 in the asymptotic region.

SUBROUTINE STRSL2

Fits the F_i's to the asymptotic form of Burke and Shey[46]. If a good fit is not obtained it automatically increases r_B and tires the expansion again. Computes $F_i(r_B)$, $F_i(r_B-HF)$.

CALLS STRSL9.

SUBROUTINE STRSL9(ALPHA, BETA, GAMMA)

Solves a difference equation for the co-efficients α_p^{jk} β_p^{jk} and γ_p^{jT} of the asymptotic expansion using $\alpha_0^{NC\,NC}$ $\beta_0^{NC\,NC}$ and $\gamma_0^{NC\,NC}$ communicated to it by STRSL2. The results are stored in the arrays ALPHA, BETA, and GAMMA. Computes IAASE i.e. the number of terms in our multipole expansion.

SUBROUTINE SETCAE (I1)

Evaluates the orthogonality integral in the 'inner' region using the trapozodial rule at each step of integration.

$$E(NMU, NIN) = \int_0^{R(IR1)} P_{IU}(r)\, F_{IV,J}(r)\, dr \qquad J = 1, 2, \ldots NIN$$

where

IU=NMVSOL(NMV)"

IV=NFEQN(NMV)

It also evaluates the integral involved in equation (2.48).

$$C(NIN) = \sum_{i=1}^{N} \int V_i F_{ij}\, dr \qquad J = 1, 2 \ldots NIN$$

SUBROUTINE SETDA (I1)

Evaluates the same integrals as SETCAE for the 'outer' region. The results are stored in the arrays I(NMU,NØUT) and D(NØUT) .

SECTION 3

SUBROUTINE MAIN3

CALLS SOLVE

SUBROUTINE SOLVE

Completes setting up the Matching matrix B1 which incorporates the requirement that the solutions be continuous over the entire range $0 \leq r \leq r_B$, and also the conditions expressed by (33) and (41) of Ref.(32). The orthogonality requirements are also expressed in the B1 matrix. The resultant set of linear equations may be expressed in matrix form

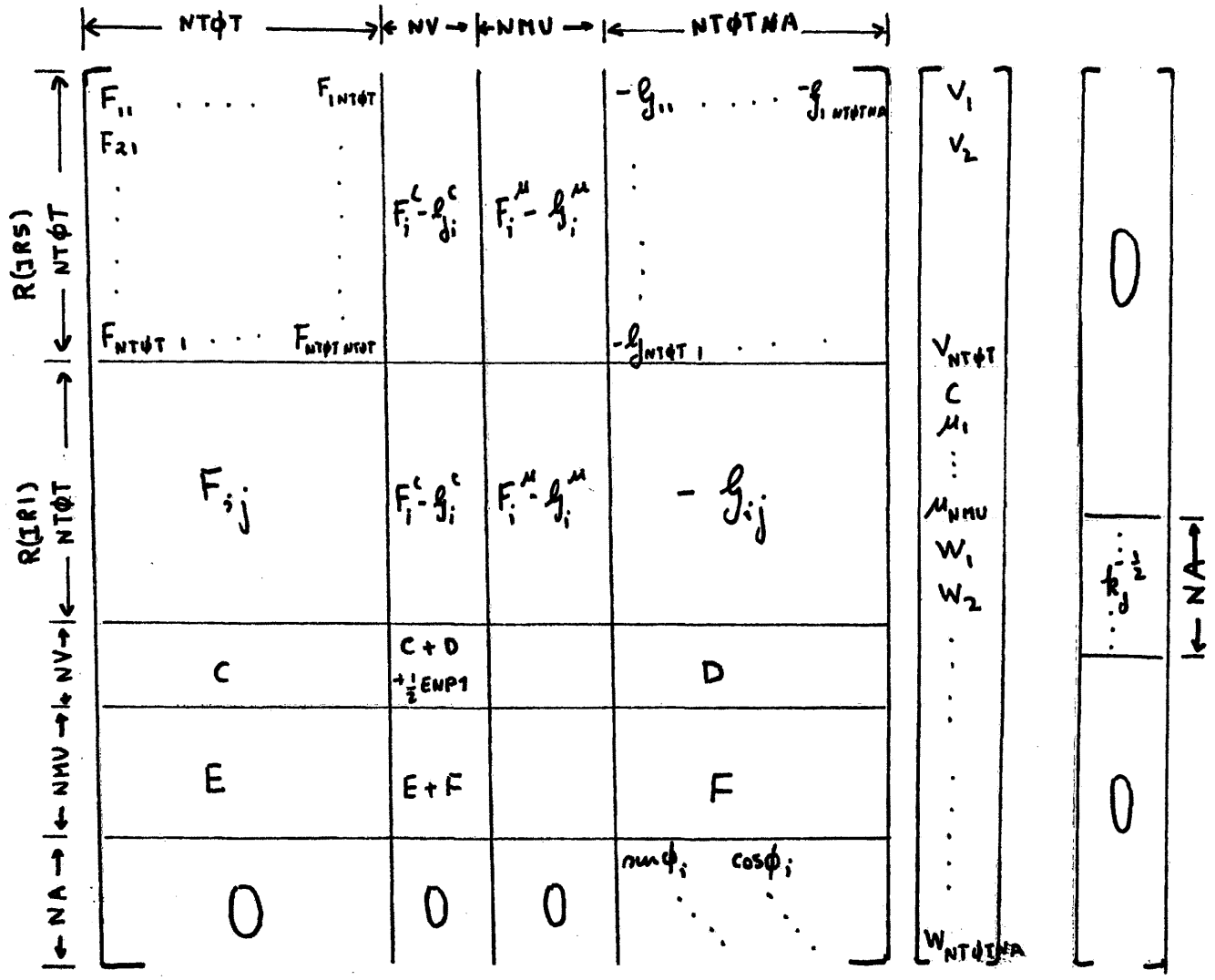

These equations are solved NA times to give the unknown co-efficients V_α^i, C^i, μ_γ^i, W_α^i i=1, NA which are stored in the array W(M,NA). The R-matrix is then computed using equation (42) of SHB. The R-matrix is daigonalized and the eigenphase shifts computed.

CALLS MATIN3,HDIAG,GAMMAR, RMSIE

SUBROUTINE MATIN3

Inverts the Bl matrix

SUBROUTINE GAMMAR(ARG1,ARG2,ARG3,ARG4)

Computes the argument of the complex gamma function

$$\arg \Gamma(ARG1 + iARG2) = \arctan(ARG4/ARG3)$$

SUBROUTINE HDIAG(H,N,IEGEN,U,NR)

Diagonzlies the NXN symmetric matrix H.

SUBROUTINE RMSIG

Calculates S and T matrixes and partial wave cross sections for the transitions $L_iS_i \to L_jS_j$. Also computes the normalization matrix $A_{r'r''}$ of Equation (2.57) and stores it in the array AB(NA,NA,NA)

SECTION 4

SUBROUTINE MAIN4

Rewinds ITAPE and reads in the solutions F which were computed at each point of the integration. Linear combinations of these solution vectors are now formed using the co-efficients computed in SOLVE and which are stored in W(M, NA). The

result is stored in the array F2(N,NA,IRA1)

CALLS PHOTO

SUBROUTINE PHOTO

This subroutine evaluates equations (20) of Ref. (4) to give the photoionization cross sections in the dipole length and dipole velocity approximations. We note that the function $g_\Gamma(E)$ (equation 2.43a) is approximated by the following expression (equation 2.43b)

$$q_\Gamma(E) = \sum_{\Gamma'} C_{\Gamma'} \left\{ (2p'|P_{\Gamma'}|F_{\Gamma\Gamma'}) - \delta_{\ell_\Gamma 0} \left[\frac{(1s'2s'|F_{\Gamma\Gamma' 2s})}{(1s'2s'|1s2s)} \times (2p'\,P_{\Gamma'}\,1s) + \frac{(1s'2s'|1s\,F_{\Gamma\Gamma'})}{(1s'2s'|1s2s)} (2p'|P_{\Gamma'}|2s) \right] \right\}$$

$$\simeq \sum_{\Gamma'} C_{\Gamma'} \left\{ (2p'|P_{\Gamma'}|F_{\Gamma\Gamma'}) - \delta_{\ell_\Gamma 0} (2s|F_{\Gamma\Gamma'})(2p'|P_{\Gamma'}|2s) \right\}$$

where we use the same notation as Ref. (41)

CALLS INTRAP

SUBROUTINE INTRAP (A,I,J,UK,RHO,IND)

Evaluates the integral

$$RHO = \int_0^{r_A} A_{ij}(r)\, UK(r)\, dr$$

using the Trapezoidal rule.

REFERENCES

1. D. R. Bates, Proc. Phys. Soc. London B 64, 805 (1951).

2. A. Dalgarno, M. B. McElroy and J.C.G. Walker, Planetary and Space Science 15, 331, (1967a).

3. I.S. Bowen, Astrophys. J., 68, 257, (1928).

4. M.J. Seaton, Proc. Phys. Soc. A231, 37, (1955).

5. M.J. Seaton, Reports Prog. Phys. 23, (1960).

6. M.J. Seaton, Advances in Atomic and Molecular Physics, Academic Press, New York, (1968).

7. Burgess A, Astrophys. J. 131, (1961).

8. B. Stromgen, Astrophys. J. 108, (1948).

9. L. Goldberg, Auto-ionization, edited by A. Temkin, Mono Book Corp., Baltimore (1966).

9a. Leo Goldberg, Andrea Dupree and John W. Allen, Annales D' Astrophysique, 28 No. 3 (1965).

10. A. Burgess, Astrophys. J. 139, (1964).

11. M.J. Seaton, Rev. Mod Physics, (1968).

12. M.J. Seaton, Lectures in Theoretical Physics IV, Boulder (1961).

13. R. Wildt, Astrophys. J. 89, (1939).

14. Vardya, Mon. N. Royal Ast. Soc. 71, (1967).

15. T. Ohmura and H. Ohmura Astrophys. J. 131, 8, (1960).

16. Mjosness and Ru el, Phys. Rev. 154, 98 (1967).

17. Smith, K. Reports on Prog. Phys. 29, 373 (1966).

18. Massey, H.S.W. and Mohr C.B.O.,(1932) Proc. Roy Soc (London) A136, 289.

19. Fesbach, H. Ann. Phys. 5, 357, (1958).

20. Fesbach, H. Ann. Phys. 19, 287, (1962).

21. Fesbach, H. Rev. Mod. Phys. 36, 1076, (1964).

REFERENCES

(continued)

22. K. Smith, Lecture Notes (unpublished).

23. A.M. Lane and R.G. Thomas, Rev. Mod, Phys. 30, 257 (1958).

24. O Malley, T.F. and S. Geltman, Phys. Rev. 137, A1344, (1965).

25. G. Brect and E. Wigner, Phys. Rev. 49, 519, (1936).

26. U. Fano, Phys. Rev., 124, 1866, (1961).

27. U. Fano and J.W. Cooper, Phys. Rev. 137, A1364, (1965).

28. P.A.M. Dirac, Physik 44, 585, (1927).

29. F.H. Mies, Phys. Rev. 175, 164, (1968).

30. B. W.Shore, Rev. Mod. Phys. 39, 439, (1967).

31. G. Racah, Phys. Rev. 63, 367, (1943).

32. K. Smith, R.J.W. Henry, and P.G. Burke, Phys. Rev 147, 21 (1966).

33. H. E. Saraph, M.J. Seaton and J. Shemming, (1968) preprint.

34. I.I. Sobelman, Introduction to the Theory of Atomic Spectra, Moscow translated by the U.S. Department of Commerce (1963).

35. C.C.J. Roothan and P.S. Kelly, Phys. Rev. 131, 1177, (1963).

36. E. Clementi, IBM, J. Res. Develop. 9, 2 (1965).

37. K. Smith, M.J. Conneely and L.A. Morgan, Phys. Rev 177, 196 (1969).

38. A. De Shalit and I. Thalmi, Nuclear Shell Theory (Academic Press, New York), 1963.

39. Rotenberg, M.R., N. Metropolis and J.K. Wooten, The 3-j and 6-j symbols. The Technology Press M.I.T., Cambridge, Mass.

40. R.J.W. Henry, P.G. Burke, and A-L Sinfailam, Phys. Rev. (in press).

41. R.J.W. Henry and Lester Lipsky, Phys. Rev. 153 51-56, (1967).

REFERENCES

(continued)

42. H. Bethe and E. Salpeter, Quantum Mechanics of One and Two Electron Systems, Academic Press Inc., New YOrk (1957).

43. S.J. Czyzak, T.K. Kruegar, H.E. Saraph and J. Shemming, Proc. Phys. Soc. (London) 92, 1146, (1967).

44. S.J. Czyzak and T.K. Kreugar, Proc. Phys. Soc. London 90, 623, (1967).

45. M.J.Seaton, Rev. Mod. Phys. 30, (1958).

46. P.G. Burke and H.M. Shey, Phys. Rev. 126, 163 (1962).

47. R.J.W. Henry, J. Chem. Phys. 48, 3635, (1968).

48. F.J. Comes and H.Elzer, Phys. Letters 25A, 374, (1967).

49. F.J. Comes and H. Elzer, Z. Naturforsch, 23A, 133, (1968).

50. P.K. Carroll, R.E. Huffman, J.C. Larrabee and Y. Tanaka Astrophy. J. 146, 535, (1966).

51. Dalgarno Henry and Stewart, Planetary and Space Science, 12, 235, (1964).

52. B.H. Armstrong, R.R. Johnston and P.S. Kelly, Technical Report No. AFWL-TK 65-17, Lockheed Missiles and Space Company, (1965).

53. M.G.Kozlov, E.I. Nickonova and G. P. Startsev, Soviet Physics Opt. and Spect. 21, 298, (1966).

54. L. A. Vainshtein and G.E. Norman, Soviet Phys. Opt and Spect. 8, 79, (1960).

55. A. Burgess, G.B. Field and R.W. Michie, Astrophys. J. 131, 529 (1960).

56. G. Peach, Mont. Not. Roy. Astron. Soc., 124, 371, (1962).

57. S. T. Manson and J. W. Cooper, Phys. Rev., 165, 126 (1968).

58. J.C. Rich, Astrophys. J. 148, 275 (1967).

59. A. Burgess and M.J. Seaton, Mon. Not. Roy. Astron. Soc. 120, 121, (1960).

60. K. Smith, Sommerfeld Memorial Meeting, Munich, Sept. (1968), to be published.

REFERENCES

(continued)

61. R.E. Huffman, J.C. Larrabee and Y. Tanaka, J. Chem. Phys. 47, 856, (1967).

62. E. J. Robinson and S. Geltman, Phys. Rev. 153, 4, (1967).

63. Yu. V. Moskvin, Soviet Phys. High Temp. 3, 765 (1965).

64. J.W. Cooper and J.B. Martin, Phys. Rev. 126, 1482 (1962).

65. R.S. Berry, C.W. Reinmann and G.N. Spokes, J. Chem. Phys. 37, 2278 (1962).

Reprinted from

PHYSICAL REVIEW VOLUME 177, NUMBER 1 5 JANUARY 1969

Trial Wave Functions in the Close-Coupling Approximation*

Kenneth Smith, M. J. Conneely, and L. A. Morgan
Behlen Laboratory of Physics, University of Nebraska, Lincoln, Nebraska 68508
(Received 13 May 1968)

The theoretical and numerical consequences of choosing different trial wave functions in the close-coupling approximation are considered. In particular, calculations are carried out on the scattering of electrons by atomic systems with configurations $1s^2 2s^2 2p^q$, $q=2,3,4$, where properly antisymmetrized bound configurations $1s^2 2s^2 2p^{q+1}$ are mixed with the trial continuum wave function. An alternative treatment, which eliminates the need for such bound configurations is presented.

I. INTRODUCTION

In order to calculate the cross section for a scattering process within the framework of nonrelativistic wave mechanics, it is necessary to approximate the Schrödinger equation. One of the most successful approximation schemes is to expand the over-all wave function of the projectile plus target in terms of the complete set of (assumed known) eigenstates of the target Hamiltonian, see Burke and Smith.[1] This method has come to be known as the "close-coupling approximation" because only a few of those atomic terms close to initial and final states are retained in the eigenfunction expansion. The unknown coefficients, $F_\alpha(r)$, in such an expansion are the solutions of coupled second-order integro-differential equations with prescribed boundary conditions, and are interpreted as describing the radial motion of the projectile relative to the target.

If there are N such coefficients, then the Schrödinger partial differential equation has been replaced by an N-channel problem in one dimension, r. Those N_A channels in which F_α oscillates as $r \to \infty$ are said to be "open", and correspond to continuum orbitals; the remaining $(N-N_A)$ channels are said to be "closed" since the associated F_α will vanish exponentially as $r \to \infty$.

The theory of the scattering of electrons by hydrogen atoms, within this approximation, was carried out by Percival and Seaton[2] and extended to hydrogen-like ions by Burke, McVicar, and Smith.[3] Two points of these papers are of interest to us here. Firstly, the eigenstates of the target Hamiltonian are known exactly; and secondly, the expansion coefficients $F_\alpha(r)$ were not orthogonalized with respect to the bound target orbital. The fact that the target eigenstate is a single exactly known orbital means that antisymmetrization of the target is a non-existent problem and no errors are introduced into the cross sections because of the bound orbital. However, since only a few states can be taken in the expansion, only a part of the full effective polarizabilities are included. A technique for improving the calculations has been suggested by Damburg and Geltman.[4] These authors recommend replacing the three degenerate $n=3$ hydrogenic target orbitals with an alternative non-degenerate trio, which results in the full effective polarizabilities being accounted for. In other words, even in the simplest collision problem, the one-electron orbitals of the target are a source of discussion.

Extensive calculations for electron collisions with positive ions with configurations is $1s^2 2s^2 2p^2$ have been carried out by Saraph *et al.*[5] They imposed the condition that the radial functions F_α should be orthogonal to the bound one-electron

orbitals with the same orbital angular momentum l_α. Physically, this can be interpreted as excluding the projectile from being captured, virtually, into incomplete subshells. This restriction on their total wave function was removed by superimposing a second configuration, ϕ, constructed entirely from bound orbitals. Their trial wave function in the close-coupling approximation was taken to be

$$\Psi(\Gamma_i) = \sum_{\Gamma_j} \psi^{\Gamma_i}(p^q(S_j L_j)k_j l_j SL\pi) + \alpha_i \phi(p^{q+1} SL\pi), \quad (1)$$

using the notation of Ref. 5, where Γ is the complete set of quantum numbers for the system and ψ is a vector-coupled antisymmetrized function constructed from one-electron orbitals. This same method was used by Czyzak and Krueger.[6] Equation (1) can be interpreted as configuration interaction: In the first term one of the electrons is in a continuum orbital, while all electrons are in bound orbitals in the ϕ term. Saraph *et al.* use the same orbitals for the terms $S_j L_j$ as well as in the ϕ configuration; these orbitals were calculated using a computer code written by Froese.[7]

The underlying reason behind choosing ϕ to be constructed from the same orbitals as ψ is that the F's are constrained to be orthogonal to these orbitals, yet without the constraint F would contain a component of the bound p^q orbitals. The unconstrained continuum orbital could be written

$$\tilde{F} = F + \alpha_i P, \quad (F,P) = 0. \quad (2)$$

However, permitting the projectile to be captured into the $2p$ subshell means that there are now $(q+1)$ equivalent electrons, not q, in the ϕ term of Eq. (1).

Seaton's method, described above, for choosing the trial wave function in the close-coupling approximation in the scattering of electrons by atomic systems with incomplete p subshells has also been used by Smith *et al.*[8] (SHB) for the same problem. The same approximation was made with respect to the orbitals of the two configurations $1s^2 2s^2 2p^q \epsilon l + 1s^2 2s 2p^{q+1}$; however, the analytic self-consistent-field (SCF) functions of Roothaan and Kelly[9] were used in the numerical calculations of Smith *et al.*[10] and of Rudd and Smith.[11] This method involves the evaluation of matrix elements

$$L_{kl}^{\alpha} = \alpha^k \langle \phi, (H_{N+1} - E) \sum_{\Gamma_i} \psi^{\Gamma_l}(\Gamma_i, \vec{x}_{N+1}) \rangle, \quad (3)$$

$$L_{kl}^{\alpha^2} = \alpha^k \alpha^l \langle \phi, (H_{N+1} - E)\phi \rangle, \quad (4)$$

in the notation of Ref. 8, who used C for the variational parameter denoted by α here. In their evaluation of these matrix elements, Smith *et al.*[8] used the orthogonality, Eq. (2), between P and F, which would not be possible if the bound orbitals of the actual p^{q+1} configuration were used in ϕ. Furthermore, they chose to antisymmetrize the additional p electron in ϕ as being inequivalent to the other q electrons. That is to say, the $(q+1)$th p electron in ϕ was treated on the same footing as the F electron in ψ. This results in ϕ not being fully antisymmetrized under the interchange of any pair of electrons. The purpose of this paper is to present the fully antisymmetrized function and to examine its effect on the results of Ref. 10 and 11, as well as to compare with the results of Ref. 5.

In Sec. 2 we evaluate the matrix elements (3) and (4) by specializing the general results of Smith and Morgan,[12] referred to henceforth as SM, to the single incomplete p-configuration problem. The results obtained are verified in Sec. 3 using the methods of deShalit and Talmi.[13] In Sec. 4 we re-examine the problem of choosing the trial function by discarding the restriction that the close-coupling functions F must be orthogonal to the bound-state orbitals P. Finally, in Sec. 5 we discuss the numerical effects of various ϕ symmetrizations on the scattering of electrons by atomic systems with configurations $2p^q$.

II. RECOUPLING COEFFICIENT METHOD

The theory of the scattering of electrons by atomic systems with any number of incomplete subshells has been developed within the Hartree-Fock, or close-coupling, approximation by Smith and Morgan.[12] These authors assumed that the bound-electron orbitals are independent of the configuration. They impose the orthogonality condition, Eq. (2), with the result that the terms linear in α (see Eq. (54) of SM) reduce to

$$L_{il,k}^{\alpha} = \sum_\mu \alpha_\mu^k (\langle il|H_1|\mu\rangle + \langle il|1/r|\mu\rangle) \quad (5)$$

which is the many-configuration generalization of Eq. (3), and where the two terms are defined in Eqs. (56) and (60), respectively, of Smith and Morgan. The sum μ runs over all the incomplete subshells included in the eigenfunction expansion. We now restrict consideration to a single incomplete p subshell, as in Saraph *et al.*,[5] so that only the $\mu = np$ term appears in Eq. (5).

The matrix element of H_1 will be nonzero only when the interacting electron is in the incomplete np subshell. In the notation of Smith and Morgan, $\rho = np = b\mu$, $N\rho = q+1$, $S_\rho{}^\mu = S$, $L_\rho{}^\mu = L$, $S_\rho{}^i = S_i$, and $L_\rho{}^i = L_i$,

since all other subshells are closed. Consequently, the first term of Eq. (5), reduces to

$$\langle il|H_1|2p\rangle = (q+1)^{\frac{1}{2}}(p^{q+1}SL\{\}p^qS_iL_i;p)\int dr\,F_{il}$$

$$\times\delta_{l_i1}\left[-\frac{1}{2}\left(\frac{d^2}{dr^2}-\frac{2}{r^2}+\frac{2Z}{r}\right)\right]P_{np}(r)\langle S_i\tfrac{1}{2},S|(S_i\tfrac{1}{2})S\rangle\langle L_il_i,L|(L_ip)L\rangle. \tag{6}$$

Since there is no recoupling of the angular momenta, both recoupling coefficients are unity. Equation (6) leads to a different leading term in Eq. (24) of Smith *et al.*[8] in that $(q+1)^{\frac{1}{2}}$ replaces $(N+1)^{\frac{1}{2}}$, where N is the total number of target electrons.

In the evaluation of the second term of Eq. (5), we note that $N_\lambda{}^i = N_\lambda{}^\mu$ for all subshells except $\lambda = 2p$. In the notation of Smith and Morgan, the outermost interacting subshell in ϕ is $\sigma = np$, and we must have $\rho_i = \rho_\mu = \rho$, which is summed over all the subshells. Furthermore, we have $\Delta P = 0$, $\bar{S}_\sigma = S$, $\bar{L}_\sigma = L_i$, S_σ and $L_\sigma{}^\mu = L$. For $\epsilon = 0$, we have $\nu = \rho$ and $\zeta = np$, which gives the spin and orbital recoupling coefficients to be

$$\begin{aligned}\langle \mathcal{S}_i|\mathcal{S}_\mu\rangle^0 &= \langle(\bar{S}_\rho\tfrac{1}{2})S_\rho\ldots S_i,\tfrac{1}{2}S|(\bar{S}_\rho\tfrac{1}{2})S_\rho\ldots(S_i\tfrac{1}{2})S\rangle = 1\\ \langle \mathcal{O}_i|\mathcal{O}_\mu\rangle^0 &= \langle[\bar{L}_\rho,(l_\rho\nu)l_\rho]L\ldots,l_i;L|(\bar{L}_\rho l_\rho)L_\rho\ldots[\bar{L}_\sigma,(\nu l_i)l_\sigma]L_\sigma;L\rangle,\end{aligned} \tag{7}$$

which is precisely the same form as the direct recoupling coefficient [see SM Eq. (49)]. The dots in Eq. (7) represent the quantum numbers, either spin or orbital, of the spectator subshells lying between the two interacting subshells $\lambda = l_\rho$ and $\lambda = l_i$.

If $\epsilon = 1$, then $\eta = np$ and $\zeta = \rho$, resulting in the recoupling coefficients

$$\begin{aligned}\langle \mathcal{S}_i|\mathcal{S}_\mu\rangle^1 &= \langle[\bar{S}_\rho\tfrac{1}{2}(N)]S_\rho\ldots,\tfrac{1}{2}(N+1);S|[\bar{S}_\rho\tfrac{1}{2}(N+1)]S_\rho\ldots,\tfrac{1}{2}(N);S\rangle\\ \langle \mathcal{O}_i|\mathcal{O}_\mu\rangle^1 &= \langle[\bar{L}_\rho,(l_\sigma\nu)l_\rho]L_\rho\ldots,l_i;L|[\bar{L}_\rho,(\nu l_i)l_\rho]L_\rho\ldots(\bar{l}_\sigma l_\sigma)L_\sigma\rangle.\end{aligned} \tag{8}$$

These recoupling coefficients are precisely those which appear in the exchange term [see SM Eq. (40)], since the order of coupling is the same in both sets of coefficients.

Substituting Eqs. (6), (7), and (8) into Eq. (5) gives the function $V_i(r)$, defined in Eq. (53a) [printed following Eq. (59)] of Smith and Morgan, as

$$\begin{aligned}V_i(r) = (q+1)^{\frac{1}{2}}\Bigg\{&\delta_{l_i1}\{(p^{q+1}LS|\}p^qL_iS_i;p)\Bigg[\left(-\frac{1}{2}\frac{d^2}{dr^2}+\frac{1}{r^2}-\frac{Z}{r}\right)P_{np}(r)\\ &+\rho\sum_{\text{closed}}2(2l_\rho+1)\Big[Y_0(nl_\rho nl_\rho;r)P_{np}(r)-\tfrac{1}{2}\textstyle\sum_t(2t+1)^{-1}(l_\rho100|t0)^2Y_t(nl_\rho np;r)P_\rho(r\Big]\Bigg]\\ &+3q\sum_{L'S'}\delta_{S_iS'}(p^{q+1}LS\{\}p^qL'S,p)[(2L'+1)(2L_i+1)]^{\frac{1}{2}}\sum_{L_2S_2}(-1)^{L_2+L+L'+L_i}(p^qL'S'\{\}p^{q-1}L_2S_2)\\ &\times(p^qL_iS_i\{\}p^{q-1}L_2S_2,p)\textstyle\sum_t(2t+1)^{-1}(1100|t0)\,W(1L'l_iL_i;Lt)\,W(1L'1L_i;L_2t)\\ &\times(1l_i00|t0)[(2l_i+1)3]^{\frac{1}{2}}Y_t(np\,np;r)P_{np}(r)\Bigg\}.\end{aligned} \tag{9}$$

This differs from Eq. (24) of Smith *et al.*[8] in the over-all $(q+1)^{\frac{1}{2}}$ factor replacing $(N+1)^{\frac{1}{2}}$ and in the sum over t in the square brackets, which was missing in Ref. 8. Equation (9) does agree with the results of Shemming,[14] which presumably were used in Refs. 5 and 6.

The incomplete antisymmetrization of ϕ used in Ref. 8 also affects the matrix elements defined in Eq. (4). This matrix element is evaluated in two parts, $\sum_{\alpha=1}^{N+1}H_1(\alpha)$ and r^{-1}, rather than computing H_N as in SM. Starting with Eq. (61) of SM, the first part can be shown to be[15]

$$\langle\phi|H_{N+1}|\phi\rangle = -\frac{1}{2}\sum_{\rho=1s}^{np}N_\rho\int dr\,P_\rho(r)\left(\frac{d^2}{dr^2}-\frac{l_\rho(l_\rho+1)}{r^2}+\frac{2Z}{r}\right)P_\rho(r)+\frac{1}{2}\sum_{\rho=1s}^{np}N_\rho(N_\rho-1)R_0(nl_\rho{}^4)$$

$$+\sum_{\rho>\sigma=1s}^{np} N_\rho N_\sigma R_0(nl_\rho nl_\sigma nl_\rho nl_\sigma) - \sum_{\rho>\sigma(s\ \text{subshell})} 2R_0(nl_\rho nl_\sigma nl_\sigma nl_\rho)$$

$$-\frac{1}{6}\sum_{\substack{\rho=p\\ \sigma\neq\rho}}^{\text{subshell}} N_\rho N_\sigma \sum_\kappa (l_\rho \kappa 00|10)^2 R_\kappa(nl_\rho nl_\sigma nl_\sigma nl_\rho)$$

$$+\frac{3q(q+1)}{5}\sum_{\bar{L}_i\bar{L}_j L'\bar{S}S'} (p^{q+1}LS\{|p^q\bar{L}_i\bar{S}_i,p)(p^{q+1}LS\{|p^qL_j\bar{S},p)$$

$$\times(p^q\bar{L}_i\bar{S}\{|p^{q-1}\bar{L}'\bar{S}',p)(p^qL_jS\{|p^{q-1}L'S',p)(-1)^{L'+L}[(2\bar{L}_i+1)(2\bar{L}_j+1)]^{\frac{1}{2}}$$

$$\times W(L_i1L_j1;L'2)W(L_i1L_j1;L2)R_2(np^4), \tag{10}$$

while the second part is still given by Eqs. (62) and (62a) of SM. It is the first part which is different from the corresponding first two terms of Eq. (25) of Ref. 8, which are simply

$$\sum_{L'S'} (p^{q+1}LS\{|p^qL'S',p)^2E_N(L'S') + \int dr\, P_{np}\left(-\frac{1}{2}\frac{d^2}{dr^2}+\frac{1}{r^2}-\frac{Z}{r}\right)P_{np}.$$

One of the principal advantages of working with Eq. (10) rather than SM Eq. (72) is the fact that it becomes unnecessary to know the energies of highly excited configurations. A detailed proof that the work of Saraph *et al.* and Smith *et al.*,[8] when the above antisymmetrization is taken into account, are proper subsets of the formulation of Smith and Morgan is given in Morgan.[15] That is to say, Refs. 5 and 8 are special cases of Ref. 12, which permits any number of configurations to be included in the trial wave function.

III. OPERATOR METHOD

Although the work of Smith and Morgan had brought to light the incomplete antisymmetrization of Ref. 8, it was thought necessary to verify the expressions for the matrix elements, Eqs. (3) and (4), given in the previous section by using an alternative method. The method chosen was the antisymmetrization operators A_N of deShalit and Talmi.[13] In this method the $(N+1)$-electron wave function for the bound term in Eq. (1) is

$$|1s^22s^22p^{q+1};LS\rangle = \frac{A_{N+1}}{[2!2!(N+1)!(q+1)!]^{\frac{1}{2}}}\,\theta(1s^2;12)\theta(2s^2;34)\theta(2p^{q+1};5,\ldots,N+1;LS), \tag{11}$$

where the q's are properly antisymmetrized for the electrons in that subshell, but A_{N+1} effects the antisymmetrization between the subshells. Using the commutators

$$[A_N, H(x_{N+1})] = 0, \text{ and } [A_N, A_{N+1}] = 0, \tag{12}$$

gives the same matrix element as Eq. (6). In order to evaluate the matrix elements of the two-electron operator $\sum_{\alpha=1}^{N+1} r_{N+1,\alpha}^{-1}$, we consider closed and open subshells separately, leading to the terms in the ρ sum of Eq. (9).

Finally, to compute the terms quadratic in α, we consider matrix elements between closed subshells, between open subshells, and then the cross terms between open and closed. For the interaction of open, l_1, with closed, l_2, we find that the matrix element of the two-electron operator is independent of the total L and is given by

$$V(l_1l_2L) = \sum_\kappa f_\kappa F^\kappa + (-1)^{l_1+l_2+S}\sum_\kappa g_\kappa G^\kappa, \tag{13}$$

where F^κ and G^κ are the usual Slater integrals, and f_κ and g_κ are geometric factors expressible in Racah algebra. For the matrix elements between a pair of closed subshells we find that the contribution

to Eq. (3) is

$$(2l+1)(2l'+1)\left[2F^0(nln'l') - \sum_\kappa (-1)^{l+l'+\kappa}\begin{pmatrix} l & l & \kappa \\ 0 & 0 & 0 \end{pmatrix} G^\kappa(nln'l')\right]. \tag{14}$$

The matrix elements of $\sum_{\alpha=1}^{N+1} H_1(x_\alpha)$ were determined as in the previous section, and the over-all results confirmed the correctness of Eqs. (9) and (10).

IV. VIRTUAL CAPTURE

In the Introduction it was emphasized that when the close-coupling functions were orthogonalized, Eq. (2), with respect to the bound orbitals, it was equivalent to neglecting virtual electron capture into open subshells. For this reason, configuration mixing via the ϕ terms was introduced in Eq. (1).

In this section, we shall discuss briefly the elimination of the orthogonalization constraint on the F's relative to the bound orbitals of the incomplete subshells; a complete discussion will be given elsewhere.[15] This discussion will be within the framework of the techniques of Fano,[16] and leads to the elimination of the so-called ϕ- dependent terms of Refs. 5, 6, 8, and 12. Consequently, virtual capture is now implicit in the close-coupling functions F.

The principal advantage of the orthogonalization procedure was the elimination of factors in the exchange term as a result of the vanishing of the overlap integral of F with a P. (It is clear that such an overlap does not occur in the direct terms, since both F's are found in the same integral.) We now have to derive an alternative expression for SM Eq. (25), with the orthogonality constraint expressed in the form

$$\int dr\, F_{ij}(r)P_\lambda(r) = \Delta(ij;\lambda)\delta_{l_i l_\lambda}, \tag{15}$$

for the incomplete subshells P_λ, but the Δ still vanish for the closed subshells.

We begin by evaluating the matrix elements of the one-electron operators $\sum_{\alpha=1}^{N+1} H_1(\alpha)$ and note that only those for $\alpha \leq N-1$ contribute equally. If we let μ_i and μ_j be the subshells containing the labels N and $N+1$ in the distributions q_i and q_j, respectively, then using the methods of SM we can show that

$$\left\langle \sum_{\alpha=1}^{N-1} H_1(\alpha) \right\rangle = \sum_{\rho,\mu_i,\mu_j} C_{\rho\mu_i\mu_j}^{ij} \int_0^\infty dr\, P_{\mu_i}(r)F_{jl}(r) \int_0^\infty dr\, F_{i\kappa}(r)P_{\mu_j}(r)$$
$$\times \int_0^\infty dr\, P_\rho(r)\left(\frac{d^2}{dr^2} - \frac{l_\rho(l_\rho+1)}{r^2} + \frac{2Z}{r}\right)P_\rho(r), \tag{16}$$

with one less integral for $H_1(N)$ and $H_1(N+1)$ on account of F and P_ρ being interchanged. The C factors are defined in Ref. 15.

A similar separation of the two-electron operator can be effected

$$\sum_{i<j}^{N+1} \langle r_{ij}^{-1}\rangle = \sum_{i<j}^{N-1} \langle r_{ij}^{-1}\rangle + \sum_{i=1}^{N-1} \langle r_{i,N}^{-1}\rangle + \sum_{i=1}^{N-1} \langle r_{i,N+1}^{-1}\rangle + \langle r_{N,N+1}^{-1}\rangle. \tag{17}$$

The final matrix element is given in SM Eq. (41), and the remaining three matrix elements can be readily evaluated by the same method after using symmetry properties.

The variational principle of SM Eq. (73) is now replaced by

$$\delta\left(\sum_{ij}\int F_{i\kappa}\mathcal{L}_{ij}F_{jl}\,dr + \sum_{ij}\int F_{i\kappa}X_{ij}^{\,l}\,dr + \sum_{\lambda,\ \text{closed}} \mathfrak{M}_\lambda \int P_\lambda F_{i\kappa}\,dr - \tfrac{1}{2}K_{\kappa l}\right) = 0, \tag{18}$$

where $\mathfrak{M}_\lambda$ are the Lagrange undetermined multipliers chosen to ensure the orthogonality of the continuum with the closed subshells, and $X_{ij}^{\,l}(r)$ is an integral operator on F with terms from Eqs. (16) and (17). The associated Euler equations are

$$\sum_j \mathcal{L}_{ij}F_{jl} + \sum_j X_{ij}^{\,l}(r) + \sum_{\lambda,\ \text{closed}} \mathfrak{M}_\lambda P_\lambda(r) = 0, \tag{19}$$

where each of the factors of the inhomogeneous X term is of the form

$$X_{ij}^{\,l}(r) = \mathcal{G}_{ij}(r)A_{ij}^{\,l}, \tag{20}$$

where $\mathcal{G}_{ij}(r)$ are known functions[15] and A_{ij} are unknown numbers dependent on F. If there are NV such inhomogeneous terms, then we can generate NV particular solutions of the inhomogeneous system by setting the A's in turn equal to unity, the remainder zero. This is a variation of the numerical method developed in Ref. 8 and is equivalent to that used by Burke and McVicar[17] for the electron-hydrogen-like-ion problem.

V. NUMERICAL RESULTS

In the preceding sections two changes have been proposed in the formalism. Firstly, there is the problem of antisymmetrization, which is now properly handled in Secs. 2 and 3; and secondly, there is the alternative approach to virtual capture described in Sec. 4. Here we shall report computations carried out on the effects of ϕ antisymmetrization.

In Table I we present results for the collision strengths of electrons incident on a variety of ions, as computed with both the partly and fully antisymmetrized ϕ functions, and we compare with the results of Saraph *et al.* We emphasize that the bound orbitals for the N-electron problem have been used in both ψ and ϕ of Eq. (1). Furthermore, in the computation of the matrix element, given in Eq. (4), we have written

$$E = \tfrac{1}{2}\kappa_1^2 + E_N(S_1L_1),$$

$$E_N \equiv \langle \phi(N) | H_N | \phi(N) \rangle, \qquad (21)$$

where S_1L_1 are the quantum numbers of the lowest term, and the actual expression for E_N is obtained from Eq. (10). Two conclusions can be drawn from Table I. Firstly, the results do depend markedly on the symmetry of ϕ; and secondly, the quite different numerical procedures and bound orbitals of Refs. 5 and 8 lead to the same collision strengths to within a few percent. When the theoretical values of Roothaan and Kelly are used in Eq. (21), the results are hardly affected at all.

The large change in the collision strengths mentioned above, brought about by the full antisymmetrization of ϕ raises the question of its

TABLE I. Collision Strengths, $\Omega(nn')$.

ION	n	n'	ϕ (SHB)	ϕ	Ref. 6
N^+	^3P	^1D	6.342	3.292	3.203
	^1D	^1S	0.677	0.428	0.424
	^3P	^1S	0.931	0.428	0.391
O^{++}	^3P	^1D	5.016	2.545	2.398
	^1D	^1S	0.438	0.294	0.319
	^3P	^1S	0.798	0.369	0.345

TABLE II. Values of conserved quantum numbers influenced by the virtual ϕ term.

Ref.	Target	$(2S+1)_{L^\pi}$		
12	O^+	$^3P^e$	$^1D^e$	$^1S^e$
9	C	$^4S^0$	$^2D^0$	$^2P^0$
	N	$^3P^e$	$^1D^e$	$^1S^e$
	O	$^2P^0$		

TABLE III. Partial-wave contributions to the excitation cross sections. Numbers in parentheses are from Ref. 10.

Target	Process	SLπ	κ^2 = 0.15	0.2	0.25	0.3	0.4	0.5	0.6	0.8	1.0	1.4	2.0	3.0	4.0
C	$^3P - {}^1D$	$^2P^0$	1.020	0.885	0.691	0.566	0.420	0.334	0.277	0.202	0.155	0.097	0.051	0.019	0.008
			(0.330)	(0.484)	(0.514)	(0.502)	(0.446)	(0.389)	(0.338)	(0.261)	(0.210)	(0.150)	(0.103)	(0.040)	(0.012)
	$^3P - {}^1S$	$^2P^0$	1.177	1.220	1.124	1.013	0.821	0.676	0.567	0.413	0.311	0.185	0.090	0.031	0.012
			(0.849)	(1.143)	(1.225)	(1.217)	(1.104)	(0.977)	(0.858)	(0.673)	(0.546)	(0.387)	(0.236)	(0.069)	(0.019)
	$^1D - {}^1S$	$^2P^0$		0.005	0.136	0.174	0.167	0.144	0.122	0.089	0.067	0.039	0.019	0.006	0.002
				(0.003)	(0.110)	(0.169)	(0.200)	(0.196)	(0.179)	(0.146)	(0.120)	(0.085)	(0.054)	(0.017)	(0.004)
	$^3P - {}^1D$	$^2P^0$		0.007	0.146	0.158	0.133	0.107	0.086	0.059	0.042	0.023	0.011	0.007	0.006
				(0.005)	(0.110)	(0.146)	(0.175)	(0.183)	(0.178)	(0.155)	(0.131)	(0.090)	(0.045)	(0.008)	(0.004)
	$^3P - {}^1S$	$^2P^0$		0.406	0.494	0.490	0.397	0.345	0.307	0.255	0.219	0.157	0.113	0.060	0.033
				(0.159)	(0.269)	(0.336)	(0.383)	(0.376)	(0.352)	(0.297)	(0.255)	(0.177)	(0.133)	(0.083)	(0.051)
	$^1D - {}^1S$	$^2P^0$				1.112	1.024	0.901	0.794	0.629	0.511	0.357	0.321	0.105	0.051
						(0.837)	(1.100)	(1.076)	(1.001)	(0.836)	(0.700)	(0.513)	(0.357)	(0.202)	(0.095)
	$^3P - {}^1P$	$^3P^e$				0.125	0.282	0.297	0.279	0.231	0.190	0.131	0.079	0.034	0.016
						(.....)	(0.133)	(0.281)	(0.327)	(0.323)	(0.290)	(0.224)	(0.157)	(0.084)	(0.036)
	$^1D - {}^1P$	$^3P^e$				0.031	0.050	0.056	0.056	0.048	0.039	0.025	0.012	0.004	0.002
						(.....)	(0.039)	(0.087)	(0.114)	(0.129)	(0.122)	(0.096)	(0.061)	(0.022)	(0.005)
	$^4S - {}^2P$	$^4D^e$					0.088	0.104	0.104	0.093	0.079	0.056	0.035	0.016	0.008
							(0.070)	(0.151)	(0.180)	(0.182)	(0.165)	(0.127)	(0.087)	(0.045)	(0.018)
O	$^3P - {}^1D$	$^2P^0$													
	$^3P - {}^1S$	$^2P^0$													
	$^1D - {}^1S$	$^2P^0$													
	$^3P - {}^1D$	$^2P^0$													
	$^3P - {}^1S$	$^2P^0$													
	$^1D - {}^1S$	$^2P^0$													
	$^4S - {}^2P$	$^4P^e$													
	$^2D - {}^2P$	$^4P^e$													
N															

TABLE IV. Partial-wave contributions to the elastic cross sections. Numbers in parentheses are from Ref. 10.

Target	Process	$SL\pi$	$\kappa_1^2 = 0.1$	0.15	0.2	0.25	0.3	0.4	0.5	0.6	0.8	1.0
C	$^3P-^3P$	$^4S^0$	1.989	2.246	2.263	2.182	2.063	1.804	1.570	1.373	1.078	0.877
			(2.462)	(3.005)	(3.096)	(2.950)	(2.735)	(2.215)	(1.754)	(1.392)	(0.914)	(0.658)
		$^2P^0$	10.623	6.429	4.157	3.001	2.429	1.829	1.496	1.275	0.996	0.829
			(3.898)	(3.747)	(3.344)	(2.804)	(2.364)	(1.681)	(1.208)	(0.884)	(0.516)	(0.344)
		$^2D^0$	8.564	5.257	4.258	3.703	3.317	2.779	2.407	2.129	1.744	1.493
			(4.163)	(4.169)	(3.970)	(3.629)	(3.240)	(2.501)	(1.916)	(1.488)	(0.965)	(0.703)
	$^1D-^1D$	$^2P^0$	0.644	2.413	2.883	2.939	2.854	2.626	2.406	2.212	1.896	1.658
			(0.893)	(2.215)	(2.858)	(3.060)	(2.994)	(2.598)	(2.192)	(1.854)	(1.397)	(1.132)
		$^2D^0$	0.350	1.831	3.100	3.619	3.788	3.722	3.492	3.244	2.814	2.448
			(0.404)	(1.393)	(3.194)	(4.064)	(4.297)	(3.907)	(3.253)	(2.642)	(0.803)	(1.355)
	$^1S-^1S$	$^2P^0$			0.026	3.143	5.852	8.684	9.727	9.972	9.540	8.754
					(0.028)	(3.321)	(6.364)	(9.124)	(9.693)	(9.367)	(8.197)	(7.146)
O	$^3P-^3P$	$^2P^0$	9.209	4.463	2.727	2.103	1.778	1.336	1.108	0.962	0.774	0.655
			(1.017)	(1.372)	(1.485)	(1.530)	(1.523)	(1.407)	(1.254)	(1.096)	(1.830)	(0.619)
	$^1D-^1D$	$^2P^0$		0.104	0.298	0.566	0.696	0.732	0.746	0.735	0.693	0.653
				(0.115)	(0.050)	(0.234)	(0.431)	(0.697)	(0.800)	(0.808)	(0.725)	(0.640)
	$^1S-^1S$	$^2P^0$						2.928	5.119	6.045	6.405	6.143
								(0.692)	(1.643)	(2.393)	(3.244)	(3.663)
N	$^4S-^4S$	$^3P^e$	25.696		8.279		5.119	4.110	3.576	3.206	2.693	2.344
			(5.349)		(6.648)		(5.373)	(4.319)	(3.540)	(2.956)	(2.146)	(1.654)
	$^2D-^2D$	$^3P^e$					1.250	1.513	1.526	1.464	1.293	1.136
							(0.965)	(1.607)	(1.696)	(1.581)	(1.237)	(0.956)
		$^1D^e$					1.529	1.790	1.739	1.596	1.285	1.033
							(1.596)	(2.248)	(2.174)	(1.899)	(1.316)	(0.893)
	$^2P-^2P$	$^3P^e$					0.244	1.073	1.536	1.760	1.874	1.812
							(. . .)	(0.421)	(1.258)	(1.675)	(1.835)	(1.708)
		$^1D^e$					0.131	0.644	0.949	1.094	1.155	1.101
							(. . .)	(0.261)	(0.786)	(1.035)	(1.100)	(0.998)

influence on the positions of the autoionized levels of oxygen, as reported in Rudd and Smith,[11] and on the cross sections presented in Ref. 8. In Table II, we list those values of the conserved quantum numbers which are affected by the ϕ problem.

In Tables III and IV we present the partial-wave contributions to the excitation and elastic cross sections, respectively, as computed with the fully antisymmetrized ϕ, and compare them with the results of Ref. 10, which are given in parentheses. The general feature of these results is that at lower impact energies the new ϕ produces larger cross sections than the partly antisymmetric ϕ, while at the higher energies the new results are lower. In this regard the new results are in no better agreement with the experimental total cross sections for electrons on either oxygen or nitrogen. Of course the effects of excited configurations which have been neglected here, may well have a significant influence. We note that the relative phases of some of the coefficients of fractional parentage used in Refs. (10), (14) and Sobel' man[18] are incorrect due to incorrect use of Eq. (19) in Racah[19].

In Table V we present the results of the two partial waves in electron-O^+ scattering which are affected by the antisymmetrization problem. For autoionized $^3P^e$ states we see that the new ϕ results are consistently higher than those of Rudd and Smith by about 0.1 ev. However, one notable feature of the new results is that we have been able to locate the low-lying $^2D_{np}$ resonances found by experiment, as well as to identify the very narrow f series. For autoionized $^1D^e$ states we see that the new ϕ has very little affect at all. Indeed, since the theoretical results of Rudd and Smith were obtained on a CDC-6600, while the present results were computed on an IBM System 360/65, the difference due to ϕ is indeed slight. A new feature of the results presented here is

TABLE V. Positions of autoionized states in atomic oxygen.

$LS\pi$	Assignment	n	old ϕ	ϕ	Experiment
1,1,even	^2Pnp	3	15.768	16.0174	15.77
		4	17.305	17.4069	17.31
		5	17.849	17.9103	
		6	18.121	18.2167	
		7	18.278	18.401	
	^2Dnp	3		14.461	14.16
		4		15.729	15.62
		5	16.121	16.204	16.22
		6	16.312	16.4818	
		7	16.507		
	^2Dnf	4		16.087	
		5			
2,0,even	^2Pnp	4	17.387	17.403	
		5	17.908	17.903	
		6	18.135	18.159	
		7	18.285		
		8	18.366		
	^2Pnf	4		17.786	
		5		18.094	
		6		18.255	
		7		18.380	

that we have been able to isolate several members of the $^2P nf$ series.

In conclusion we note that the numerical results presented in this paper are based on a formalism which largely neglects polarization of the target by the impinging electron. To account for such polarization, we could include excited configurations such as $1s^2 2s\, 2pq + 1$ and $1s^2 2s^2 2pq - 13d$, etc. as in SM, or we could take the dipole distortion of the atom produced by the incident electron into account by using the method of polarized orbitals as used by Henry.[20] Calculations based on the SM formalism are under way, and comparison will be made against the results of the polarized orbital method. Since no rigorous criteria exist for complex targets for selecting one approximation scheme over another, one can only compare theoretical predictions with known experimental results to determine which features of the model are important before computing physical processes which have not been investigated experimentally.

Note added in proof: Henry *et al.* (unpublished) have carried out the calculations in Table IV to lower energies and have analyzed the low-energy peaks predicted here as "shape" resonances.

ACKNOWLEDGMENT

The authors are indebted to Professor M. J. Seaton for discussions and a helpful exchange of correspondence.

---

*Work supported by the National Science Foundation, the U. K. Science Research Council and by the Air Force Weapons Laboratory, Kirtland AFB, New Mexico, under contract No. AF29(601)-68-C-0052 with Quantum Systems, Inc., Albuquerque, New Mexico.

[1]P. G. Burke and K. Smith, Rev. Mod. Phys. 34, 458 (1962).

[2]I. C. Percival and M. J. Seaton, Proc. Cambridge Phil. Soc. 53, 654 (1957).

[3]P. G. Burke, D. D. McVicar, and K. Smith, Proc. Phys. Soc. (London) 83, 397 (1964).

[4]R. J. Damburg and S. Geltman, Phys. Rev. Letters 20, 485 (1968).

[5]H. E. Saraph, M. J. Seaton, and J. Shemming, Proc. Phys. Soc. (London) 89, 27 (1966).

[6]S. J. Czyzak and T. K. Krueger, Proc. Phys. Soc. (London) 90, 623 (1967).

[7]C. Froese, Canad. J. Phys. 41, 1895 (1963).

[8]K. Smith, R. J. W. Henry and P. G. Burke, Phys. Rev. 147, 21 (1966).

[9]C. C. J. Roothaan and P. S. Kelly, Phys. Rev. 131, 1177 (1963).

[10]K. Smith, R. J. W. Henry and P. G. Burke, Phys. Rev. 157, 51 (1967).

[11]M. E. Rudd and K. Smith, Phys. Rev. 169, 79 (1968).

[12]K. Smith and L. A. Morgan, Phys. Rev. 165, 110 (1968).

[13]A. deShalit and I. Talmi, Nuclear Shell Theory (Academic Press Inc., New York 1963), p. 470.

[14]J. Shemming, Ph.D. thesis, University of London, 1965, (unpublished).

[15]L. A. Morgan, Ph.D. thesis, University of London, 1968, (unpublished).

[16]U. Fano, Phys. Rev. 140, A67 (1965).

[17]P. G. Burke and D. D. McVicar, Proc. Phys. Soc. (London) 86, 989 (1965).

[18]I. I. Sobel'man, Introduction to the Theory of Complex Spectra, (Moscow 1963), Translated by the Foreign Technology Division, Wright-Patterson AFB, 1967.

[19]G. Racah, Phys. Rev. 63, 367 (1943).

[20]R. J. W. Henry, Phys. Rev. 162, 56 (1967).

PHOTOIONIZATION OF ATOMS WITH CONFIGURATIONS $1s^2 2s^2 2p^6 3s^2 3p^q$

M. Conneely, L. Lipsky, K. Smith

(Royal Holloway College, Englefield Green, Egham, Surrey, England).

The abundance of some atoms in the second row of the periodic table (Al, Si, P, S) in the sun is comparatively large, being approximately one tenth that of C, N, or O but ten times that of Fe [1]. Therefore, it is expected that their contributions to the solar spectrum will be significant. In particular, the photoabsorption cross sections for Al and Si are large

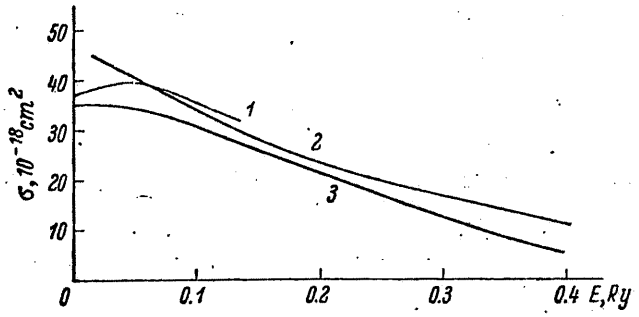

Fig. 1. Photoionization cross section σ of $(3p)^2\ ^3P$ silicon.
1 — experimental; *2* — this work; *3* — quantum defect.

enough to virtually obliterate light originating in the photosphere for certain parts of the spectrum. Recently, shock-tube experiments have been performed to determine these cross sections [2]. General interest in the inert gases has caused several experimental groups to measure the photoabsorption of argon [3, 4]. It is therefore useful to have theoretical results avai-

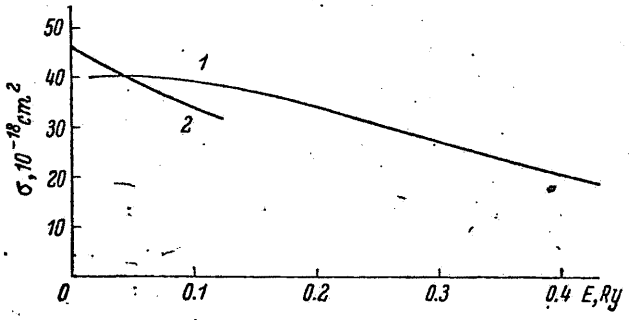

Fig. 2. Photoionization cross section σ of $(3p)^2 {}^1S$ silicon.
1 — this work; *2* — quantum defect.

lable for the $(3p)^q$ elements. The quantum defect method [5] has been used extensively to calculate cross sections, but it becomes unreliable when applied to the 3*p*-shell. This is due to the fact that the quantum defects of the singly excited states of these (and heavier) atoms are not smooth functions of n, the principle quantum number, and therefore it is difficult to extrapolate to above threshold.

The procedure followed here, in calculating the photoionization cross sections, is described in Henry and Lipsky [6]. Briefly, we calculate the wave functions for an electron scattering of a particular ion, assuming L—S

coupling, using the close coupling code of Smith, Henry and Burke [7]. These functions are then used to calculate the dipole matrix elements between states of an outgoing electron in a particular channel and a state of the ini-

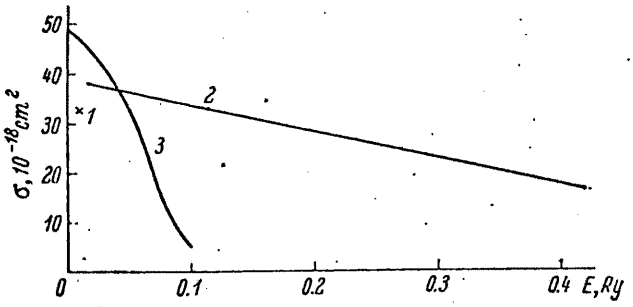

Fig. 3. Photoionization cross section σ of $(3p)^2\ {}^1D$ silicon.
1 — experimental; *2* — this work; *3* — guantum defect.

tial atom. The analytic Hartree—Fock functions of Clementi [8] are used to represent the wave functions of the atoms and residual ions.

Some calculations have already been completed, and the results for silicon and argon are reproduced in fig. 1—4, together with available experi-

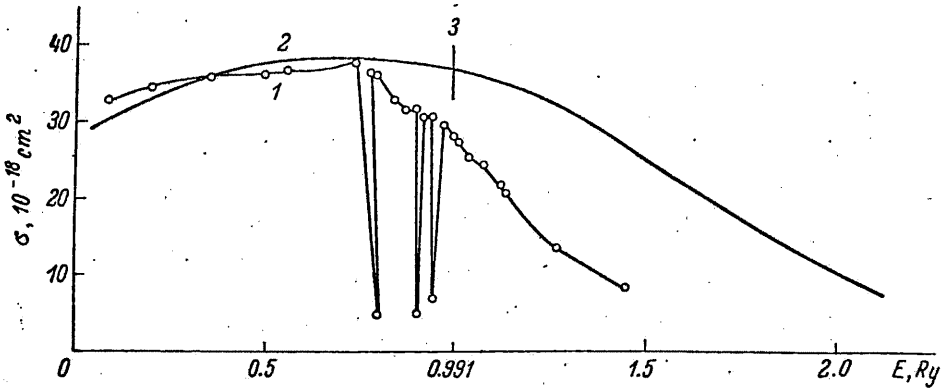

Fig. 4. Photoionization cross section σ of argon.
1 — experiment; *2* — this work; *3*—$3s3p^6$ edge.

mental data. The experimental data as well as the quantum defect curves for silicon are taken from Rich [2]. The argon data was given to the authors by Edérer et al. [4], in advance of publication. The dipole length calculations agree fairly well with experiment for energies below the excited state thresholds, whereas the dipole velocity approximation gives values $^1/_2$ to $^2/_3$ that of experiment.

REFERENCES

1. L. Goldberg, E. Q. Müller, L. H. Aller, Astrop. J. Suppl., 5, 1 (1960).
2. J. C. Rich, Astrop. J. (to be published).
3. J. A. R. Samson, G. C. A. Technical Report, № 63-N (1964).
4. D. Ederer, K. Codling, R. Madden (private communication).
5. Burgess, Seaton, Rev. Mod. Phys. (1960).
6. R. J. W. Henry, L. Lipsky, Phys. Rev. (1967).
7. Kenneth Smith, R. J. W. Henry, P. G. Burke, Phys. Rev., 147, 21 (1966).
8. E. Clementi. Table of atomic functions, I. B. M. J. Res. Develop., 9, 2 (1965).